



TESIS DOCTORAL

OPTIMIZACIÓN DEL MANEJO DE CULTIVOS LEÑOSOS A TRAVÉS DEL ANÁLISIS AUTOMATIZADO DE IMÁGENES OBTENIDAS CON VEHÍCULOS AÉREOS NO TRIPULADOS

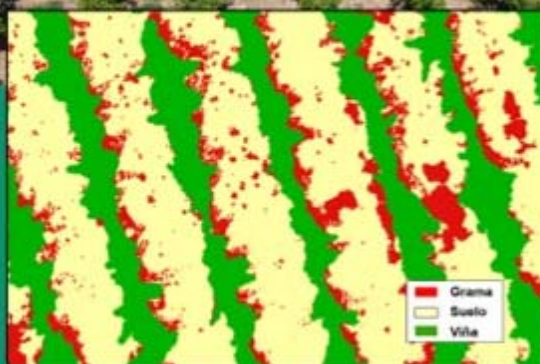
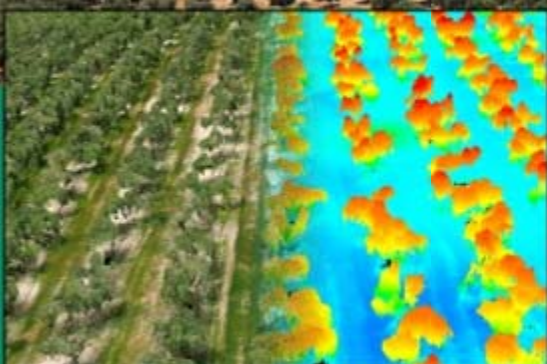
Francisco Manuel
Jiménez Brenes

Directoras

Dra. Francisca López Granados
Dra. Ana Isabel de Castro Megías



Córdoba, Septiembre de 2019



**TITULO: OPTIMIZACIÓN DEL MANEJO DE CULTIVOS LEÑOSOS A TRAVÉS
DEL ANÁLISIS AUTOMATIZADO DE IMÁGENES OBTENIDAS CON
VEHÍCULOS AEREOSEN NO TRIPULADOS**

AUTOR: *Francisco Manuel Jiménez Brenes*

© Edita: UCOPress. 2019
Campus de Rabanales
Ctra. Nacional IV, Km. 396 A
14071 Córdoba

<https://www.uco.es/ucopress/index.php/es/>
ucopress@uco.es



UNIVERSIDAD
DE
CÓRDOBA



CSIC
CONSEJO SUPERIOR DE INVESTIGACIONES CIENTÍFICAS

INSTITUTO DE
AGRICULTURA
SOSTENIBLE



Programa de Doctorado en Ingeniería Agraria, Alimentaria, Forestal y de Desarrollo Rural Sostenible

TESIS DOCTORAL

OPTIMIZACIÓN DEL MANEJO DE CULTIVOS LEÑOSOS A TRAVÉS DEL ANÁLISIS AUTOMATIZADO DE IMÁGENES OBTENIDAS CON VEHÍCULOS AÉREOS NO TRIPULADOS

OPTIMIZING WOODY CROP MANAGEMENT THROUGH
AUTOMATED ANALYSIS OF IMAGERY TAKEN
BY UNMANNED AERIAL VEHICLES

Presentada por **Francisco Manuel Jiménez Brenes** para la obtención
del título de Doctor Ingeniero de Montes

Directoras:

Dra. Francisca López Granados
Dra. Ana Isabel de Castro Megías

Tutor:

Dr. Alfonso García-Ferrer Porras

Córdoba, Septiembre de 2019



TÍTULO DE LA TESIS: Optimización del manejo de cultivos leñosos a través del análisis automatizado de imágenes obtenidas con vehículos aéreos no tripulados

DOCTORANDO: Francisco Manuel Jiménez Brenes

INFORME RAZONADO DE LAS DIRECTORAS DE LA TESIS

La **Dra. Francisca López Granados, Investigadora Científica-CSIC**, y la **Dra. Ana Isabel de Castro Megías, Investigadora Postdoctoral**, ambas adscritas al Instituto de Agricultura Sostenible de Córdoba (IAS-CSIC), como Directoras de la Tesis Doctoral titulada “**OPTIMIZACIÓN DEL MANEJO DE CULTIVOS LEÑOSOS A TRAVÉS DEL ANÁLISIS AUTOMATIZADO DE IMÁGENES OBTENIDAS CON VEHÍCULOS AÉREOS NO TRIPULADOS**” realizada por Francisco Manuel Jiménez Brenes,

INFORMAN QUE:

- Dicha Tesis Doctoral ha sido desarrollada bajo su dirección.
- Ha tenido como principal objetivo la contribución a la mejora del manejo de cultivos leñosos de forma eficiente, económica y sostenible en el contexto de la agricultura de precisión mediante la combinación de tecnología UAV, modelos tridimensionales a partir de técnicas fotogramétricas y desarrollo de procedimientos automáticos de análisis de imagen basados en OBIA.
- Tanto la metodología como el trabajo de investigación, las conclusiones y los resultados obtenidos son satisfactorios.
- En el desarrollo de su etapa predoctoral, Francisco Manuel Jiménez Brenes ha colaborado en diferentes líneas de trabajo, varias de las cuales se han realizado expresamente en el marco de su Tesis Doctoral, así como en otros Proyectos de Investigación del grupo en los que el doctorando se ha incorporado. De estos trabajos se han derivado las siguientes publicaciones, señalándose con asterisco las directamente relacionadas con los objetivos de su Tesis Doctoral:

REVISTAS INCLUIDAS EN EL SCIENCE CITATION INDEX:

1. LÓPEZ-GRANADOS, F.; TORRES-SÁNCHEZ, J.; **JIMÉNEZ-BRENES, F.M.**; ARQUERO, O.; LOVERA, M.; DE CASTRO, A.I. (2019). An efficient RGB-UAV-based platform for field almond tree phenotyping: 3-D architecture and flowering traits. *Plant Methods* (Under review).
2. * **JIMÉNEZ-BRENES, F.M.**; LÓPEZ-GRANADOS, F.; TORRES-SÁNCHEZ, J.; PEÑA, J.M.; RAMÍREZ, P.; CASTILLEJO-GONZÁLEZ, I.L.; DE CASTRO, A.I. (2019). Automatic UAV-based detection of *Cynodon dactylon* for site-specific vineyard management. *PLoS ONE*, 14(6): e0218132.
<https://doi.org/10.1371/journal.pone.0218132> (Open Access).
3. DE CASTRO, A.I.; RALLO, P.; SUÁREZ, M.P.; TORRES-SÁNCHEZ, J.; CASANOVA, L.; **JIMÉNEZ-BRENES, F.M.**; MORALES-SILLERO, A.; JIMÉNEZ, R.; LÓPEZ-GRANADOS, F. (2019). High-throughput system for the early quantification of major architectural traits in olive breeding trials using UAV images and OBIA techniques. *Frontiers in Plant Science* (Under review).
4. JURADO-EXPÓSITO, M.; DE CASTRO, A.I.; TORRES-SÁNCHEZ, J.; **JIMÉNEZ-BRENES, F.M.**; LÓPEZ-GRANADOS, F. (2019). *Papaver rhoeas* L. mapping with cokriging using UAV imagery. *Precision Agriculture*, 20(5): 1045-1067.
<https://doi.org/10.1007/s11119-019-09635-z>
5. TORRES-SÁNCHEZ, J.; DE CASTRO, A.I.; PEÑA, J.M.; **JIMÉNEZ-BRENES, F.M.**; ARQUERO, O.; LOVERA, M.; LÓPEZ-GRANADOS, F. (2018). Mapping the 3D structure of almond trees using UAV acquired photogrammetric point clouds and object-based image analysis. *Biosystems Engineering*, 176:172-184.
doi:10.1016/j.biosystemseng.2018.10.018
6. * DE CASTRO, A.I.; **JIMÉNEZ-BRENES, F.M.**; TORRES-SÁNCHEZ, J.; PEÑA, J.M.; BORRA-SERRANO, I.; LÓPEZ-GRANADOS, F. (2018). 3-D characterization of vineyards using a novel UAV imagery-based OBIA procedure for precision viticulture applications. *Remote Sensing*, 10(4): 584. doi:10.3390/rs10040584 (Open Access).
7. DE CASTRO, A.I.; TORRES-SÁNCHEZ, J.; PEÑA, J.M.; **JIMÉNEZ-BRENES, F.M.**; CSILLIK, O.; LÓPEZ-GRANADOS, F. (2018). An automatic random forest-OBIA algorithm for early weed mapping between and within crop rows using UAV imagery. *Remote Sensing*, 10(2), 285.
doi:10.3390/rs10020285 (Open Access).
8. * **JIMÉNEZ-BRENES, F.M.**; LÓPEZ-GRANADOS, F.; DE CASTRO, A.I.; TORRES-SÁNCHEZ, J.; CASTILLO, N.; PEÑA, J.M. (2017). Quantifying pruning impacts on olive tree architecture and annual canopy growth by using UAV-based 3D modelling. *Plant Methods*, 13:55.
doi:10.1186/s13007-017-0205-3 (Open Access).

REVISTAS NO INCLUIDAS EN EL SCIENCE CITATION INDEX:

1. **JIMÉNEZ BRENES, F.M.**; DE CASTRO, A.I.; TORRES SÁNCHEZ, J.; PEÑA, J.M.; LÓPEZ-GRANADOS, F. (2018). Detección temprana de malas hierbas dentro y fuera de la línea de cultivo utilizando imágenes UAV y procedimientos automatizados de análisis. *Tierras - Agricultura*, 264: 22-27.
2. DE CASTRO, A.I.; PEÑA, J.M.; TORRES SÁNCHEZ, J.; **JIMÉNEZ BRENES, F.M.**; LÓPEZ-GRANADOS, F. (2017). Uso de drones (UAV) para la detección de grama en cubiertas de viña. *Interempresas - Grandes Cultivos*, 12: 4-8.

APORTACIONES EN CONGRESOS INTERNACIONALES:

1. * TORRES-SÁNCHEZ, J.; MARÍN, D.; DE CASTRO, A.I.; ORIA, I.; **JIMÉNEZ-BRENES, F.M.**; MIRANDA, C.; SANTESTEBAN, L.G.; LÓPEZ-GRANADOS, F. (2019). Assessment of vineyard trimming and leaf removal using UAV photogrammetry. *12th European Conference on Precision Agriculture*, 8th-11th July 2019. Montpellier, Francia, pp: 187-192.
2. TORRES-SÁNCHEZ, J.; DE CASTRO, A.I.; RALLO, P.; SUÁREZ, M.P.; PEÑA, J.M.; **JIMÉNEZ-BRENES, F.M.**; MORALES, A.; CASANOVA, L.; JIMÉNEZ, R.; LÓPEZ-GRANADOS, F. (2018). Olive breeding trials 3D characterization using UAV acquired photogrammetric point clouds. *6th International Conference on Olive Tree and Olive Products (Olive Bioteq'18)*, 15th-19th October 2018. Sevilla, España. p. 65.
3. * DE CASTRO, A.I.; PEÑA, J.M.; TORRES-SÁNCHEZ, J.; **JIMÉNEZ-BRENES, F.M.**; LÓPEZ-GRANADOS, F. (2017). Mapping *Cynodon dactylon* in vineyards using UAV images for site-specific weed control. *11th European Conference on Precision Agriculture*, 16th-20th July 2017. Edinburgh, Reino Unido, pp: 267-271.
4. * MESAS-CARRASCOSA, F.J.; PEÑA, J.M.; DE CASTRO, A.I.; TORRES-SÁNCHEZ, J.; **JIMÉNEZ-BRENES, F.M.**; GARCÍA-FERRER, A.; LÓPEZ-GRANADOS, F. (2017). Generation of canopy height model based on point clouds and spectral data: a case study on grapevine. *5th UAS4Enviro*, 28th-30th June 2017. Vila Real, Portugal, p. 11.
5. * PEÑA-BARRAGÁN, J.M.; **JIMÉNEZ-BRENES, F.M.**; TORRES-SÁNCHEZ, J.; LÓPEZ-GRANADOS, F.; DE CASTRO, A.I.; SERRANO, N. (2016). Assessment of pruning intensity from 3-D olive-tree models generated with UAV technology. *VII International Olive Symposium*, 10th-14th October 2016. Split, Croacia. p. 86.

APORTACIONES EN CONGRESOS NACIONALES:

1. RECASENS, J.; CABRERA, C.; VALENCIA-GREDILLA, F.; DE CASTRO, A.I.; ROYO-ESNAL, A.; TORRES-SÁNCHEZ, J.; CIVIT, J.; **JIMÉNEZ-BRENES, F.M.**; LÓPEZ-GRANADOS, F. (2019). Manejo, dinámica espacio-temporal y detección aérea de rodales de *Cynodon dactylon* en viñedos con cubierta vegetal. *XVII*

Congreso de la Sociedad Española de Malherbología-SEMh, 8-10 Octubre, 2019. Vigo, España.

2. * DE CASTRO, A.I.; **JIMÉNEZ-BRENES, F.M.**; TORRES-SÁNCHEZ, J.; PEÑA, J.M.; LÓPEZ-GRANADOS, F. (2018). Aplicación de tecnología UAV para monitorización multitemporal de cultivos leñosos: caso práctico poda del olivo. *III Symposium Nacional de Ingeniería Hortícola – I Symposium Ibérico de Ingeniería Hortícola*, 21-23 de Febrero 2018. Lugo, España. pp: 396-400.
3. * TORRES-SÁNCHEZ, J.; LÓPEZ-GRANADOS, F.; DE CASTRO, A.I.; **JIMÉNEZ-BRENES, F.M.**; PEÑA, J.M. (2017). Detección temprana de malas hierbas dentro y fuera de la línea de cultivo mediante imágenes-UAV y modelos 3D. *XVI Congreso de la Sociedad Española de Malherbología-SEMh*, 25-27 Octubre, 2017. Pamplona, España. pp: 407-412.
4. * DE CASTRO, A.I.; PEÑA, J.M.; TORRES-SÁNCHEZ, J.; **JIMÉNEZ-BRENES, F.M.**; RECASENS, J., VALENCIA, F.; LÓPEZ-GRANADOS, F. (2017). Cartografía de *Cynodon dactylon* en viñedo mediante imágenes UAV y tecnología OBIA para un uso sostenible y localizado de herbicidas. *XVI Congreso de la Sociedad Española de Malherbología-SEMh*, 25-27 Octubre, 2017. Pamplona, España. pp: 395-400.
5. PEÑA, J.M.; DE CASTRO, A.I.; TORRES-SÁNCHEZ, J.; **JIMÉNEZ-BRENES, F.M.**; VALENCIA, F.; LÓPEZ-GRANADOS, F. (2017). Principales variables para la detección de plántulas de amapola (*Papaver rhoeas*) en imágenes tomadas con un vehículo aéreo no tripulado. *XVI Congreso de la Sociedad Española de Malherbología-SEMh*, 25-27 Octubre, 2017. Pamplona, España. pp: 425-430.
6. JURADO-EXPÓSITO, M.; DE CASTRO, A.I.; TORRES-SÁNCHEZ, J.; **JIMÉNEZ-BRENES, F.M.**; LÓPEZ-GRANADOS, F. (2017). Optimización de la cartografía de malas hierbas mediante técnicas geoestadísticas y teledetección con UAV. *XVI Congreso de la Sociedad Española de Malherbología-SEMh*, 25-27 Octubre, 2017. Pamplona, España. pp: 419-424.
7. * **JIMÉNEZ-BRENES, F.M.**; LÓPEZ-GRANADOS, F.; TORRES-SÁNCHEZ, J.; DE CASTRO, A.I.; CASTILLO, N.; PEÑA, J.M. (2017). Cuantificación de la influencia de la poda sobre la arquitectura 3D del olivo mediante tecnología UAV. *Symposium Científico-Técnico en XVIII Feria Internacional del Aceite de Oliva e Industrias Afines - EXPOLIVA*, 10-12 de Mayo de 2017. Jaén, España.
8. * DE CASTRO, A.I.; PEÑA-BARRAGÁN, J.M.; TORRES-SÁNCHEZ, J.; **JIMÉNEZ-BRENES, F.M.**; VALENCIA, F.; LÓPEZ-GRANADOS, F. (2016). Detección de grama (*Cynodon dactylon*) en viña mediante imágenes adquiridas por un vehículo aéreo no tripulado (UAV). *II Jornadas del Grupo de Viticultura de la Sociedad Española de Ciencias Hortícolas-SECH*, 3 y 4 de Noviembre de 2016. Escuela Técnica Superior de Ingeniería Agronómica. Madrid. pp: 243-248.
9. * TORRES-SÁNCHEZ, J., LÓPEZ-GRANADOS, F.; DE CASTRO, A.I.; **JIMÉNEZ-BRENES, F.M.**; PEÑA-BARRAGÁN, J.M. (2016). Caracterización 3-D de viñas mediante imágenes procedentes de un vehículo aéreo no tripulado para el diseño de

tratamientos localizados. *II Jornadas del Grupo de Viticultura de la Sociedad Española de Ciencias Hortícolas (SECH)*, 3 y 4 de Noviembre de 2016. Escuela Técnica Superior de Ingeniería Agronómica. Madrid. pp: 267-272.

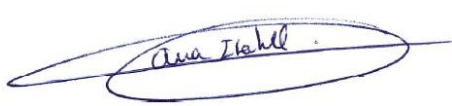
Por todo lo anterior, consideran que el trabajo realizado cumple los requisitos necesarios para su presentación y, en consecuencia, se autoriza la lectura y defensa públicas de la Tesis Doctoral.

Córdoba, 5 de Septiembre de 2019.

Firma de las Directoras



Fdo.: Dra. Francisca López Granados



Fdo.: Dra. Ana Isabel de Castro Megías



TÍTULO DE LA TESIS: Optimización del manejo de cultivos leñosos a través del análisis automatizado de imágenes obtenidas con vehículos aéreos no tripulados

DOCTORANDO: Francisco Manuel Jiménez Brenes

INFORME RAZONADO DEL TUTOR

Dr. ALFONSO GARCÍA-FERRER PORRAS, Catedrático del Departamento de Ingeniería Gráfica y Geomática de la Universidad de Córdoba y Responsable de la Línea de Investigación “Ingeniería Geomática y Agricultura de Precisión” del Programa de Doctorado “Ingeniería Agraria, Alimentaria, Forestal y de Desarrollo Rural Sostenible” de la Universidad de Córdoba,

INFORMA:

Que la investigación sobre “**Optimización del manejo de cultivos leñosos a través del análisis automatizado de imágenes obtenidas con vehículos aéreos no tripulados**” llevada a cabo por el Ingeniero de Montes D. Francisco Manuel Jiménez Brenes, bajo la dirección de la Dra. Francisca López Granados, Investigadora Científica-CSIC, y la Dra. Ana Isabel de Castro Megías, Investigadora Postdoctoral, ambas adscritas al Instituto de Agricultura Sostenible de Córdoba (IAS-CSIC), y la tutoría del que subscribe, ha sido desarrollada con éxito y alcanzado los objetivos inicialmente propuestos. Los resultados de la investigación realizada constituyen una aportación científica innovadora y relevante para el manejo de cultivos leñosos de forma eficiente, económica y sostenible en el contexto de la agricultura de precisión mediante la combinación de tecnología UAV, modelos tridimensionales a partir de técnicas fotogramétricas y desarrollo de procedimientos automáticos de análisis de imagen basados en OBIA.

En consecuencia, como tutor de la Tesis Doctoral que comprende dicha investigación, considero que puede ser presentada para su exposición y defensa públicas en la Universidad de Córdoba y ratifico la consideración favorable emitida por las Directoras de la Tesis Doctoral a tal efecto.

Por todo ello, se autoriza la presentación de la Tesis Doctoral.

Córdoba, 5 de Septiembre de 2019.

Firma del Tutor y Responsable de la Línea de Investigación
del Programa de Doctorado

GARCIA FERRER
PORRAS ALFONSO -
30417127H

 Firmado digitalmente por GARCIA FERRER PORRAS
ALFONSO - 30417127H
Nombre da reconocimiento (DNI): c=ES,
serialNumber=IDCES-30417127H,
givenName=ALFONSO, sn=GARCIA FERRER PORRAS,
cn=GARCIA FERRER PORRAS ALFONSO - 30417127H
Fecha: 2019.09.04 12:26:42 +02'00'

Fdo.: Dr. Alfonso García-Ferrer Porras

*Con especial cariño a mi hija,
Ana Jiménez Moyano,
por regalarnos diariamente su sonrisa y su luz*

Agradecimientos

En las siguientes líneas me gustaría dar las gracias a todas aquellas personas que de una u otra forma me han ayudado a llegar hasta aquí.

En primer lugar, doy las gracias a las Directoras de esta Tesis Doctoral ya que sin su ayuda no hubiese sido posible el desarrollo y conclusión de dicho trabajo. Me habéis transmitido la importancia del rigor científico y de los muestreos de campo, y me habéis enseñado a contestar las correcciones y sugerencias de los *referees*, una de las tareas más laboriosas de la actividad investigadora. Ante todo, gracias por la empatía e ilusión que transmitís al hacer cualquier cosa y por estar siempre dispuestas a ayudar; es un placer trabajar y aprender a vuestro lado:

- Dra. Francisca López Granados, Investigadora Científica del Instituto de Agricultura Sostenible (IAS) de Córdoba, centro perteneciente al Consejo Superior de Investigaciones Científicas (CSIC), y responsable del Grupo de Investigación “imaPing” al que pertenezco. Paquita, gracias por acogerme en tu grupo, por tus sabios consejos y por cuidarnos tanto.

- Dra. Ana Isabel de Castro Megías, Investigadora Postdoctoral en el Grupo “imaPing” (IAS-CSIC). Ana, gracias por tu amistad, paciencia y por tantos y buenos momentos.

Al Dr. José Manuel Peña Barragán, Científico Titular en el Instituto de Ciencias Agrarias de Madrid (ICA-CSIC), quien dirigió mi trabajo Fin de Máster y de este modo, mis inicios en investigación. Me gustaría destacar su amabilidad y atención constantes conmigo. Muchas gracias por todo, JM.

Al Dr. Alfonso García-Ferrer Porras, Catedrático de la Universidad de Córdoba, por haber sido el Tutor de esta Tesis Doctoral y mostrarme su disponibilidad y ayuda siempre que lo necesité.

Al Dr. Jorge Torres Sánchez, Investigador Postdoctoral en el Grupo imaPing, amigo, compañero de carrera y de trabajo. Han sido muchos los buenos momentos que hemos compartido juntos, esperando que sean muchos más. Muchas gracias por tu ayuda, ya que por estar sentado a mi lado has tenido que “sufrirme” en numerosas ocasiones dando respuesta a mis dudas. Gracias por estar siempre ahí.

Al resto de mis compañeros/as del Grupo imaPing: Amparo Torre, Angélica Serrano, Clara Bazzo, Irene Borra, Juanjo Caballero, María Pérez y Montse Jurado. Aunque algunos/as ya no trabajan en el Grupo ha sido un placer conocerlos/as y aprender de ellos/as. Nunca olvidaré los buenos ratos durante los trabajos de campo y esos viajes por la vasta geografía española en busca de parcelas para realizar los trabajos de campo.

A todos/as los/as investigadores/as que he conocido personalmente y con los/as que hemos colaborado durante esta etapa pertenecientes a las siguientes instituciones: Universidad de Córdoba, Universitat de Lleida, ICA-CSIC (Madrid), IFAPA de Cabra, Universidad Pública de Navarra, IFAPA Alameda del Obispo (Córdoba) y CAR-CSIC (Madrid). Gracias a todos por vuestra ayuda en los muestreos de campo y por los buenos ratos de camaradería que venían después.

A todos/as mis compañeros/as y profesores/as de Ingeniería de Montes de la Universidad de Córdoba e Ingeniería Técnica Forestal de la Universidad de Huelva. Gracias por todo lo que me habéis aportado.

A mis tíos/as, primos/as, amigos/as y profesores/as de mi pueblo, Arahal (Sevilla), ya que forjaron mi infancia y adolescencia, y con ello, una de las etapas más importantes de mi vida. Gracias a todos/as.

A mis suegros y cuñado, Miguel, Francisca y Alfonso, por toda su ayuda y por estar siempre ahí cuando lo necesito. En definitiva, a todos los integrantes de la familia “Moyano” y de la familia “García” por ser mi familia cordobesa. Gracias a todos por vuestro cariño.

A mi mujer Ana María Moyano García, quien está siempre a mi lado, animándome cuando lo necesito... Por su amor y por ser una madre ejemplar. Y a mi hija, mi otra Ana, a quien dedico especialmente esta Tesis y quien seguramente dentro de unos añitos estará leyendo todo esto. Gracias por todo a las dos.

Como la base de todo, doy las gracias a mis padres, Pepe y Pepa, porque gracias a su esfuerzo, ánimos y consejos he podido llegar hasta aquí. Muchas gracias por todo papá y mamá, sois un ejemplo para mí. También a María Dolores, mi hermana mayor, por haberme enseñado tantas cosas, por haberme ayudado tanto a lo largo de mi vida y por estar siempre pendiente de mí. Gracias, hermana.

No puedo olvidarme de los Proyectos “AGL2014-52465-C4-4-R”, “AGL2017-83325-C4-4-R” e Intramurales-CSIC “201640E025” y “201840E002” (IP: Dra. Francisca López Granados), ya que han aportado la financiación necesaria para el desarrollo de esta Tesis Doctoral.

Y aunque suene un poco raro también doy las gracias a mi guitarra flamenca, mi gran afición, la que me permite evadirme y desconectar de la rutina, con la que también me enfado y sonrío...

Francisco Manuel Jiménez Brenes

*“Necesitamos especialmente de la imaginación en las ciencias.
No todo es matemáticas y no todo es simple lógica,
también se trata de un poco de belleza y poesía”*

María Montessori

INDICE DE CONTENIDOS

Resumen	1
Summary	3
Prefacio	5

Capítulo 1. Introducción7

1. Historia de la Agricultura: Un Breve Recorrido.....9
2. Agricultura Sostenible.....10
3. Agricultura de Precisión.....12
4. Uso Sostenible de Fitosanitarios 14
5. Teledetección Aplicada a la Agricultura de Precisión 16
5.1. Definición y utilidad de la teledetección en agricultura.....16
5.2. Tipos de plataformas más frecuentes utilizadas en agricultura.....19
5.3. Principales características de los UAV23
5.4. Análisis de imágenes basado en objetos (OBIA)24
5.5. Cartografía de la estructura 3D de cultivos leñosos: del LiDAR terrestre al UAV27
5.6. Detección y cartografía de malas hierbas a través de tecnología UAV y OBIA.. 30
6. Objetivos de la Tesis Doctoral.....32
7. Referencias 35

Capítulo 2. Quantifying pruning impacts on olive tree architecture and annual canopy growth by using UAV-based 3D modelling51

1. Resumen 53
2. Abstract.....54
3. Introduction.....55
4. Results 58
4.1. Technological objectives: multi-temporal quantification of the tree 3D features (location, projected canopy area, tree height and crown volume) at the field scale58
4.2. Agronomic objectives: impact of every pruning treatment on the tree architecture, annual tree growth and tree restoration64
5. Discussion.....68
6. Conclusions.....70

7. Methods	71
7.1. Study area and description of the pruning treatments	71
7.2. Multi-temporal UAV flights and the generation of geo-spatial products	72
7.3. Object-based image analysis algorithm for computing the 3D tree features	75
7.4. Data analysis.....	79
8. Acknowledgements	79
9. References	79

Capítulo 3. 3-D characterization of vineyard using a novel UAV imagery-based OBIA procedure for precision viticulture applications **85**

1. Resumen	87
2. Abstract.....	87
3. Introduction.....	88
4. Materials and Methods.....	90
4.1. Study fields and UAV flights.....	90
4.2. DSM and orthomosaic generation.....	92
4.3. OBIA algorithm	93
4.4. Validation	97
4.4.1 <i>Grapevine classification and gap detection</i>	97
4.4.2 <i>Grapevine height</i>	99
5. Results and Discussion.....	99
5.1. Vine classification.....	99
5.2. Vine gap detection	101
5.3. Vine height quantification.....	102
5.4. Potential algorithm result applications	105
6. Conclusions.....	108
7. Acknowledgments	109
8. References	109

Capítulo 4. Automatic UAV-based detection of *Cynodon dactylon* for site-specific vineyard management..... **115**

1. Resumen	117
2. Abstract.....	117
3. Introduction.....	118
4. Materials and methods.....	120
4.1. Study sites description and UAV flights	120

4.2. Geomatic products generation	121
4.3. Ground truth data.....	123
4.4. Spectral analysis: optimum vegetation index	124
4.5. Image analysis: bermudagrass mapping.....	127
4.5.1 <i>OBIA algorithm</i>	127
4.5.2 <i>Bermudagrass map validation</i>	129
5. Results and Discussion.....	129
5.1. Spectral analysis: vegetation index selected	129
5.2. Image analysis	131
5.2.1 <i>Classified maps</i>	131
5.2.2 <i>Bermudagrass mapping accuracy</i>	134
5.2.3 <i>Site-specific weed management</i>	137
6. Conclusions.....	139
7. References	140
Capítulo 5. Conclusiones.....	149

INDICE DE TABLAS

Capítulo 2.

Table 1. A sample of the output dataset delivered by the customized OBIA algorithm.....	58
Table 2. Number and percentage of trees correctly photo-reconstructed on one of the three study dates (columns Date 1, Date 2 and Date 3) and on all the three study dates (column 1-2-3).	59
Table 3. Impact of tree pruning treatment on the tree architecture, when computed as the differences in the projected canopy area, tree height, and crown volume between dates 2 (after pruning) and 1 (before pruning).....	65
Table 4. Impact of tree pruning treatment on annual tree growth, computed as the differences of projected canopy area, tree height, and crown volume between the date 3 (1-year after pruning) and the date 2 (after pruning).....	66
Table 5. Impact of the tree pruning treatment on tree restoration, when computed as the differences in the canopy area, tree height, and crown volume between date 3 (1-year after pruning) and date 1 (before pruning).....	67

Capítulo 3.

Table 1. Main characteristics of the studied fields. Coordinates are in the WGS84, UTM zone 31N reference system	90
Table 2. Technical specifications of the imaging sensor on board the Unmanned Aerial Vehicle (UAV).....	91
Table 3. Processing parameters selected for Digital Surface Model (DSM) and orthomosaic generation procedure by Agisoft Photoscan software.	93
Table 4. Error matrix schema for validation of vineyard classification.....	98
Table 5. Classification statistics (Overall accuracy and Kappa index) obtained in confusion matrix at every location and date	99
Table 6. Results of the gap detection in vine rows. Percentages were calculated over the total length of gaps in the field	102
Table 7. A sample of the output data file delivered by the OBIA algorithm for vine of field A-September.....	106

Capítulo 4.

Table 1. Spectral vegetation indices and their equations used for both cameras	126
Table 2. Vegetation indices analyzed with the highest values of M-statistical obtained for each camera.....	130
Table 3. Classified area of grapevine, bermudagrass and bare soil obtained from the RGB and RGNIR images analyses at every location and year studied.....	133

Table 4. Classification statistics obtained in confusion matrix for each year, field and camera.....	135
Table 5. Omission error statistics obtained for each year and field using RGB camera....	136
Table 6. Herbicide saving obtained from herbicide application maps as affected by treatment thresholds for RGB imagery by year and field analyzed.....	139

INDICE DE FIGURAS

Capítulo 1.

Figura 1. Objetivos relativos a seguridad alimentaria (parte superior) y medioambientales (parte inferior) marcado para las próximas décadas. Los signos (+) y (-) indican si es necesario un aumento o reducción de la variable, respectivamente.	10
Figura 2. La sostenibilidad, en el centro, rodeada por sus tres principales objetivos.....	11
Figura 3. Curva de reflectancia espectral de la vegetación	18
Figura 4. Campo de algodón infestado de malas hierbas (algunos ejemplos en círculos rojos) en época temprana en el que se constata la similar respuesta espectral del cultivo y malas hierbas.....	20
Figura 5. Rodales de grama (<i>Cynodon dactylon</i>) (algunos ejemplos en círculos rojos) infestando un viñedo con cubiertas vegetales entre hileras de cepas.....	21
Figura 6. Rodales de grama (<i>Cynodon dactylon</i>) (algunos ejemplos en círculos rojos) infestando un viñedo en estado avanzado de crecimiento y sin cubierta vegetal entre hileras de cepas	21
Figura 7. Esquema comparativo de resoluciones espaciales medias conseguidas por aviones tripulados y no tripulados y capacidad para la obtención de modelos bidimensionales (2-D) y tridimensionales (3D) en un cultivo de olivar.	23
Figura 8. Relación entre los elementos a analizar en una imagen bajo distintas resoluciones espaciales: a) baja resolución: píxeles significativamente mayores que los elementos de interés, se necesitan técnicas de análisis basados en subpíxeles; b) resolución media: el tamaño de los píxeles y de los elementos a analizar es el mismo, por lo que serían apropiadas técnicas de análisis de píxel por píxel; c) alta resolución: los píxeles son significativamente más pequeños que los elementos a analizar, por lo que sería necesaria la regionalización de los píxeles en grupos de píxeles (objetos).....	25
Figura 9. a) Vista parcial de ortomosaico obtenido a partir de imágenes UAV al que se acopló una cámara RGB y correspondiente a una parcela de viñedo en espaldera; Diferentes segmentaciones del tipo multirresolución según distintos valores de escala (E) y homogeneidad (forma-F y compacidad-C): b) E= 50, F= 0,1 y C= 0,5; c) E= 200, F= 0,1 y C= 0,5; d) E= 50, F= 0,8 y C= 1; (e) E= 200, F= 0,8 y C= 1	26
Figura 10. Deriva y exceso de aplicación de producto fitosanitario en: a) almendro en seto, y b) viñedo en espaldera	28

Capítulo 2.

Figure 1. Graphical scheme of the stages and specific technological and agronomic objectives of this investigation	57
Figure 2. Four-level representation of the projected tree canopy areas as computed on the three study dates. The letters indicate the pruning treatments as follows: TP (traditional), AP (adapted), and MP (mechanical). In the axes, coordinate system UTM zone 30N, datum WGS84	61

Figure 3. Four-level representation of the tree heights as computed on the three study dates. The letters indicate the pruning treatments as follows: TP (traditional), AP (adapted), and MP (mechanical). In the axes, coordinate system UTM zone 30N, datum WGS84.....	62
Figure 4. Four-level representation of the tree crown volumes as computed on the three study dates. The letters indicate the pruning treatments as follows: TP (traditional), AP (adapted), and MP (mechanical). In the axes, coordinate system UTM zone 30N, datum WGS84	63
Figure 5. Four-level representation of the pruning impact on tree volume (differences in tree volume between dates 2 and 1). The letters indicate the pruning treatments as follows: TP (traditional), AP (adapted), and MP (mechanical). In the axes, coordinate system UTM zone 30N, datum WGS84.....	64
Figure 6. Four-level representation of the annual growth on tree volume after the pruning task (differences in tree volume between dates 3 and 2). The letters indicate the pruning treatments as follows: TP (traditional), AP (adapted), and MP (mechanical). In the axes, coordinate system UTM zone 30N, datum WGS84.	65
Figure 7. Four-level representation of the tree restoration in terms of volume (differences in tree volume between dates 3 and 1). The letters indicate the pruning treatments as follows: TP (traditional), AP (adapted), and MP (mechanical). In the axes, coordinate system UTM zone 30N, datum WGS84.....	67
Figure 8. Percentage of annual tree growth after pruning as affected by the pruning severity and type of pruning treatment. Lines over the columns indicate the standard deviations	68
Figure 9. Description of the three pruning treatments evaluated in this investigation.....	72
Figure 10. The quadcopter UAV and the Red-Green-Blue (RGB) camera used to acquire the remote images of the olive trees	73
Figure 11. A partial view of the 3-D point cloud for the olive grove studied in this investigation, which was produced by the photogrammetric processing of the remote images taken with the UAV	74
Figure 12. Flowchart of the OBIA algorithm developed in this investigation.....	76
Figure 13. Partial views of the primary OBIA algorithm outputs: a) the 4-band multi-layer file with the RGB (a1) and the DSM (a2) layers, showing the results of mechanical and adapted pruning as applied to the trees on the two top and bottom rows, respectively; b) chessboard segmentation output; c) the coarse classification of the tree (pink colour) and bare soil (white colour) objects based on the difference in DSM (height) values; d) the coarse classification of the tree borders (blue color); e) pixel-based segmentation of the tree borders; f) the fine classification of the tree (green colour) objects; and g) the tree and the bare-soil objects were joined with separately. As a result of the whole procedure, the algorithm computed the 3D tree geometric features (projected area, height and volume) and exported the values as vector and table files for further analysis.....	78

Capítulo 3.

-
- Figure 1.** Images of the studied fields at different growth stages: a) inter-row cover crop growing in Field C in July; b) the UAV flying over Field B; c) and d) comparison between the field situations (green cover crops, vines and bare soil) between July and September in Field B.....91
- Figure 2.** A partial view of the 3-D point cloud for the vineyard field A in July, which was produced by the photogrammetric processing of the remote images taken with the UAV.. 93
- Figure 3.** Flowchart and graphical examples of the Object Based Image Analysis (OBIA) procedure outputs for automatic vine characterization 96
- Figure 4.** Experimental set for validating the results: a) validation point grid in Field A on July; b) a vector squares used for classification validation (yellow points indicate the positions of 40 true height data, and the white square is the artificial target placed in the field); c) measurement of the vine height.....97
- Figure 5.** Example of 2 x 2 validation frame in field A-July: (a) manually classified orthomosaicked image (R-G-B composition); (b) DSM-OBIA-based classification 100
- Figure 6.** Graphic comparing DSM-OBIA estimated and vine height for all data corresponding to the three fields and both dates (July and September). The root mean square error (RMSE) and correlation coefficient (R^2) derived from the regression fit are included ($p < 0.0001$). The solid line is the fitted linear function and the pink dashed line represents the 1:1 line.103
- Figure 7.** DSM-OBIA detected height vs. measured vine height divided by field and date. The root mean square error (RMSE) derived from the regression fit are included ($p<0.0001$). The solid line is the fitted linear function and the pink dashed lines represent the 1:1 line.....104
- Figure 8.** Four-level representation of the estimated vine canopy volume as computed on the three fields in July, from left to right: From left to right: Field A, Field B and Field C. In the axes, coordinate system UTM zone 31 N, datum WGS84107
- Figure 9.** Height, area and volume values in two dates (July and September, corresponding to different growth stages) from the left side to the row. Every data corresponded to 0.10 m length segments of the vine row.108

Capítulo 4.

-
- Figure 1.** a) Quadcopter microdrone MD4-1000 with the Red-Green-Near Infrared (RGNIR) camera attached, flying over one of the vineyards and b) detail of an RGB-image taken by the UAV from field A-2017. The circles in blue color represent bermudagrass patches growing in the inter-rows.....121
- Figure 2.** RGNIR orthomosaic corresponding to field A-2016.....122
- Figure 3.** a) Placing and georeferencing the frames in field A-2017 and b) detail of a frame covering bermudagrass and bare soil classes. The individuals in this manuscript have given written informed consent (as outlined in PLoS consent form) to publish these case details.123

Figure 4. Detail of RGB-orthomosaic of field A-2017 showing: a) sampling frames covering bermudagrass and bare soil and b) manual classification of bermudagrass (green color) and bare soil (brown color) classes that made up the ground truth data.....	124
Figure 5. Several stages of the OBIA algorithm for an enlarged view belonging to field A-2016 and RGB camera. a) the RGB bands, b) the DSM of the orthomosaic, c) vine line classification (grapevines in green color and no-vineyard objects in white color), and d) classified map (grapevines in green color, bermudagrass patches in red color, and bare soil in yellow color)	128
Figure 6. Classified maps developed by the OBIA-algorithm using RGB-imagery for field A in: a) 2016 and b) 2017.....	132
Figure 7. Classified maps developed by the OBIA-algorithm using RGNIR-imagery for field A in: a) 2016 and b) 2017.....	133
Figure 8. Site-specific treatment maps for bermudagrass patches in field A-2016 according treatment thresholds: a) 0%, b) 2.5%, and c) 5%.....	138

RESUMEN

La actividad agrícola ha seguido un largo proceso de evolución y de intensificación para incrementar la producción de los cultivos y satisfacer la creciente demanda de alimentos, pienso y fibra. Las técnicas empleadas en agricultura durante la “Revolución Verde” (1960-1980) tuvieron como principal objetivo el aumento de la producción sin prestar especial atención a la calidad nutricional ni a la conservación de los recursos naturales, es decir, a la sostenibilidad de la actividad agrícola. A causa de ello, en las últimas décadas han surgido inconvenientes de diversa índole relacionados, entre otros, con la contaminación de acuíferos y la erosión de suelos, la reducción notable de biodiversidad y la aparición de resistencias y nuevas plagas, enfermedades y malas hierbas. La sensibilización y la preocupación de la sociedad por la conservación del medio ambiente han originado una búsqueda del equilibrio entre producción y sostenibilidad.

En este contexto, han surgido nuevas formas de agricultura sostenible entre las que destaca la Agricultura de Precisión, cuyo desarrollo se ve potenciado por la Digitalización de la Agricultura creándose un nuevo paradigma conocido como “Agricultura 4.0”. Una de las tecnologías con más proyección para este fin es la Teledetección, debido a la disponibilidad de nuevas plataformas para la adquisición de imágenes y al aumento del poder computacional de los equipos informáticos para el análisis de éstas. Ambos factores han permitido la aplicación de técnicas de análisis de imagen basado en objetos (OBIA) y aprendizaje automático, contribuyendo a resolver parte de las dificultades relacionadas con la adopción práctica de la Agricultura de Precisión. En esta Tesis Doctoral se han desarrollado un conjunto de trabajos mediante la combinación del uso de un vehículo aéreo no tripulado (UAV), modelos tridimensionales a partir de técnicas fotogramétricas y el desarrollo de procedimientos automáticos OBIA. El UAV fue equipado con sensores en distinto rangopectral para la adquisición de información de diferentes variables agronómicas y escenarios en el contexto de la agricultura de precisión.

A partir de lo anterior, la presente Tesis Doctoral se ha centrado en contribuir en la generación de conocimiento para la optimización del manejo de dos cultivos leñosos de gran relevancia agronómica y socioeconómica (olivar y viñedo) de manera eficiente, económica y sostenible, principalmente en cuanto al uso sostenible de fitosanitarios. Por un lado, se ha abordado la caracterización tridimensional de ambos cultivos para llevar a cabo una monitorización multitemporal de la arquitectura de cada uno de los olivos, o cepas (en el caso de viñedo), presentes en las parcelas analizadas para la cuantificación del crecimiento vegetativo en viñedo según diferentes fechas y distintas podas en olivar, y por otro, se ha puesto a punto una metodología para la detección y cartografía de la mala hierba gramínea y perenne, conocida como grama (*Cynodon dactylon* L.), cuya presencia en los viñedos de diferentes zonas geográficas del país está ocasionando serios problemas de competencia y control. Los resultados obtenidos ponen de manifiesto el potencial de la combinación UAV-OBIA para llevar a cabo estrategias de manejo localizado y contribuir a la Digitalización de la Agricultura. Además, con los ajustes oportunos, los algoritmos OBIA de análisis de imágenes UAV desarrollados podrían ser adaptables y transferibles a otros cultivos leñosos, ya sea para la caracterización tridimensional con otros objetivos como el fenotipado de variedades, o para la cartografía de otras malas hierbas problemáticas o de difícil control.

SUMMARY

The agricultural activity has followed a long process of evolution and intensification to increase crop production and meet the growing demand for food, feed and fiber. The techniques used in agriculture during the "Green Revolution" (1960-1980) had as their main objective the increase of production without paying special attention neither to the nutritional quality nor to the conservation of natural resources, i.e., to the sustainability of the agricultural activity. As a result, serious problems have arisen in last decades, including water pollution and soil erosion, a significant reduction in biodiversity and the emergence of resistances and new pests, diseases and weeds. Society's awareness and concern for environmental conservation have led to a search for a balance between production and sustainability.

In this context, new forms of sustainable agriculture have emerged, including Precision Agriculture, whose development is strengthened by the Digitalization of Agriculture creating a new paradigm known as "Agriculture 4.0". One of the technologies with more projection for this purpose is Remote Sensing due to the availability of new platforms for acquiring images and the increase in the computational power of computer equipment for their analysis. Both factors have allowed the application of object-based image analysis (OBIA) and automatic learning techniques, contributing to solve part of the difficulties related to the practical adoption of Precision Agriculture. In this Doctoral Thesis, a set of works have been developed by combining the use of an unmanned aerial vehicle (UAV), three-dimensional models based on photogrammetric techniques and the design of automatic OBIA procedures. The UAV was equipped with sensors in different spectral range for acquiring information of several agronomic variables and scenarios in the context of precision agriculture.

On this basis, this Doctoral Thesis has focused on contributing to the generation of knowledge for the optimization of the management of two woody crops of great agronomic and socioeconomic relevance (olive orchard and vineyard) in an efficient, economic and sustainable way, mainly in terms of sustainable use of phytosanitary applications. The three-dimensional characterization of both crops has been used to carry out a multitemporal monitoring of the architecture of each one of the olive trees or vines, present in the analyzed fields, for quantifying the vegetative growth in olive orchards according to different prunings and in vineyards, and on the other hand, a methodology has been developed for detecting and mapping bermudagrass (*Cynodon dactylon* L.), a perennial weed whose presence in vineyards of different geographical areas of the country is causing serious problems of competition and control. The results obtained show the potential of the UAV-OBIA combination to address site-specific management strategies and contribute to the Digitization of Agriculture. In addition, it is discussed that with the appropriate adjustments, the OBIA algorithms developed for analyzing the UAV images could be adaptable and transferable to other woody crops, either for three-dimensional characterization with other objectives such as the phenotyping of varieties, or for mapping other weeds difficult to control.

Prefacio

Los inicios de la agricultura datan del Neolítico (9.000 a.C.) surgiendo a lo largo del Creciente Fértil, entre los cursos de los ríos Tigris y Éufrates. En esa época, el ser humano abandona el nomadismo, se asienta en lugares concretos y se convierte en productor de sus alimentos por medio de la siembra de una amplia variedad de vegetales y de la recolección de frutos, semillas y raíces para consumo e incluso almacenaje. A partir de ese momento, la agricultura ha evolucionado enormemente pasando de técnicas rudimentarias al sistema actual de producción altamente tecnificado. A pesar de que el progreso ha sido constante, el cambio más relevante del desarrollo agrícola se produjo en el siglo XX (1960-1980) con la denominada “Revolución Verde”, promovida por el ingeniero agrónomo estadounidense Norman Borlaug (Premio Nobel de la Paz en 1970 por su lucha para prevenir el hambre en los países en vías de desarrollo). Esta agricultura se caracterizó por la utilización de nuevas variedades de cereales de alto rendimiento (principalmente trigo, maíz y arroz) y el uso generalizado de la mecanización y los agroquímicos, siendo su principal objetivo el aumento de la producción sin prestar especial atención a la calidad nutricional ni a la conservación de los recursos naturales, es decir, a la sostenibilidad de la actividad agrícola. A causa de ello, en las últimas décadas han surgido inconvenientes de diversa índole relacionados, entre otros, con la contaminación de acuíferos y la erosión de suelos, la reducción notable de biodiversidad y la aparición de resistencias y nuevas plagas, enfermedades y malas hierbas. Sin embargo, la sensibilización y la preocupación de la sociedad por la conservación del medio ambiente han originado una búsqueda del equilibrio entre producción y sostenibilidad, surgiendo nuevas tecnologías que están contribuyendo a avanzar en dicho objetivo. La presente Tesis Doctoral se encuadra en esa dirección y en el contexto de la agricultura de precisión, abordando nuevas herramientas que armonicen la productividad, la protección agroambiental y la rentabilidad económica de la actividad agraria.

Esta Tesis Doctoral cumple el requisito establecido por la Universidad de Córdoba para su presentación como compendio de artículos, consistente en un mínimo de 3 artículos publicados o aceptados en revistas incluidas en los tres primeros cuartiles de la relación de revistas del ámbito de la especialidad y referenciadas en la última relación publicada por el Journal Citation Reports (SCI y/o SSCI). Gran parte de la bibliografía citada en la Introducción (Capítulo 1) está recogida en los tres artículos (Capítulos 2, 3 y 4) que componen la Tesis con el fin de revisar los trabajos previos de los que parten los procedimientos desarrollados así como los resultados obtenidos. Además de estas citas, se han incorporado en dicho capítulo otras referencias recientes, fechadas en 2018 y 2019, que no fueron incluidas en las tres publicaciones de la Tesis, ya sea por restricciones de las editoriales en cuanto al número de páginas o a la cantidad admitida de referencias por artículo, o porque han sido publicadas después de los tres trabajos mencionados. Por ello, en el Capítulo 1 se ha llevado a cabo una revisión bibliográfica más completa y actualizada que en los trabajos que conforman esta Tesis Doctoral.

Capítulo 1

Introducción



1. Historia de la Agricultura: Un Breve Recorrido

La actividad agrícola ha seguido un largo proceso de evolución y de intensificación para incrementar la producción de los cultivos y satisfacer así la creciente demanda de alimentos, pienso y fibra (FAO, 2004). La Revolución Verde, corriente iniciada en la década de los 60s, trajo consigo cambios muy relevantes en la producción agrícola a nivel mundial, generando importantes transformaciones en la gestión de las parcelas agrícolas, como la aplicación de técnicas bioquímicas, de mejora genética y de ingeniería moderna para el incremento de los rendimientos. Este modelo productivo se centró en: i) uso masivo de nuevas variedades e híbridos de cereal de alto rendimiento obtenidos mediante mejora genética (principalmente trigo, arroz y maíz) en zonas de elevado potencial (García Olmedo, 1998; Gollin et al., 2005); ii) mecanización generalizada de las tareas agrícolas (laboreo, tratamientos agroquímicos); y iii) aplicación de insumos como fertilizantes de obtención industrial (de síntesis) y fitosanitarios (herbicidas, insecticidas y fungicidas). Estas técnicas consiguieron maximizar los rendimientos de los cultivos, siendo así posible satisfacer las necesidades alimentarias de gran parte de la población mundial teniendo en cuenta el crecimiento exponencial que ésta ha ido experimentando (según Naciones Unidas la población mundial creció de 2.600 a 6.000 millones de personas en el período 1950-1999, pudiendo alcanzar los 10.000 millones en 2050). Sin embargo, dichas técnicas no prestaban atención a la conservación de los recursos naturales, apareciendo problemas asociados tales como: i) encarecimiento de los agroquímicos (fertilizantes y fitosanitarios) y petróleo; ii) contaminación de las aguas subterráneas, sobreexplotación y aumento de la erosión del suelo y la desertificación; iii) aumento de la liberación de gases de efecto invernadero, pérdida de la diversidad genética de los cultivos, eutrofización de ríos, pantanos y otros sistemas acuíferos; y iv) aparición de especies de insectos-plaga, enfermedades y malas hierbas invasoras, resistentes y/o de difícil control, entre otros (Matson et al., 1997; Shaner & Beckie, 2014; Vitousek et al., 1997).

Para hacer frente a los problemas ocasionados por la agricultura productivista o convencional, gracias a la sensibilización de la población, en las últimas décadas se han desarrollado esfuerzos en la búsqueda de prácticas con menor coste medioambiental y sin una disminución sustancial en los rendimientos obtenidos, lo cual ha sido y será un enorme desafío dada la complejidad económica de la agricultura y sus sectores asociados (Figura 1).



Figura 1. Objetivos relativos a seguridad alimentaria (parte superior) y medioambientales (parte inferior) marcado para las próximas décadas. Los signos (+) y (-) indican si es necesario un aumento o reducción de la variable, respectivamente. Fuente: adaptada a partir de Atzberger (2013).

2. Agricultura Sostenible

Debido a los umbrales de insostenibilidad que alcanzaron los efectos de la agricultura convencional, a finales del siglo pasado surgió una nueva técnica de gestión alternativa conocida como **Agricultura Sostenible**. Han sido muchos los autores y organizaciones a nivel internacional que han dado su propia definición del concepto agricultura sostenible. Mientras que algunos hablan de la capacidad de los sistemas agrarios para mantener su productividad a lo largo del tiempo (Ikerd, 1993), otros la consideran como el conjunto de estrategias de manejo para abordar las principales preocupaciones de la sociedad sobre la calidad de los alimentos o la protección del medio ambiente (Francis, 1987). Otros autores se centran en la flexibilidad o capacidad de adaptación de la agricultura para ajustarse a los cambios futuros (Gafsi et al., 2006). No obstante, todos coinciden en que los sistemas agrarios son sostenibles si se mantienen durante un largo período de tiempo, es decir, si son económicamente viables, ambientalmente seguros y socialmente justos (Lichtfouse et al., 2009) (Figura 2).

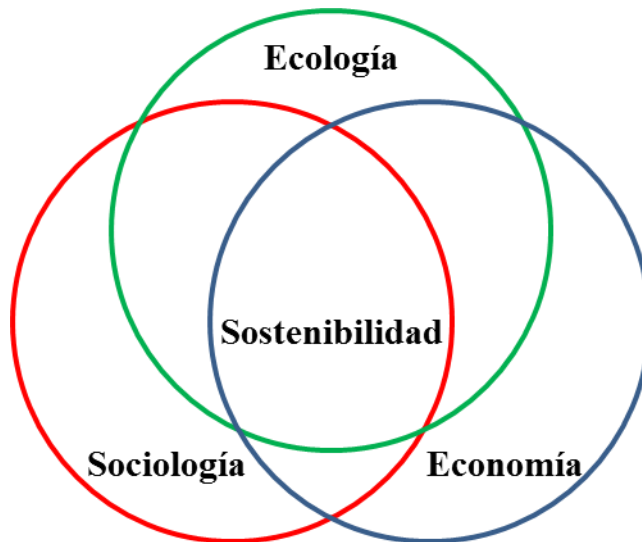


Figura 2. La sostenibilidad, en el centro, rodeada por sus tres principales objetivos. Fuente: adaptada a partir de Bongiovanni & Lowenberg-Deboer (2004).

Entre los sistemas de producción agrícola sostenible se encuentran las técnicas de manejo contempladas en la **Agricultura de Conservación** (García-Torres et al., 2003; Knowler & Bradshaw, 2007). Según la FAO, esta agricultura tiene como objetivo conservar, mejorar y hacer un uso más eficiente de los recursos naturales que sustentan la agricultura (suelo, agua, biodiversidad y atmósfera), contribuyendo a un aumento de los rendimientos utilizando técnicas que incluyen principalmente producción integrada, no-laboreo, mínimo laboreo y siembra directa. La finalidad es mantener una cobertura vegetal permanente de los suelos agrícolas, una mínima alteración mecánica de éstos y la diversificación de especies vegetales a través de una rotación de cultivos adecuada. Todos ellos representan los tres principios de la agricultura de conservación. En definitiva, este sistema agrícola potencia la biodiversidad y los procesos biológicos edáficos del suelo, lo cual contribuye a un mayor aprovechamiento del agua, reducir la erosión y una mayor eficiencia en el uso de nutrientes, así como a la mejora y sostenibilidad de la producción de cultivos.

Por otro lado, la **Agricultura Ecológica** u *Organic Agriculture*, en inglés, constituye otro tipo de agricultura sostenible, diferenciándose principalmente de la agricultura convencional por no emplear agroquímicos de síntesis en la producción de cultivos (Bengtsson et al., 2005). Diferentes investigaciones han puesto de manifiesto que las prácticas desarrolladas en la agricultura ecológica generan una menor lixiviación de nutrientes y un mayor almacenamiento de carbono (Drinkwater et al., 1995), así como una menor erosión (Reganold et al., 1987) y concentración de niveles de fitosanitarios en los sistemas hídricos (Maeder et al., 2002). Además, este tipo de agricultura ha demostrado aumentar la biodiversidad de los paisajes agrícolas (Paoletti et al., 1992). Sin embargo, y aunque existe un claro aumento de la superficie cultivada siguiendo estas técnicas para

surtir a un sector de mercado y población que prefieren su consumo (en el caso de Andalucía ha evolucionado de 100.000 a 1.000.000 de hectáreas en el período 2001-2015, Junta de Andalucía (2016)), entre sus inconvenientes está su limitada capacidad de producir alimentos (ej.: cereales como trigo, maíz, arroz) a escala mundial.

De entre los sistemas posibles de producción de agricultura sostenible, la conocida como **Agricultura de Precisión**, se está consolidando como uno de sus pilares fundamentales.

3. Agricultura de Precisión

La Agricultura de Precisión (AP) es una técnica de gestión de parcelas agrícolas basada en la variabilidad existente en las mismas y el manejo localizado de inputs (en inglés *Precision Agriculture* o *Site-Specific Management SSM*), que se desarrolló a finales del siglo XX paralelamente a grandes avances tecnológicos. Estas técnicas abordan el sistema agrario de una forma global para alcanzar una agricultura de alta eficiencia, sostenibilidad y de bajos insumos (Shibusawa, 1998), cuyo objetivo es reducir costes, optimizar la producción agrícola, aumentar la rentabilidad para los productores y obtener beneficios ecológicos y ambientales (Robert, 2002).

La variabilidad espacial y temporal intra-parcelaria de los factores implicados en el crecimiento y desarrollo de un cultivo ha sido siempre un hecho conocido por todos los actores involucrados en la actividad agrícola (agricultores, investigadores, empresas del sector), aceptando que una misma parcela presentara diferencias entre zonas en cuanto a rendimiento, presencia de malas hierbas, enfermedades o plagas, estado nutricional o estructura foliar, en cuyo caso estas diferencias pueden apreciarse a nivel individuo (árbol o cepa de viñedo) cuando se trata de cultivos leñosos. No obstante, esta variabilidad no había podido ser cartografiada debido a la carencia de herramientas tecnológicas que pudieran localizar y cuantificar dicha variabilidad. La emergencia de nuevas tecnologías en las últimas décadas del siglo XX, entre las que destacan: i) desarrollo de tecnologías informáticas (hardware y software), geoespaciales y de la información (sistemas de posicionamiento global, GPS; sistemas de información geográfica, SIG); ii) sensores y controladores de maquinaria agrícola; y iii) sistemas de teledetección de alta resolución espacial, hace posible el desarrollo de la AP, resultando ser una de las diez revoluciones con mayor impacto en agricultura permitiendo la generación de conocimiento para el manejo de precisión de las explotaciones agrarias (Crookston, 2006; Mulla, 2013). La creación de los Congresos Internacional y Europeo de Agricultura de Precisión y de la revista **Precision Agriculture** (revista científica con más impacto de su área) indica que el

progreso de este tipo de agricultura es imparable y que se genera abundante investigación internacional de calidad en las numerosas áreas que abarca el manejo localizado de los cultivos.

Como se ha mencionado, la AP persigue la eficiencia agrícola estudiando y cuantificando la variabilidad intrínseca de los factores implicados en el rendimiento de los cultivos, presentándose la Tecnología Digital como una de las herramientas más potentes y robustas para obtener y analizar dicha información. Ello permite una mejora de la productividad del cultivo y por lo tanto, un aumento de la rentabilidad obtenida gracias a una gestión optimizada de los insumos agrícolas y una mayor protección del medio ambiente (Tian, 2002). De este modo, la agricultura sostenible y la AP están íntimamente relacionadas, representando esta última un cambio de paradigma en las prácticas agrícolas al modular las actuaciones según las necesidades de cada parcela, en contraposición con el manejo uniforme llevado a cabo en la agricultura convencional (Aubert et al., 2012).

No obstante, y aunque la información publicada es numerosa y variada, la práctica real de la AP es aún limitada. Con el fin de estudiar los progresos en SSM, Paustian & Theuvsen (2017) estudiaron qué factores afectan la adopción o no de estas técnicas en Alemania. Los resultados fueron que, de 227 agricultores, 68 implementaban SSM, siendo los agricultores jóvenes (25-34 años) con formación (ingeniero técnico) y con experiencia (al menos 5 años al frente de una explotación) los más receptivos a los cambios tecnológicos para emprender estas prácticas agrícolas. Lindblom et al. (2017) identificaron en Suecia “*el problema de la implementación*”, entendido como la diferencia entre las decisiones apoyadas en el conocimiento científico y las basadas en el conocimiento tácito del agricultor y sus necesidades reales. Estos autores argumentan que la adopción de SSM está influenciada por: i) elevada complejidad de las operaciones e insuficiente conocimiento de los usuarios; ii) escasa adaptación de los programas informáticos a las condiciones concretas de su cultivo; iii) carencia de incentivos económicos de instituciones públicas para aprender nuevas técnicas; iv) falta de compromiso por mejorar sus explotaciones; y v) recelo a que una vez que deciden adoptar estas técnicas, falte un interlocutor técnico que los aconseje (ej.: sustitución del técnico inicial por parte de la empresa que le suministró equipos caros y de cierta complejidad). Aunque algunas de estas causas están muy arraigadas, sugieren una serie de soluciones para que el empresario agrícola las considere: i) formarse en tecnologías de la información, integrarse en consorcios para proyectos de investigación o de transferencia, interaccionar con otros agricultores para compartir gastos y conocimientos así como asistir a jornadas de demostraciones en campo; ii) aspirar a profesionalizar su actividad agrícola y no considerarla como una actividad menor y tradicional; y iii) empezar con pequeñas actuaciones y estudiar resultados.

En la actualidad, el sector está inmerso en un nuevo paradigma, conocido como **Agricultura 4.0**, que persigue la **Transformación Digital** de la actividad agrícola aplicando un conjunto de tecnologías digitales como: i) análisis de grandes cantidades de datos (*Big Data, Machine Learning*); ii) computación en la nube (*Cloud Computing*); iii) internet de las cosas (*Internet of Things –IoT*); y iv) teledetección y nuevas plataformas, automatización, sensores, redes y robótica (Taylor, 2018). Todo ello contribuye a la Digitalización de la agricultura y se presenta como una de las **prioridades de la política europea de I+D+i para los próximos años**, estando incorporada a la Política Agraria Común (PAC) a través de uno de sus objetivos *transversales* cuya finalidad es “*modernizar el sector a través del fomento y la puesta en común del conocimiento, la innovación y la digitalización en las zonas agrícolas y rurales*” (Comisión Europea, 2018). Entre las nuevas tecnologías, destaca la **teledetección**, que se presenta como una de las herramientas con mayor contribución para resolver las dificultades para la adopción generalizada de la AP por parte de los agricultores, impulsando así la implementación de estrategias de AP para mejorar la competitividad y la sostenibilidad del sector (JRC-EC, 2014). Recientemente, Annosi et al. (2019) han analizado el grado de acogida e implementación de la tecnología digital 4.0 en pequeños y medianos empresarios agrícolas en Italia en función de las diferentes tecnologías disponibles (riego inteligente, vehículos aéreos no tripulados, software para análisis de datos, sistemas para monitorizar condiciones edáficas e incidencias en el cultivo) concluyendo que aunque la adopción es lenta, tiene aún un amplio recorrido dado que conlleva la adaptación a procesos complejos.

4. Uso Sostenible de Fitosanitarios

La agricultura actual requiere un alto consumo de fitosanitarios como herramienta esencial para mantener las necesidades de calidad y cantidad que demanda la población. Estos productos fitosanitarios incluyen principalmente herbicidas, insecticidas y fungicidas, y supusieron para España (el país europeo que más productos fitosanitarios consume) un gasto de 859 millones de euros en el período 2011-2015 (AEPLA, 2016). Ello no solo genera un elevado gasto de los productos, sino también el coste inherente a las aplicaciones relacionado con combustible, maquinaria y mano de obra. Todo ello ha originado una sensibilización y preocupación medioambiental y económica en la sociedad, y en distintos ámbitos administrativos, que se han movilizado para minimizar el impacto del uso de los fitosanitarios a través de diferentes legislaciones. Así, la Comisión Europea publicó el **Reglamento (CE) 1107/2009** para la **Comercialización de Productos Fitosanitarios** dentro del cual se definió la **Directiva 2009/128/CE** para el **Uso Sostenible de Plaguicidas** que recoge legislación específica para su utilización. En ella se destacan como elementos clave “*el fomento del bajo consumo (reducción de las*

aplicaciones) y la utilización de dosis adecuadas y ajustadas de fitosanitarios”, elementos incluidos en el fundamento agronómico de la Agricultura de Precisión. Esta Directiva fue traspuesta al **Real Decreto 1311/2012** (BOE nº 223) en el que se establece **el marco de actuación** para conseguir **un uso sostenible de los productos fitosanitarios**, lo que permite también disminuir el uso de energía. En este Real Decreto se recoge la importancia de reducir en la medida de lo posible la dependencia del empleo de estos productos con el objetivo de minimizar los riesgos potenciales y sus efectos de su uso sobre la salud humana y el medio ambiente. Para ello, se propone el fomento de la gestión integrada y de planteamientos o técnicas alternativas, como los métodos no químicos para el control de insectos-plaga, enfermedades y malas hierbas. Para aportar soluciones a lo anteriormente expuesto, esta **Tesis Doctoral se enmarca en la optimización del uso de herbicidas y de fitosanitarios foliares en cultivos leñosos**.

Existen 4 pasos fundamentales para la aplicación de estrategias de manejo localizado de malas hierbas y fitosanitarios foliares de los cultivos: i) percepción y monitorización para localizar e identificar la incidencia (ej.: malas hierbas, enfermedades foliares) por medio de muestreos *in-situ* o con técnicas de detección; ii) toma de decisiones y planificación de la actuación (qué aplicar, cómo, cuándo y dónde); iii) actuación en campo o ejecución de SSW; y iv) evaluación de la rentabilidad económica y medioambiental de las operaciones realizadas en campo para programar acciones el año siguiente (Fernández-Quintanilla et al., 2018; López-Granados, 2011; Srinivasan, 2006). En los últimos años se ha avanzado en los pasos ii) y iii) del ciclo anterior, de tal forma que hay maquinaria agronómica disponible para realizar con éxito, tanto aplicaciones localizadas de herbicidas, como pulverizaciones de precisión dirigidas al dosel vegetal del cultivo. Sin embargo, el paso i), es decir, la monitorización de las malas hierbas en los cultivos y la obtención de información tridimensional de la copa de cada árbol en cultivos leñosos, constituyen dos componentes críticos para la adopción de SSM y están identificados a nivel empresarial y científico como el principal cuello de botella de esta estrategia de gestión (Paustian & Theuvsen, 2017).

Con relación a la gestión sostenible de productos fitosanitarios en agricultura, se han logrado avances considerables en la reducción de la aplicación de estos productos utilizando tecnologías de aplicación variable (*Variable Technologies-VT*, en inglés). Rosell & Sanz, (2012) revisaron las diferentes metodologías que permiten la **caracterización 3D de cultivos** frutales y viñedo para su aplicación en **tratamientos inteligentes de fitosanitarios foliares** para la optimización de su uso según tamaño de copa. Más recientemente, Miranda-Fuentes et al. (2016) obtuvieron la reducción del uso de fitosanitarios mediante aplicaciones ajustadas al volumen y estructura de la copa en olivar. En la sección 5.5, así como en los **capítulos 2 y 3 de esta Tesis**, se incluye una revisión bibliográfica sobre el estado actual de la **cartografía 3D de cultivos leñosos para aplicaciones variables de fitosanitarios**.

Referente al **control localizado de malas hierbas** con el fin de reducir el uso de herbicidas u otras prácticas agrícolas que requieren gasto de combustible y de mano de obra, la sección 5.6 y el **capítulo 4 de esta Tesis** contienen una revisión sobre el estado actual de la detección y cartografía de malas hierbas y la optimización de su control mediante el diseño de mapas de aplicaciones localizadas. Abundando en lo anterior, en Fernández-Quintanilla et al. (2018) se recogen los trabajos más recientes sobre esta línea de investigación, detallando los ahorros herbicidas alcanzados en los principales cultivos y discutiendo las limitaciones y oportunidades de los diferentes métodos y equipos empleados, tanto remotos como próximos, para monitorizar la presencia de malas hierbas en los cultivos así como los desafíos pendientes de resolver.

A modo de resumen, se indica que los **capítulos 2 y 3** de esta **Tesis Doctoral** presentan una serie de procedimientos y técnicas que se han desarrollado con el fin de obtener resultados de alta precisión sobre la **caracterización 3D de cada olivo y cada cepa en parcelas de olivar y viñedo**, respectivamente, mientras que en el **capítulo 4** se **aborda la detección y manejo localizado de malas hierbas, concretamente la especie Cynodon dactylon L. (grama) en viñedo**. Según lo indicado anteriormente, en cada uno de los capítulos se expone una revisión bibliográfica exhaustiva de las líneas de investigación desarrolladas. Es relevante resaltar que el conjunto tecnológico propuesto sería potencialmente extrapolable a otros cultivos y escenarios similares con los correspondientes ajustes.

Como se ha mencionado en el epígrafe anterior, la **Teledetección** se presenta como una de las herramientas más útiles y eficaces para implementar estrategias de manejo localizado (Thorp & Tian, 2004). Para la consecución de los trabajos que se proponen en esta Tesis se utiliza esta tecnología, por lo que en los apartados siguientes se describen brevemente los aspectos fundamentales de la misma.

5. Teledetección Aplicada a la Agricultura de Precisión

5.1. Definición y utilidad de la teledetección en agricultura

El concepto de teledetección ha sido ampliamente definido como la tecnología que se ocupa de obtener e interpretar información sobre un objeto, área o fenómeno obtenida por sensores que no están en contacto con el objeto de observación (Jensen, 2007). La interacción de la radiación electromagnética incidente con la vegetación o el suelo constituye la base de las aplicaciones de teledetección en agricultura. Específicamente, la teledetección comprende la medición de la radiación reflejada por el agua o por cualquier objeto presente en la superficie de la tierra (Mulla, 2013). En el caso de los cultivos, la

radiación reflejada por la planta, o curva de reflectancia, varía en función de la longitud de onda de la radiación incidente y está directamente relacionada con sus características fenológicas, fisiológicas y morfológicas (Schmidt & Skidmore, 2003), especialmente con el contenido de pigmentos fotosintéticos presentes en la hoja. En la Figura 3 se muestran las distintas longitudes de onda del espectro electromagnético en las que se pueden estudiar diferentes aspectos relacionados con el cultivo (pigmentos foliares, estructura foliar, contenido hídrico, entre otros). Los contrastes en el comportamiento de la radiación reflejada en diferentes longitudes de onda han motivado el desarrollo de índices espetrales, que son ratios o combinaciones matemáticas de los valores de reflectancia en las distintas regiones del espectro y que permiten mejorar la evaluación de los atributos o incidencias en el cultivo (estructura foliar, contenido en clorofila, índice de área foliar, presencia de malas hierbas o enfermedades, etc.) (Mulla, 2013).

El amplio uso de la teledetección se ha visto motivado por una gran cantidad de ventajas, entre las que cabe destacar: i) es un método no destructivo para recopilar información sobre las características de la Tierra mediante el análisis de las imágenes remotas; ii) los datos pueden obtenerse de forma sistemática en zonas geográficas extensas, en lugar de limitarse a observaciones puntuales e inaccesibles para la exploración humana y además, permite eliminar el sesgo de muestreo; y iii) proporciona información biofísica fundamental que puede ser utilizada en diversas áreas del conocimiento (Liaghat & Balasundram, 2010). Hoy en día, la teledetección se aplica en numerosos campos de estudio, como: astronomía, ingeniería y arquitectura civil, monitorización de catástrofes o incidencias naturales y medioambientales, calidad y control de productos industriales, y agronomía, entre otras. En este último caso, permite obtener información precisa y en el momento oportuno de grandes áreas de cultivo. En el ámbito que nos ocupa en esta Tesis Doctoral y como se detallará en los siguientes apartados, han sido numerosos los autores que han puesto de manifiesto el gran impacto que el análisis de las imágenes adquiridas por las distintas plataformas remotas está teniendo en el sector agrario y en el SSM, en particular. Instituciones como la FAO o la Comisión Europea a través de la próxima PAC (2021-2027) recalcan la necesidad de utilizar técnicas de teledetección en agricultura ya que facilitan el seguimiento y monitorización de las actividades agrícolas, que se podrían resumir en: i) la estacionalidad del desarrollo de los cultivos que puede verse perturbado por los efectos del cambio climático (ej.: subida de las temperaturas); y ii) evaluar el rendimiento potencial esperado y que puede verse afectado por factores abióticos (ej.: estreses hídrico o nutricional) y bióticos (ej.: presencia malas hierbas, enfermedades, insectos-plaga). Por lo tanto, la gran ventaja de la teledetección es que permite cartografiar o monitorizar todas estas variables tan cambiantes espacio-temporalmente (Atzberger, 2013) y de las que, de otra manera, sería muy complicado obtener la información necesaria

en grandes superficies y en poca cantidad de tiempo para solventar el problema agronómico.

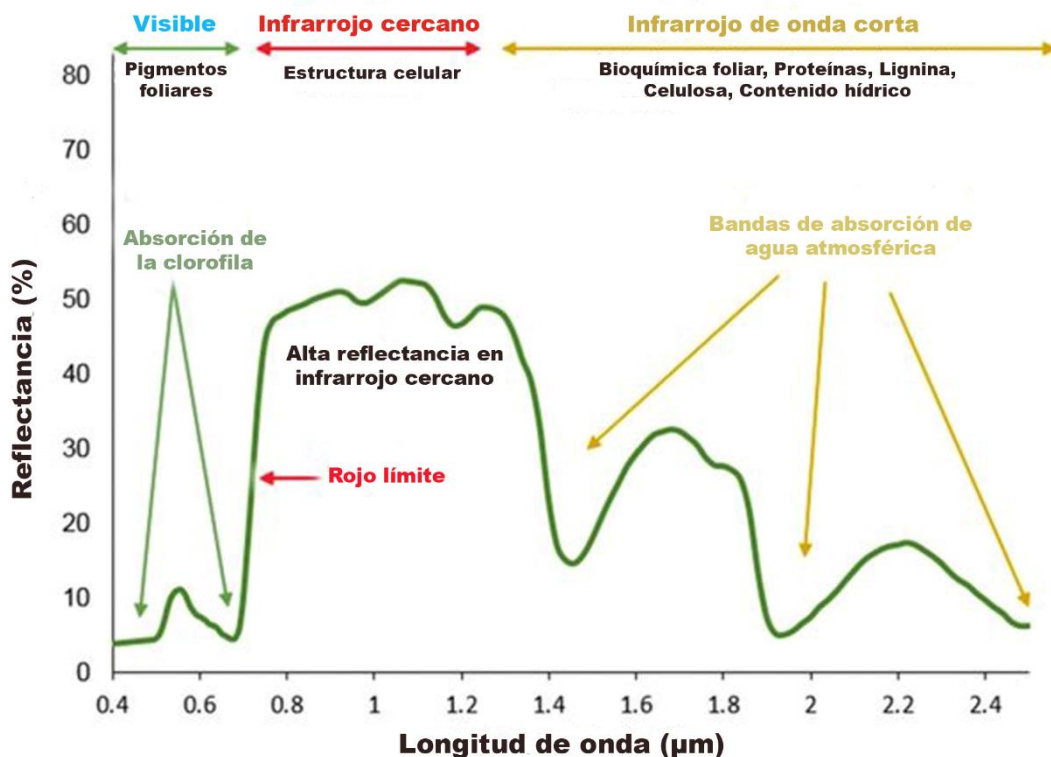


Figura 3. Curva de reflectancia espectral de la vegetación. Fuente: adaptada a partir de Roman & Ursu (2016).

Entre las aplicaciones de teledetección en agricultura de precisión pueden destacarse las relativas a estudios de cartografía de infestaciones de malas hierbas en cultivos (López-Granados, 2011; Peña et al., 2015), caracterización tridimensional (3D) de cultivos leñosos (Ribeiro et al., 2017; Torres-Sánchez et al., 2015), evaluación del desarrollo fenológico de cultivos (Lausch et al., 2015; Ostos-Garrido et al., 2019), monitorización del vigor vegetativo y estrés hídrico (Bandyopadhyay et al., 2017; Gago et al., 2015), detección de enfermedades (Abdulridha et al., 2018; de Castro et al., 2015), estimaciones de biomasa y rendimiento de los cultivos (Wang et al., 2016; You et al., 2017), cálculo de las superficies de cultivo (Ambika et al., 2016; Mosleh et al., 2015) y cartografía de los cambios de usos de suelo (Lark et al., 2017; Yalew et al., 2016). En los **capítulos 2, 3 y 4 de** esta Tesis Doctoral se abordarán las dos primeras aplicaciones citadas anteriormente: caracterización 3D y detección de malas hierbas en cultivos leñosos.

5.2. Tipos de plataformas más frecuentes utilizadas en agricultura

El uso de la teledetección en agricultura se remonta a 1929, año en que se usó la fotografía aérea analógica para cartografiar los recursos del suelo (Seelan et al., 2003). A partir de entonces y dependiendo de los objetivos o necesidades de cada estudio, se han utilizado diferentes tipos de plataformas de teledetección: remotas (*espaciales o aéreas*) y próximas (*vehículos o estructuras terrestres*) (López-Granados, 2011). En este apartado sólo se presentan las distintas plataformas remotas más empleadas en agricultura.

Los **satélites** son plataformas espaciales ampliamente usadas en agricultura desde 1972, año en que se lanzó Landsat 1. Los sensores de escáner multiespectral de Landsat 1 captaban información en las bandas espectrales del verde, rojo y en dos bandas del infrarrojo cercano (NIR: *Near infrared*), con una resolución espacial de 80 metros y una frecuencia de revisita de 18 días. Bauer & Cipra (1973) usaron las imágenes de Landsat 1 para clasificar paisajes agrícolas del medio oeste estadounidense en campos de maíz o soja obteniendo una precisión global del 83%. Debido a la limitada resolución espacial de Landsat y a los elevados requerimientos de ésta en agricultura de precisión, en 1999 se lanzó el satélite IKONOS, que proporcionaba imágenes con una resolución espacial de 4 metros en las bandas azul, verde, rojo y NIR, y una frecuencia de revisita de 5 días. Las imágenes de este satélite fueron usadas por Seelan et al. (2003) para estudiar la eficiencia de fungicidas en trigo y deficiencias de nitrógeno en remolacha azucarera. Los avances en la tecnología espacial permitieron lanzar en 2001 el satélite QuickBird, con una resolución espacial de 0,6 a 2,4 metros y una frecuencia de revisita de 1 a 3 días. Las imágenes QuickBird han sido utilizadas para realizar estimaciones de área cultivada, número de olivos, marcos de plantación y predicción de producción (García Torres et al., 2008) y cartografiar rodales de malas hierbas crucíferas en estado fenológico tardío en más de 260 campos de cultivo de trigo (de Castro et al., 2013). A estos satélites les siguieron otros, apareciendo en 2015 el satélite Sentinel-2 (revisita 5 días, desde 10 m de resolución espacial, espectro visible+infrarrojo cercano+infrarrojo de onda corta), que se está utilizando para monitorización de sistemas de cultivo para fines agrícolas y estudiar las interacciones socioeconómicas y medioambientales en zonas rurales (Bégué et al., 2018). A pesar de los trabajos mencionados anteriormente, la resolución espacial y la limitada revisita que presentan no son suficientes para generar la información de detalle y a tiempo que requiere la cartografía para determinadas aplicaciones de agricultura de precisión, como son la detección de malas hierbas cuando su comportamiento spectral es similar al del cultivo (ej.: estado fenológico temprano) o la caracterización 3D de cada individuo (árbol o cepa de viñedo) en cultivos leñosos.

Por otro lado, a diferencia de los satélites, las **plataformas aéreas tripuladas** con sensores a bordo pueden operar bajo la cubierta de nubes pudiendo ofrecer imágenes con

una resolución espacial mucho mayor. Los sistemas aerotransportados están disponibles prácticamente en todo el mundo y se han utilizado desde hace décadas para numerosos objetivos en aplicaciones forestales y de cobertura y uso de la tierra (Chen et al., 2002; Coulter et al., 2000; Franklin, 2001). En agricultura de precisión también se han utilizado con éxito en la detección de malas hierbas en estado fenológico tardío (floración o inicio senescencia), tanto en cultivos de trigo como girasol, mediante el análisis de imágenes de 40 cm de píxel (López-Granados et al., 2006; Peña-Barragán et al., 2007) y en la detección temprana de infestaciones del hongo *Raffaelea lauricola* en aguacate en imágenes de 15 cm de píxel (de Castro et al., 2015). Sin embargo, para lograr discriminar y cartografiar otro tipo de factores que también afectan al rendimiento de los cultivos, se necesita contar con información de mayor detalle y en momentos críticos del crecimiento del cultivo, aportando herramientas que ayuden a decidir la actuación a realizar en el momento óptimo. Por ejemplo, el control de malas hierbas en cultivos herbáceos y en post-emergencia temprana tiene una ventana de acción muy reducida ya que debe realizarse cuando cultivo y mala hierba se encuentran en fase fenológica temprana (desde el estado de plántula a 2-6 hojas verdaderas). Por tanto, la detección debe realizarse en ese momento fenológico cuando además existe una gran similitud espectral entre cultivo y mala hierba (Fernández-Quintanilla et al., 2018; López-Granados, 2011) (Figura 4).



Figura 4. Campo de algodón infestado de malas hierbas (algunos ejemplos en círculos rojos) en época temprana en el que se constata la similar respuesta espectral del cultivo y malas hierbas. Fuente: grupo imaPing.

Una situación análoga se presenta cuando una especie de mala hierba emerge en un cultivo leñoso y, dependiendo de su ciclo fenológico, puede presentar similitud espectral bien con el suelo desnudo (Figura 5), bien con el cultivo (Figura 6), como es el caso de las

infestaciones de grama (*Cynodon dactylon*) en viñedo, dificultándose en ambos escenarios su detección y cartografía.



Figura 5. Rodales de grama (*Cynodon dactylon*) (algunos ejemplos en círculos rojos) infestando un viñedo con cubiertas vegetales entre hileras de cepas. Se observa la similitud espectral de dichos rodales con la cubierta vegetal, restos vegetales (ej.: poda) y suelo desnudo. Fuente: grupo imaPing.



Figura 6. Rodales de grama (*Cynodon dactylon*) (algunos ejemplos en círculos rojos) infestando un viñedo en estado avanzado de crecimiento y sin cubierta vegetal entre hileras de cepas. Se puede comprobar que los rodales de grama y el dosel de las cepas guardan un comportamiento espectral similar. Fuente: grupo imaPing.

En las situaciones agronómicas mencionadas, son necesarias imágenes de mayor resolución espacial (ej.: píxel < 5 cm) a las generadas con aviones tripulados, de lo contrario no es posible abordar estos objetivos agronómicos. Además, a esta carencia hay que añadir que el uso limitado de los aviones tripulados en agricultura de precisión se debe también a la complejidad operacional (necesidad de aeropuertos cerca de los cultivos a estudiar, necesidad de contratar el servicio con días de antelación), elevados costes y desfases o retrasos en la entrega de las imágenes tomadas (Rango et al., 2009; Zhang et al., 2006).

Desde hace unos años, la disponibilidad de **plataformas aéreas no tripuladas, drones, o UAV** (por sus siglas en inglés de *Unmanned Aerial Vehicles*) y los continuos avances en miniaturización, precisión, flexibilidad y reducción de costes de los sensores han ofrecido al sector una poderosa herramienta capaz de llevar a cabo estudios con gran nivel de detalle en agricultura de precisión (Torres-Sánchez et al., 2013; Zhang & Kovacs, 2012), fenotipado de variedades de cultivos herbáceos y de leñosos en programas de mejora (Yang et al., 2017) o reconstrucción 3D de cultivos (Colomina & Molina, 2014; Nex & Remondino, 2014). Las citas anteriores son revisiones bibliográficas y en ellas se recogen numerosos trabajos en los se pone de manifiesto cómo la utilización de imágenes UAV ha supuesto una revolución en la teledetección agronómica de precisión. Si nos referimos a trabajos más específicos para estudiar los procedimientos y técnicas desarrollados, se han publicado investigaciones sobre caracterización 3D de cultivos leñosos (Díaz-Varela et al., 2015; Torres-Sánchez et al., 2015; Zarco-Tejada et al., 2014), detección y cartografía de malas hierbas en fase temprana (de Castro et al., 2018; López-Granados, 2011; Peña et al., 2013), estrés hídrico (Gago et al., 2015; González-Dugo et al., 2013; Santesteban et al., 2017), clasificación de cultivos (Lottes et al., 2017; Park & Park, 2015; Senthilnath et al., 2016), detección de enfermedades (García-Ruiz et al., 2013; Yue et al., 2012) o estimación del contenido de nitrógeno (Pöllönen et al., 2013; Zhu et al., 2009), entre otras. Estas publicaciones destacan las ventajas que presentan los UAV en comparación con los aviones tripulados y satélites: elevada resolución espacial (resolución centimétrica) (Figura 7), bajos costes y posibilidad de adquisición de las imágenes con una gran versatilidad y flexibilidad coincidiendo con los requerimientos del cultivo.

El uso de estas plataformas en España está regulado por la Agencia Estatal de Seguridad Aérea (AESa) a través del Real Decreto 1036/2017 (AESa, 2017).

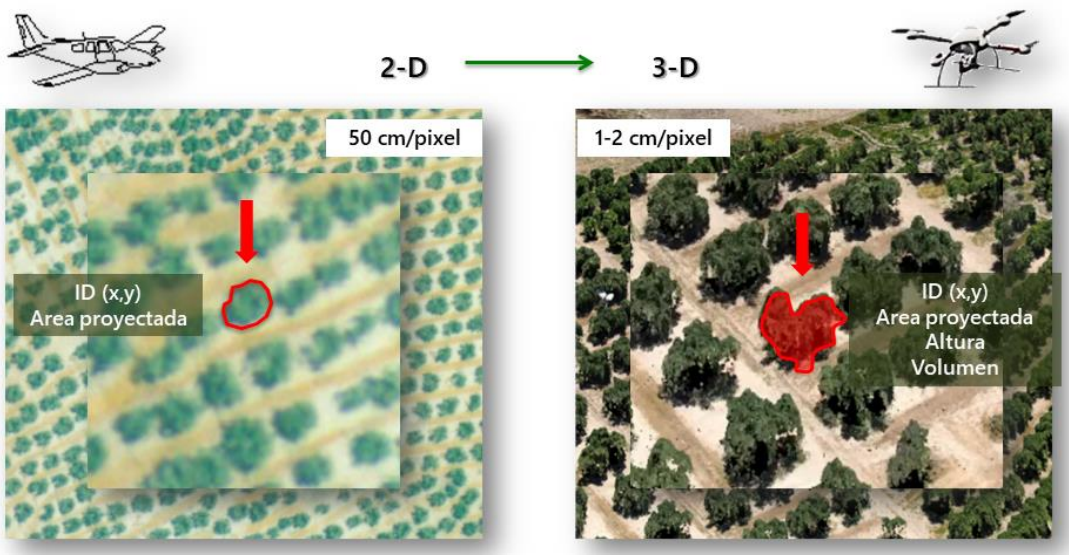


Figura 7. Esquema comparativo de resoluciones espaciales medias conseguidas por aviones tripulados y no tripulados y capacidad para la obtención de modelos bidimensionales (2-D) y tridimensionales (3D) en un cultivo de olivar. Fuente: grupo imaPing.

5.3. Principales características de los UAV

Como se ha indicado en el epígrafe anterior, los UAV encuadrados dentro de los sistemas de teledetección a baja altitud (LARS- *Low Altitude Remote Sensing*), han demostrado ser una eficiente alternativa a las plataformas tradicionales para llevar a cabo estudios de teledetección en distintos ámbitos de la agricultura de precisión. A continuación, se detallan las principales características de los UAV:

- Su uso no requiere de una excesiva planificación previa (Hardin & Hardin, 2010; Lelong et al., 2008; Nebiker et al., 2008), los costes inherentes a su uso son menores en comparación a los de otras tecnologías (Andújar et al., 2019; Rueda-Ayala et al., 2019) y posibilitan la obtención de información multitemporal (Torres-Sánchez et al., 2014), pudiendo efectuar vuelos sobre el cultivo con la frecuencia deseada dentro de una misma temporada sin incremento de los costes.
- Los avances en diseño y miniaturización de sensores, así como en la electrónica, han permitido que actualmente exista una amplia variedad de éstos que pueden ser acoplados en los UAV, permitiendo el intercambio fácil y rápido de sensores adecuado al objetivo planteado.
- Los vuelos pueden programarse a baja altura (ej.: < 120 m según AESA para línea de visión del UAV) y velocidad, lo que posibilita la toma de imágenes con una elevada resolución espacial (centimétrica, ej.: < 5 cm), generando una cartografía con un mayor

nivel de detalle. No obstante, se debe tener en cuenta que la altura de vuelo condiciona la superficie de terreno captada por el sensor, por lo que las imágenes adquiridas a baja altura, además de requerir una georreferenciación espacial y corrección geométrica como cualquier fotografía aérea, precisan ser unidas en una única imagen u ortomosaico que comprenda la totalidad de la zona de estudio. Para ello, se requiere diseñar un plan de vuelo definiendo los adecuados porcentajes de solapamiento longitudinal y transversal que permitan generar un ortomosaico de alta calidad (Mesas-Carrascosa et al., 2017, 2015; Xiang & Tian, 2011).

La elevada resolución espacial mencionada resulta muy útil para la generación de Modelos Digitales de Superficie (DSM- *Digital Surface Model*) por medio de métodos de foto-reconstrucción automática basados en técnicas de “*Structure from Motion*” (SfM) que permiten la reconstrucción 3D de los cultivos (de Castro et al., 2018; Torres-Sánchez et al., 2015).

Todas estas características han convertido la tecnología UAV en una herramienta de alta versatilidad para ser utilizada en el sector agrícola, ámbito en el que el momento de adquisición de imágenes es decisivo para monitorizar el problema y actuar lo más rápidamente posible para solventarlo.

5.4. Análisis de imágenes basado en objetos (OBIA)

Uno de los problemas intrínsecos asociados al análisis de imágenes de elevada resolución espacial adquiridas con UAV es la elevada variabilidad espectral intra-clase, originada por la gran cantidad de píxeles que componen cada uno de los elementos a detectar (Figura 8), apareciendo dificultades para separar estadísticamente las clases de estudio si únicamente se utiliza un análisis basado en los valores espectrales de los píxeles (Woodcock & Strahler, 1987). Consecuentemente, los píxeles individuales no representan las características de los elementos que se van a clasificar y se obtendría una menor precisión en la clasificación de la imagen usando métodos convencionales basados únicamente en características espectrales (Hunt et al., 2013; Yu et al., 2006).

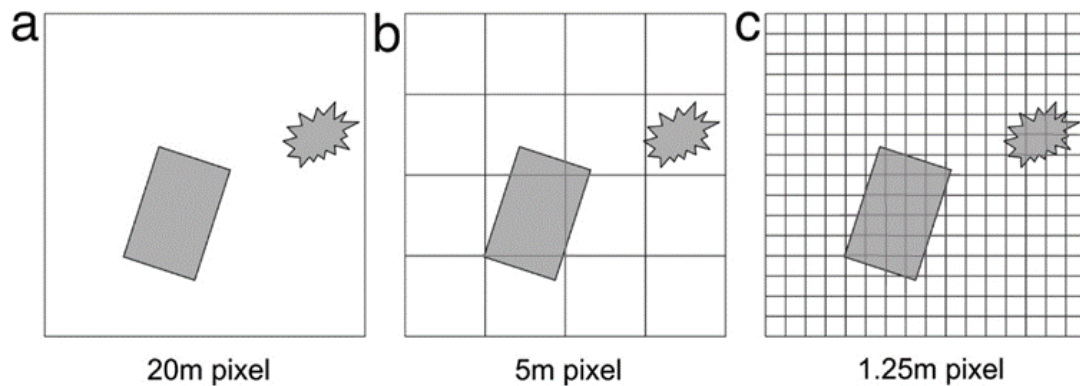


Figura 8. Relación entre los elementos a analizar en una imagen bajo distintas resoluciones espaciales: a) baja resolución: píxeles significativamente mayores que los elementos de interés, se necesitan técnicas de análisis basados en subpíxeles; b) resolución media: el tamaño de los píxeles y de los elementos a analizar es el mismo, por lo que serían apropiadas técnicas de análisis de píxel por píxel; c) alta resolución: los píxeles son significativamente más pequeños que los elementos a analizar, por lo que sería necesaria la regionalización de los píxeles en grupos de píxeles (objetos). Fuente: adaptada a partir de Blaschke (2010).

La aparición del paradigma de análisis de imagen basado en objetos (OBIA- *Object-Based Image Analysis*, en inglés) desarrollado por Blaschke (2010) ha representado un avance relevante en teledetección ofreciendo una alternativa eficaz a los métodos tradicionales de análisis basados en píxeles. El análisis OBIA se basa principalmente en dos fases: identificación automática de *objetos* homogéneos en la imagen a través del proceso de *segmentación* y *clasificación* de estos objetos incorporando información espectral, espacial, jerárquica y contextual. Por ejemplo, para discriminar malas hierbas en un cultivo de viña, la segmentación consistiría en crear regiones multi-píxel (*objetos*) representando malas hierbas, viñedo y suelo desnudo. Por lo tanto, la fase de segmentación es crucial para obtener una clasificación robusta y la elección del tipo de algoritmo a utilizar depende del objetivo a alcanzar, ya que influye directamente sobre el tamaño de los objetos creados y por lo tanto, sobre la heterogeneidad interna de los mismos, lo que a su vez afecta a la precisión de la clasificación (Drăguț et al., 2010; Moffett & Gorelick, 2013).

En la Figura 9a, en la que se muestra un fragmento de un ortomosaico a partir de un vuelo con UAV al que se acopló una cámara RGB, y correspondiente a una parcela de viñedo en espaldera, se exponen distintas segmentaciones (9b, 9c, 9d y 9e) del tipo multiresolución (algoritmo *multiresolution segmentation*) (Baatz & Schäpe, 2000) seleccionando diferentes valores para los parámetros escala y homogeneidad. De esta forma se obtienen objetos que se ajustan en mayor o menor medida a las clases presentes en la imagen.

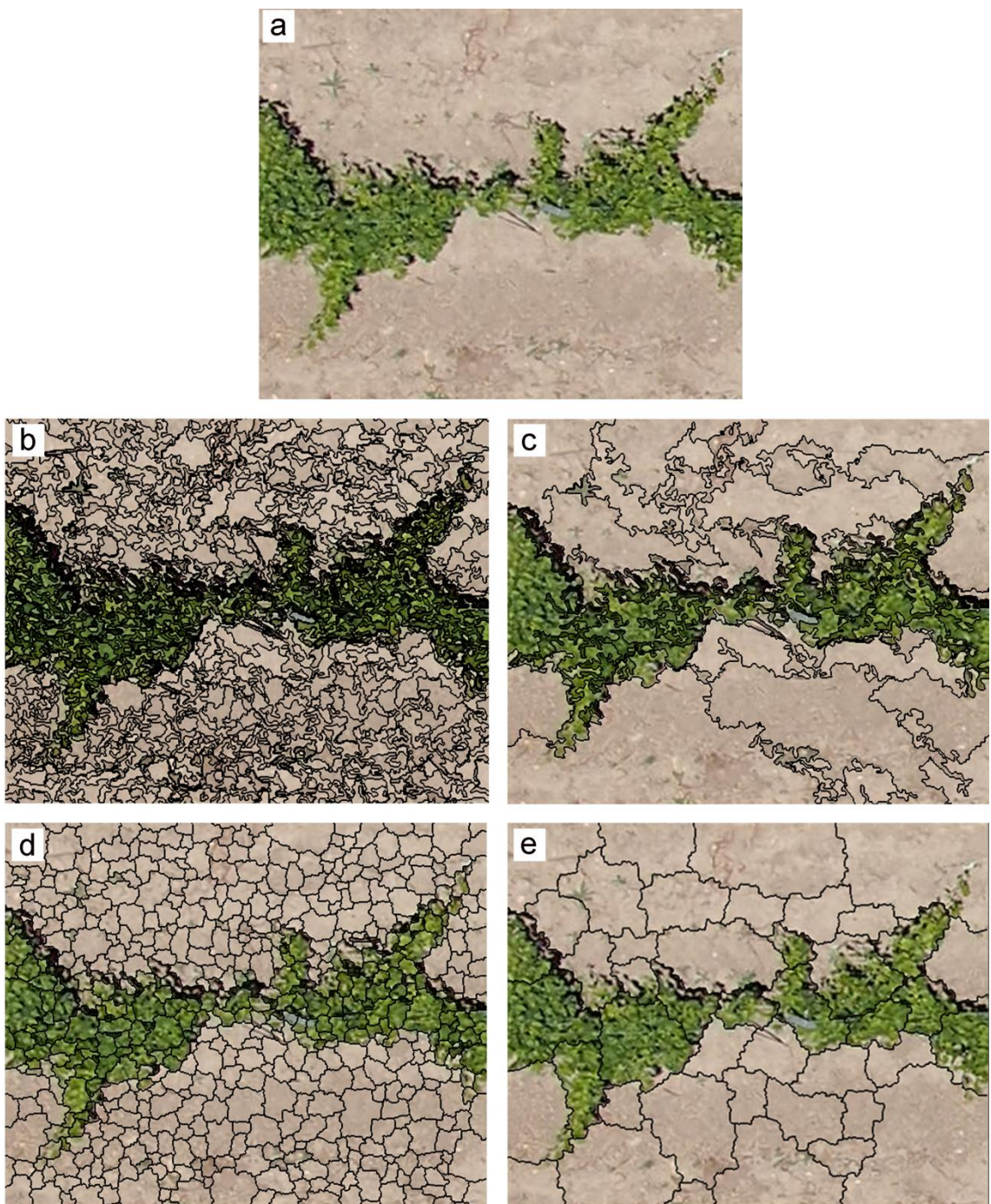


Figura 9. a) Vista parcial de ortomosaico obtenido a partir de imágenes UAV al que se acopló una cámara RGB y correspondiente a una parcela de viñedo en espaldera; Diferentes segmentaciones del tipo multirresolución según distintos valores de escala (E) y homogeneidad (forma- F y compacidad- C): b) $E=50$, $F=0,1$ y $C=0,5$; c) $E=200$, $F=0,1$ y $C=0,5$; d) $E=50$, $F=0,8$ y $C=1$; (e) $E=200$, $F=0,8$ y $C=1$. Fuente: grupo imaPing.

Además, las técnicas OBIA permiten el uso de información contextual (ej.: relaciones de orientación y posición de los objetos con sus vecinos), jerárquica (establecimiento de comparaciones entre objetos de diferente nivel) y morfológica, además de la espectral, para

desarrollar algoritmos de clasificación de los objetos creados, de manera que se reduce la variabilidad intra-clase y se solventan los problemas de similitud espectral típicos de los escenarios agrícolas. Otra ventaja adicional es que OBIA permite generar desarrollos y algoritmos totalmente automatizados, lo que supone grandes ahorros en tiempo y recursos.

Otra de las aportaciones de OBIA es la transferibilidad de los algoritmos generados que permite que éstos sean implementados, con mínimos ajustes en los parámetros y umbrales de segmentación para alcanzar el mismo objetivo, en otras áreas de la misma parcela, otras localidades e incluso en imágenes obtenidas con otro sensor (Laliberte et al., 2011). Hay que añadir que durante el proceso de desarrollo de OBIA, el analista debe incorporar su conocimiento sobre el objetivo a alcanzar y su forma de reconocer los objetos siguiendo algoritmos similares a los que utiliza el cerebro humano para registrar los objetos en el mundo real (Torres-Sánchez, 2017).

En el ámbito de la agricultura de precisión, varias investigaciones han demostrado la eficiencia de la metodología OBIA para extraer gran cantidad de información de forma automatizada de imágenes adquiridas por UAV y generar mapas útiles para la monitorización de objetivos agronómicos (López-Granados et al., 2016a; Mathews, 2014; Peña et al., 2013; Souza et al., 2017). En las secciones siguientes se revisan dos de las principales aplicaciones de la tecnología UAV y los algoritmos OBIA en relación con los objetivos de esta Tesis Doctoral: caracterización 3D de cultivos leñosos y cartografía de malas hierbas en cultivos leñosos.

5.5. Cartografía de la estructura 3D de cultivos leñosos: del LiDAR terrestre al UAV

Como se ha explicado en secciones anteriores, el conocimiento de la variabilidad inherente de los cultivos permite dirigir estrategias de agricultura de precisión, lo que conduce a optimizar la producción y la rentabilidad de los mismos a través de una aplicación de insumos dirigidos a las zonas en las que sean necesarios. Para alcanzar estos objetivos y en el caso de los cultivos leñosos, es fundamental llevar a cabo una caracterización de *alto rendimiento* (traducción literal del término ampliamente utilizado en inglés: *high-throughput*) de la arquitectura de cada árbol o cepa de vid en la parcela, es decir, una cuantificación de la estructura 3D de su copa o dosel incluyendo parámetros como altura, anchura, área proyectada y volumen. Esto proporcionaría información muy útil para: i) monitorizar el estado y fisiología de cada individuo del cultivo; ii) analizar su potencial rendimiento; y iii) optimizar un gran número de aspectos agronómicos tales como necesidades de poda o evolución de poda realizada, uso localizado de riego, nutrientes o fitosanitarios foliares para el control de plagas y enfermedades (Torres-Sánchez et al.,

2015). En el caso del uso de aplicaciones de fitosanitarios foliares en cultivos leñosos hay que evitar al máximo las actuaciones generalizadas, que consisten en una deriva indeseada, a veces ≥ 1 m y un goteo por exceso de producto (Figura 10) ocasionando problemas de contaminación medioambiental, gasto innecesario de producto y potencial aparición de resistencias.



Figura 10. Deriva y exceso de aplicación de producto fitosanitario en: a) almendro en seto, y b) viñedo en espaldera. Fuente: grupo imaping.

Tradicionalmente, la caracterización de la arquitectura de cultivos leñosos se ha realizado de manera manual mediante la medición de las principales dimensiones de varios árboles (ej.: altura, diámetro de tronco y de copa) de una serie de individuos, y la posterior modelización del volumen de copa aplicando ecuaciones que tratan a los árboles como si fuesen sólidos geométricos del tipo de cono, elipsoide, hemi-esferas u ovoides (Miranda-Fuentes et al., 2015; West, 2009). Sin embargo, esta tarea no resulta eficiente y genera

resultados inconsistentes debido a la irregular geometría de cada árbol (ej.: distinto hábito vegetativo de cada individuo con relación a una mayor o menor ramificación). Estos inconvenientes se han ido subsanando con el uso de métodos terrestres de escaneo con sensores activos (*non-imaging sensors*) de ultrasonido (Escolà et al., 2011; Llorens et al., 2010) o LiDAR (por sus siglas en inglés de *Light Detection and Ranging*) (Pfeiffer et al., 2018), siendo este último el más utilizado debido a la reducción de su precio y a la posibilidad de generar mayor número de parámetros (Sanz et al., 2018). Recientemente, Colaço et al. (2018) revisaron las aplicaciones de ambos tipos de sensores activos y las oportunidades futuras en el ámbito del fenotipado de variedades y la aplicación localizada de fitosanitarios según las dimensiones de cada individuo en cultivos hortícolas, enfatizando los grandes avances que estas técnicas han supuesto en cultivos leñosos (frutales, olivar, viñedo).

Aunque las ventajas de los sensores LiDAR a bordo de vehículos terrestres son relevantes ya que adquieren información con alta precisión implicando una elevada capacidad de clasificación, estos sensores presentan ciertas limitaciones para su uso de agricultura, como: i) inconvenientes para acceder a zonas de difícil acceso de una parcela (pendiente inclinada) o a partes altas de cada árbol cuando presentan un elevado crecimiento vegetativo; ii) escasa velocidad de avance del vehículo (unos 4-5 km/h) que implica más tiempo de adquisición de información en campo; iii) necesidad de alinear la información LiDAR en ambas caras del árbol, lo que requiere recorrer y tomar información con el vehículo primero en una hilera del cultivo y luego la contigua, lo que ocasiona a veces problemas de georreferenciación; y iv) falta de información espectral (Escolà et al., 2017; Luo et al., 2018; Underwood et al., 2016).

Como alternativa para solventar estas limitaciones, la tecnología UAV con sensores en el rango visible o NIR ha mostrado gran utilidad para la reconstrucción 3D de cada árbol y reconocimiento de cultivares en estudios de mejora genética mediante índices de vegetación en olivos (Avola et al., 2019) y generando Modelos Digitales de Superficie y métodos *Structure from Motion* (SfM) también en olivar (Díaz-Varela et al., 2015) o en cultivos de nogal (Marques et al., 2019) y lychee (Johansen et al., 2018). Asimismo, la metodología OBIA ha sido aplicada a imágenes UAV para generar cartografía del vigor en viñedo (Mathews, 2014), y altura, área proyectada y volumen en almendro (Torres-Sánchez et al., 2018), revelando su gran utilidad en estos objetivos.

En definitiva, el uso combinado de imágenes UAV y técnicas OBIA ofrece un gran potencial para la monitorización eficiente de cada uno de los individuos de la plantación, generando información de la estructura 3D que puede ser utilizada para diseñar aplicaciones de fitosanitarios foliares según las dimensiones de los individuos presentes en la parcela. Los avances en miniaturización de sensores LiDAR (peso \approx 1kg) han permitido

también su uso en UAV para inventario y estimación de tamaño de copa en el ámbito forestal (Wallace et al., 2012; Wu et al., 2019), abriendo nuevas líneas de investigación para su uso en cartografía 3D de cultivos leñosos.

En los **capítulos 2 y 3 de esta Tesis Doctoral** se aborda la caracterización 3D multitemporal de dos cultivos con alta importancia agroeconómica (olivar y viñedo, respectivamente) mediante la combinación tecnológica UAV-OBIA. En ambos artículos, el algoritmo desarrollado generó mapas de alta precisión de forma automática y sin necesidad de intervención del usuario. En la cartografía obtenida se han cuantificado las variables geométricas (altura, anchura, área proyectada o volumen) de cada olivo o cepa de vid sentando las bases para ajustar el volumen de aplicación de fitosanitarios al tamaño de los individuos de la parcela.

5.6. Detección y cartografía de malas hierbas a través de tecnología UAV y OBIA

Según WSSA (2016), una mala hierba es aquella planta que causa pérdidas económicas o daños ecológicos, crea problemas de salud a seres humanos o animales o simplemente es indeseable en el lugar donde crece. Oerke (2006) estimó que la presencia de malas hierbas provoca un 35 % de pérdidas de cosecha a escala mundial en diez de los principales cultivos (cebada, trigo, algodón, maíz, colza, patatas, arroz, soja, remolacha y tomate). Este valor de pérdidas es superior al causado por hongos patógenos (15 %), virus-bacterias (4 %) o insectos-plaga (18 %). España es el país europeo con mayor consumo de productos fitosanitarios, con un gasto total de 859 M € durante el período 2011-2015, de los cuales el 36 % representa el gasto relativo a herbicidas (AEPLA, 2016). Por otro lado, numerosos estudios han demostrado que las malas hierbas que infestan los cultivos muestran una alta dependencia espacial y se distribuyen formando en rodales y/o a lo largo de las hileras de siembra (Gerhards & Christensen, 2006; Jurado-Expósito et al., 2004; Marshall, 1988). Por ello, una cartografía precisa de las infestaciones es crucial para planificar estrategias de control localizado en función de la posición del rodal y de la cobertura o grado de infestación de las malas hierbas presentes, con el consiguiente ahorro de herbicidas (u otras prácticas de control) que supondría la no actuación en zonas en las que no existen malas hierbas.

Como se ha indicado en la sección 5.2, las investigaciones realizadas en detección de malas hierbas en cultivos herbáceos en estado fenológico temprano (desde estado de plántula a 2-6 hojas verdaderas) presentan un grave problema de similitud espectral, que ha sido solventado mediante el desarrollo de procedimientos OBIA en imágenes UAV incorporando en los algoritmos información espectral, de posición de las malas hierbas con

respecto a las líneas de cultivo y otros parámetros de textura de las hojas y de forma y tamaño de las plantas (López-Granados et al., 2016b, 2016a; Peña et al., 2015, 2013; Pérez-Ortiz et al., 2015). La hipótesis de trabajo de estas investigaciones citadas fue que todos los objetos de vegetación que estaban fuera de la línea de cultivo, es decir, *entre* las hileras de siembra, eran considerados malas hierbas. Estos resultados sentaron las bases para nuevas investigaciones sobre cartografía de malas hierbas localizadas no sólo *entre* las líneas de cultivo, sino también *dentro* de la hilera de siembra añadiendo a los algoritmos OBIA técnicas de aprendizaje automático (*Machine Learning*) (de Castro et al., 2018; Pérez-Ortiz et al., 2016).

Aunque la mayoría de las investigaciones anteriores sobre teledetección de malas hierbas se centran en cultivos herbáceos, la consecución de un manejo optimizado de malas hierbas en cultivos leñosos resulta también imprescindible para un control eficiente de las mismas. Cuando el objetivo planteado es discriminar malas hierbas en cultivos leñosos como olivar o viñedo, el problema inicial se centra en la necesidad de identificar las hileras de árboles o cepas (viñedos) y a continuación, detectar de forma precisa los rodales de la/s mala/s hierba/s presente/s en la parcela para diseñar mapas de control localizado dirigido únicamente a las zonas infestadas. Si el control se realiza con herbicidas como glifosato, terbutilazina u oxyfluorfen, hay que tener en cuenta que una aplicación inadecuada puede ocasionar problemas de resistencia, como es el caso de varias especies de *Conyza* (Tahmasebi et al., 2018), o de contaminación de suelo y acuíferos debido en parte a su baja solubilidad en agua (Calderón et al., 2016).

En el caso de viñedo, una de las malas hierbas más problemáticas es la especie gramínea perenne de desarrollo estival *C. dactylon* (grama), que compite por nutrientes y agua y presenta grandes dificultades para un control efectivo, ya que se propaga por estolones y rizomas (Hernández et al., 2000; Recasens et al., 2019). En el caso de viñedos ecológicos, el control de grama se realiza mediante laboreo superficial (hasta unos 15 cm para no dañar las raíces de las cepas), escarda manual o con desbrozadora o intercepas, y ninguna de estas actuaciones produce una acción eficaz de control ya que el laboreo aumenta la presencia de la grama favoreciendo su dispersión (Valencia et al., 2017), los rizomas que están a más profundidad de 15 cm pueden rebotar, y la siega de la parte aérea no afecta ni a estolones ni a rizomas. Si el viñedo no es ecológico, la presencia de grama se controla con herbicidas como glifosato hasta que la viña empieza a brotar. Una alternativa para el control de las malas hierbas es la implementación de una cubierta vegetal (Baumgartner et al., 2008), entre las que destaca el uso de cubiertas perennes (*Medicago sativa*) o gramíneas anuales (*Festuca arundinacea*, *Hordeum vulgare*) ya que compiten de forma eficiente con grama y son potenciales reductoras de sus infestaciones (Valencia et al., 2017).

La detección de *C. dactylon* en viñedo mediante imágenes UAV podría abordarse mediante dos estrategias. La primera de ellas consiste en la adquisición de imágenes en parada vegetativa (comúnmente diciembre-enero) y generación de mapas para su control localizado antes de que la viña empiece a brotar, si para ello se utiliza glifosato. La dificultad principal de esta estrategia radica en el similar comportamiento espectral de los rodales de grama con suelo desnudo, restos de poda y cosecha y otras especies, en caso de que las infestaciones de grama vayan unidas a la presencia de cubiertas vegetales entre calles (Figura 5). Esta aproximación metodológica fue la elegida por de Castro et al. (2017) quienes obtuvieron mapas de *C. dactylon* en parcelas de viñedo con cubierta vegetal de *F. arundinacea*. Por otro lado, la segunda estrategia sería tomar imágenes en primavera tardía (comúnmente principios-mediados de junio) en escenarios en los que el viñedo ha iniciado su crecimiento vegetativo y no cuente con cubiertas vegetales. En este escenario, la similitud espectral sería entre la vegetación de las cepas y los rodales de grama (Figura 6). El mapa generado de *C. dactylon* en esta situación podría utilizarse los días siguientes para control mecánico (ej.: intercepas) o para tratamiento localizado con herbicida (ej.: glifosato) en la siguiente campaña, ya que los rodales no controlados de grama persisten en su localización (Recasens et al., 2019).

Dados los resultados satisfactorios alcanzados por de Castro et al. (2017), en el **capítulo 4** de esta Tesis Doctoral se ha seguido la segunda estrategia dentro del marco de la detección y cartografía de malas hierbas en viñedo para un manejo sostenible. A través de los diferentes pasos del algoritmo automatizado OBIA, desarrollado en imágenes multitemporales UAV, se generaron mapas de infestación de los rodales de grama estableciéndose diferentes umbrales de tratamiento que permitieron la aplicación de distintas estrategias de manejo localizado.

6. Objetivos de la Tesis Doctoral

El *objetivo global* de esta Tesis Doctoral ha sido contribuir a la mejora del manejo de cultivos leñosos de forma eficiente, económica y sostenible en el contexto de la agricultura de precisión mediante la combinación de tecnología UAV, modelos tridimensionales a partir de técnicas fotogramétricas y el desarrollo de procedimientos automáticos de análisis de imagen basados en OBIA.

Este objetivo general se ha llevado a cabo a través de los siguientes *objetivos específicos*:

- a) Monitorización multitemporal 3D de cada árbol de una parcela de olivar bajo marco de plantación intensivo para cuantificar la influencia de tres tipos diferentes de poda

(adaptada, tradicional y mecánica) sobre los parámetros morfológicos de la copa (altura, área proyectada y volumen), así como evaluar su respuesta vegetativa después de un año de realizarse cada tratamiento de poda.

- b) Caracterización espacio-temporal 3D de alto rendimiento (*high-throughput*) de la arquitectura de cada cepa en tres viñedos en espaldera en dos momentos fenológicos distintos para computar los parámetros morfológicos de cada cepa, detectar huecos por marras en la parcela y sentar las bases metodológicas para crear mapas de tratamientos foliares de fitosanitarios según tamaño del dosel.
- c) Detección y cartografía multitemporal automática de las infestaciones de la mala hierba gramínea y perenne *Cynodon dactylon* L. (grama) en dos viñedos en espaldera durante dos años consecutivos para establecer estrategias de control localizado incorporando un rango de umbrales de tratamiento según niveles de infestación permitiendo una racionalización de su manejo.

El desarrollo de los objetivos general y específicos ha permitido la publicación de tres trabajos de investigación en revistas científicas del área con formato *Open Access* y revisión anónima por pares que motivan la presentación del presente manuscrito de Tesis Doctoral como compendio de artículos (*Art. 24 de la Propuesta por la Comisión de Másteres y Doctorado de 14 de diciembre de 2011, aprobada por Consejo de Gobierno de 21 de diciembre de 2011* y modificada por el mismo órgano el *29 de mayo de 2013 y el 23 de julio de 2013*, de la Universidad de Córdoba). **Estas tres publicaciones científicas están expuestas en los Capítulos 2, 3 y 4** de esta Tesis Doctoral, siendo el **Capítulo 1 una Introducción** en la que se describen brevemente los conceptos de las materias en las que se basa esta Tesis, así como la evolución y estado actual de los trabajos previos relacionados con los objetivos específicos planteados.

El artículo presentado en el **Capítulo 2** aborda el primer objetivo específico y se centró en la descripción y evaluación de la misión aérea programada para la adquisición de imágenes mediante una cámara con rangopectral RGB, de bajo coste, a bordo de un UAV así como la posterior generación de un modelo 3D para identificar y clasificar cada árbol en una parcela de olivar. Esta parcela contaba con 648 olivos que fueron divididos en tres zonas de igual tamaño y en cada una de las cuales se llevó a cabo un tipo de poda diferente: mecánica, adaptada y tradicional. A continuación, se desarrolló un algoritmo robusto capaz de analizar el modelo 3D y generar de forma automática los parámetros morfológicos (altura, área proyectada y volumen) de cada olivo. Este conjunto tecnológico y metodológico permitió la monitorización 3D multitemporal del efecto de los tratamientos de poda sobre la arquitectura de cada olivo, cuantificando la variación de sus parámetros morfológicos inmediatamente después de la poda y transcurrido un año de ésta. Este trabajo mostró que la tecnología y metodología utilizadas podrían transferirse con éxito a

otros cultivos y otros objetivos agronómicos similares, permitiendo el análisis de las tareas realizadas y el diseño de estrategias de manejo localizado en agricultura de precisión.

JIMÉNEZ-BRENES, F.M.; LÓPEZ-GRANADOS, F.; DE CASTRO, A.I.; TORRES-SÁNCHEZ, J.; CASTILLO, N.; PEÑA, J.M. (2017). Quantifying pruning impacts on olive tree architecture and annual canopy growth by using UAV-based 3D modelling. *Plant Methods*, 13:55. doi:10.1186/s13007-017-0205-3 (Open Access).

El **Capítulo 3** comprende el segundo objetivo específico cuya finalidad fue la caracterización tridimensional de alto rendimiento de cada cepa en tres parcelas de viñedo en espaldera en dos momentos fenológicos distintos y con presencia de cubierta vegetal entre las hileras de cepas. Se desarrolló un procedimiento OBIA de análisis de imágenes adquiridas con un sensor RGB a bordo de un UAV, y se utilizaron técnicas fotogramétricas basadas en el Modelo Digital de Superficie para resolver los problemas de similitud espectral entre las vides y la cubierta presente entre las calles. La modelización 3D permitió la identificación automática de cada cepa en los viñedos y la obtención de información cuantitativa de sus parámetros geométricos (altura, área proyectada y volumen), detectándose asimismo los huecos por marras en cada hilera de cultivo. Esta metodología se validó mediante mediciones georreferenciadas de altura en un conjunto de cepas seleccionadas en cada viñedo. Finalmente, se abordó la potencialidad de esta tecnología en otras aplicaciones agronómicas como puede ser el manejo de las cubiertas vegetales con el fin de supervisar su crecimiento, decidir el momento de la siega y evitar la competencia por agua, nutrientes y luz con las cepas.

DE CASTRO, A.I.; JIMÉNEZ-BRENES, F.M.; TORRES-SÁNCHEZ, J.; PEÑA, J.M.; BORRA-SERRANO, I.; LÓPEZ-GRANADOS, F. (2018). 3D characterization of vineyards using a novel UAV imagery-based OBIA procedure for precision viticulture applications. *Remote Sensing*, 10(4): 584. doi:10.3390/rs10040584 (Open Access).

El artículo presentado en el **Capítulo 4** recoge el tercer objetivo específico y se focalizó en la detección y cartografía de malas hierbas para optimizar su control como una de las principales tareas agrícolas del manejo de cultivos leñosos. Concretamente, se centró en la detección de *C. dactylon* (grama), una especie de mala hierba gramínea y perenne que causa graves pérdidas en el viñedo. Para la consecución de este objetivo se utilizó tecnología UAV y dos sensores que, colocados de forma independiente en la configuración de los vuelos, generaron imágenes con distinto rango espectral (RGB y RGNIR) durante dos campañas agrícolas. Sobre estas imágenes se realizó en primer lugar un análisis espectral analizando diferentes índices de vegetación, seleccionándose aquéllos que de forma más precisa fueron capaces de separar los rodales de grama y suelo desnudo según el sensor utilizado. Posteriormente, se desarrolló un algoritmo automatizado basado en OBIA,

modelización 3D y los índices espetrales seleccionados anteriormente para proceder a discriminar cada cepa de viñedo, los rodales de grama y el suelo desnudo. Estos procedimientos fueron validados mediante el muestreo georreferenciado de las emergencias de *C. dactylon* en una serie de áreas verda-terreno en cada parcela de viñedo. El algoritmo exportó de forma automática el mapa para cada sensor evaluado con la localización exacta de cada cepa y de los rodales de grama de cada parcela estudiada, lo que permitió el análisis de la expansión de las emergencias de grama dentro de cada viñedo. Según la precisión de los resultados de la clasificación, se determinó el tipo de sensor más idóneo para este tipo de investigación.

JIMÉNEZ-BRENES, F.M.; LÓPEZ-GRANADOS, F.; TORRES-SÁNCHEZ, J.; PEÑA, J.M.; RAMÍREZ, P.; CASTILLEJO-GONZÁLEZ, I.L.; DE CASTRO, A.I. (2019). Automatic UAV-based detection of *Cynodon dactylon* for site-specific vineyard management. *PLoS ONE*, 14(6): e0218132. <https://doi.org/10.1371/journal.pone.0218132> (Open Access).

Las investigaciones desarrolladas en los Capítulos 2, 3 y 4 han generado resultados de alta precisión proporcionando información continua de la totalidad de las parcelas analizadas, lo que supone un avance significativo frente a los resultados de otros trabajos basados en muestreos de campo de pocos individuos (árboles o cepas) o de análisis discretos de emergencias de malas hierbas. Ello permite la obtención de mapas, e información tabulada de la variable objeto de interés, en toda el área de estudio con potencialidad para utilizarse en la optimización de las aplicaciones de fitosanitarios u otras actuaciones en campo que poseen gran relevancia, como es la decisión del tipo de poda a efectuar en un cultivo leñoso.

Por último, **en el Capítulo 5 se exponen las conclusiones** de cada uno de los capítulos anteriores de la presente Tesis Doctoral y se detallan las líneas de investigación programadas como continuación a esta Tesis.

7. Referencias

- Abdulridha, J., Ampatzidis, Y., Ehsani, R., de Castro, A.I., 2018. Evaluating the performance of spectral features and multivariate analysis tools to detect laurel wilt disease and nutritional deficiency in avocado. *Comput. Electron. Agric.* 155, 203–211. <https://doi.org/10.1016/j.compag.2018.10.016>
- AEPLA, 2016. Memoria AEPLA 2015. http://www.aepla.es/tmp/images/publicaciones/P0022_Memoria_AEPLA_2015.pdf

AESA, 2017. Real Decreto 1036/2017, de 15 de diciembre, por el que se regula la utilización civil de las aeronaves pilotadas por control remoto.

<https://www.boe.es/buscar/doc.php?id=BOE-A-2017-15721>

Ambika, A.K., Wardlow, B., Mishra, V., 2016. Remotely sensed high resolution irrigated area mapping in India for 2000 to 2015. *Sci. Data* 3, 160118.

<https://doi.org/10.1038/sdata.2016.118>

Andújar, D., Moreno, H., Bengochea-Guevara, J.M., de Castro, A., Ribeiro, A., 2019. Aerial imagery or on-ground detection? An economic analysis for vineyard crops. *Comput. Electron. Agric.* 157, 351–358. <https://doi.org/10.1016/j.compag.2019.01.007>

Annosi, M.C., Brunetta, F., Monti, A., Nati, F., 2019. Is the trend your friend? An analysis of technology 4.0 investment decisions in agricultural SMEs. *Comput. Ind.* 109, 59–71. <https://doi.org/10.1016/j.compind.2019.04.003>

Atzberger, C., 2013. Advances in Remote Sensing of Agriculture: Context description, existing operational monitoring systems and major information needs. *Remote Sens.* 5, 949–981. <https://doi.org/10.3390/rs5020949>

Aubert, B.A., Schroeder, A., Grimaudo, J., 2012. IT as enabler of sustainable farming: An empirical analysis of farmers' adoption decision of precision agriculture technology. *Decis. Support Syst.* 54, 510–520. <https://doi.org/10.1016/j.dss.2012.07.002>

Avola, G., Di Gennaro, S.F., Cantini, C., Riggi, E., Muratore, F., Tornambè, C., Matese, A., 2019. Remotely sensed vegetation indices to discriminate field-grown olive cultivars. *Remote Sens.* 11, 1242. <https://doi.org/10.3390/rs11101242>

Baatz, M., Schäpe, A., 2000. Multiresolution segmentation: an optimization approach for high quality multi-scale image segmentation. http://www.ecognition.com/sites/default/files/405_baatz_fp_12.pdf

Bandyopadhyay, D., Bhavsar, D., Pandey, K., Gupta, S., Roy, A., 2017. Red edge index as an indicator of vegetation growth and vigor using hyperspectral remote sensing data. *Proc. Natl. Acad. Sci. India Sect. Phys. Sci.* 87, 879–888. <https://doi.org/10.1007/s40010-017-0456-4>

Bauer, M., Cipra, J., 1973. Identification of agricultural crops by computer processing of ERTS MSS data. *LARS Tech. Rep.* https://docs.lib.psu.edu/cgi/viewcontent.cgi?referer=https://www.google.com/&httpsredir=1&article=1019&context=larstechnical_papers

Baumgartner, K., Steenwerth, K.L., Veilleux, L., 2008. Cover-crop systems affect weed communities in a California vineyard. *Weed Sci.* 56, 596–605. <https://doi.org/10.1614/WS-07-181.1>

- Bégué, A., Arvor, D., Bellon, B., Betbeder, J., de Abelleyra, D., P. D. Ferraz, R., Lebourgeois, V., Lelong, C., Simões, M., R. Verón, S., 2018. Remote sensing and cropping practices: a review. *Remote Sens.* 10, 99. <https://doi.org/10.3390/rs10010099>
- Bengtsson, J., Ahnström, J., Weibull, A.-C., 2005. The effects of organic agriculture on biodiversity and abundance: a meta-analysis. *J. Appl. Ecol.* 42, 261–269. <https://doi.org/10.1111/j.1365-2664.2005.01005.x>
- Blaschke, T., 2010. Object based image analysis for remote sensing. *ISPRS J. Photogramm. Remote Sens.* 65, 2–16. <https://doi.org/10.1016/j.isprsjprs.2009.06.004>
- Bongiovanni, R., Lowenberg-Deboer, J., 2004. Precision agriculture and sustainability. *Precis. Agric.* 5, 359–387. <https://doi.org/10.1023/B:PRAG.0000040806.39604.aa>
- Calderón, M.J., De Luna, E., Gómez, J.A., Hermosín, M.C., 2016. Herbicide monitoring in soil, runoff waters and sediments in an olive orchard. *Sci. Total Environ.* 569–570, 416–422. <https://doi.org/10.1016/j.scitotenv.2016.06.126>
- Chen, D., Stow, D., Getis, A., 2002. Multi-resolution classification framework for improving land use/cover mapping, in: Walsh, S.J., Crews-Meyer, K.A. (Eds.), *Linking People, Place, and Policy: A GIScience Approach*. Springer US, Boston, MA, pp. 235–261. https://doi.org/10.1007/978-1-4615-0985-1_11
- Colaço, A.F., Molin, J.P., Rosell-Polo, J.R., Escolà, A., 2018. Application of light detection and ranging and ultrasonic sensors to high-throughput phenotyping and precision horticulture: current status and challenges. *Hortic. Res.* 5, 1–11. <https://doi.org/10.1038/s41438-018-0043-0>
- Colomina, I., Molina, P., 2014. Unmanned aerial systems for photogrammetry and remote sensing: a review. *ISPRS J. Photogramm. Remote Sens.* 92, 79–97. <https://doi.org/10.1016/j.isprsjprs.2014.02.013>
- Comisión Europea, 2018. Reglamento del Parlamento Europeo y del Consejo por el que se establecen normas en relación con la ayuda a los planes estratégicos que deben elaborar los Estados miembros en el marco de la política agrícola común (planes estratégicos de la PAC), financiada con cargo al Fondo Europeo Agrícola de Garantía (FEAGA) y al Fondo Europeo Agrícola de Desarrollo Rural (Feader), y por el que se derogan el Reglamento (UE) n.º 1305/2013 del Parlamento Europeo y del Consejo y el Reglamento (UE) n.º 1307/2013 del Parlamento Europeo y del Consejo. <https://eur-lex.europa.eu/legal-content/ES/TXT/HTML/?uri=CELEX:52018PC0392&from=ES>
- Coulter, L., Stow, D., Hope, A., O’Leary, J., Turner, D., Longmire, P., Peterson, S., Kaiser, J., 2000. Comparison of high spatial resolution imagery for efficient generation of GIS vegetation layers. *PEampRS Photogramm. Eng. Remote Sens.* 66, 1329–1335.

- Crookston, R.K., 2006. A top 10 list of developments and issues impacting crop management and ecology during the past 50 years. *Crop Sci.* 46, 2253–2262. <https://doi.org/10.2135/cropsci2005.11.0416gas>
- de Castro, A.I., Ehsani, R., Ploetz, R., Crane, J.H., Abdulridha, J., 2015. Optimum spectral and geometric parameters for early detection of laurel wilt disease in avocado. *Remote Sens. Environ.* 171, 33–44. <https://doi.org/10.1016/j.rse.2015.09.011>
- de Castro, A.I., Peña, J.M., Torres-Sánchez, J., Jiménez-Brenes, F., López-Granados, F., 2017. Mapping *Cynodon dactylon* in vineyards using UAV images for site-specific weed control. *Adv. Anim. Biosci.* 8, 267–271. <https://doi.org/10.1017/S2040470017000826>
- de Castro, A.I., Torres-Sánchez, J., Peña, J.M., Jiménez-Brenes, F.M., Csillik, O., López-Granados, F., 2018. An automatic random forest-OBIA algorithm for early weed mapping between and within crop rows using UAV imagery. *Remote Sens.* 10, 285. <https://doi.org/10.3390/rs10020285>
- de Castro, A.I. de, López Granados, F., Jurado-Expósito, M., 2013. Broad-scale cruciferous weed patch classification in winter wheat using QuickBird imagery for in-season site-specific control. *Precis. Agric.* 14(4): 392–413. <https://doi.org/10.1007/S11119-013-9304-Y>
- Díaz-Varela, R.A., de la Rosa, R., León, L., Zarco-Tejada, P.J., 2015. High-resolution airborne UAV imagery to assess olive tree crown parameters using 3D photo reconstruction: application in breeding trials. *Remote Sens.* 7, 4213–4232. <https://doi.org/10.3390/rs70404213>
- Directiva 128, 2009. Directiva 2009/128/CE del Parlamento Europeo y del Consejo, de 21 de octubre de 2009, por la que se establece el marco de la actuación comunitaria para conseguir un uso sostenible de los plaguicidas. <https://eur-lex.europa.eu/LexUriServ/LexUriServ.do?uri=OJ:L:2009:309:0071:0086:ES:PDF>
- Drăguț, L., Tiede, D., Levick, S.R., 2010. ESP: a tool to estimate scale parameter for multiresolution image segmentation of remotely sensed data. *Int. J. Geogr. Inf. Sci.* 24, 859–871. <https://doi.org/10.1080/13658810903174803>
- Drinkwater, L.E., Letourneau, D.K., Workneh, F., Bruggen, A.H.C. van, Shennan, C., 1995. Fundamental differences between conventional and organic tomato agroecosystems in California. *Ecol. Appl.* 5, 1098–1112. <https://doi.org/10.2307/2269357>
- Escolà, A., Martínez-Casasnovas, J.A., Rufat, J., Arnó, J., Arbonés, A., Sebé, F., Pascual, M., Gregorio, E., Rosell-Polo, J.R., 2017. Mobile terrestrial laser scanner applications in precision fruticulture/horticulture and tools to extract information from canopy point clouds. *Precis. Agric.* 18, 111–132. <https://doi.org/10.1007/s11119-016-9474-5>

- Escolà, A., Planas, S., Rosell, J.R., Pomar, J., Camp, F., Solanelles, F., Gracia, F., Llorens, J., Gil, E., 2011. Performance of an ultrasonic ranging sensor in apple tree canopies. *Sensors* 11, 2459–2477. <https://doi.org/10.3390/s110302459>
- FAO, 2004. La ética de la intensificación sostenible de la agricultura. Roma.
- Fernández-Quintanilla, C., Peña, J.M., Andújar, D., Dorado, J., Ribeiro, A., López-Granados, F., 2018. Is the current state of the art of weed monitoring suitable for site-specific weed management in arable crops?. *Weed Res.* 58, 259–272. <https://doi.org/10.1111/wre.12307>
- Francis, C.A., 1987. Search for a sustainable agriculture: reduced inputs and increased profits. *Crops Soils* 39, 12–14.
- Franklin, S.E., 2001. Remote sensing for sustainable forest management. CRC Press. <https://doi.org/10.1201/9781420032857>
- Gafsi, M., Legagneux, B., Nguyen, G., Robin, P., 2006. Towards sustainable farming systems: effectiveness and deficiency of the French procedure of sustainable agriculture. *Agric. Syst.* 90, 226–242. <https://doi.org/10.1016/j.agrsy.2006.01.002>
- Gago, J., Douthe, C., Coopman, R.E., Gallego, P.P., Ribas-Carbo, M., Flexas, J., Escalona, J., Medrano, H., 2015. UAVs challenge to assess water stress for sustainable agriculture. *Agric. Water Manag.* 153, 9–19. <https://doi.org/10.1016/j.agwat.2015.01.020>
- García Olmedo, F., 1998. La tercera revolución verde. Plantas con luz propia. Debate.
- García Torres, L., Peña-Barragán, J.M., López-Granados, F., Jurado-Expósito, M., Fernández-Escobar, R., 2008. Automatic assessment of agro-environmental indicators from remotely sensed images of tree orchards and its evaluation using olive plantations. *Comput. Electron. Agric.* 61, 179–191. <https://doi.org/10.1016/j.compag.2007.11.004>
- García-Ruiz, F., Sankaran, S., Maja, J.M., Lee, W.S., Rasmussen, J., Ehsani, R., 2013. Comparison of two aerial imaging platforms for identification of Huanglongbing-infected citrus trees. *Comput. Electron. Agric.* 91, 106–115. <https://doi.org/10.1016/j.compag.2012.12.002>
- García-Torres, L., Benites, J., Martínez-Vilela, A., Holgado-Cabrera, A. (Eds.), 2003. Conservation agriculture: environment, farmers experiences, innovations, socio-economy, policy. Springer Netherlands.
- Gerhards, R., Christensen, S., 2006. Site-specific weed management, in: handbook of precision agriculture: principles and applications. New York, NY, pp. 185–206.
- Gollin, D., Morris, M., Byerlee, D., 2005. Technology adoption in intensive post-green revolution systems. *Am. J. Agric. Econ.* 87, 1310–1316.

- González-Dugo, V., Zarco-Tejada, P., Nicolás, E., Nortes, P.A., Alarcón, J.J., Intrigliolo, D.S., Fereres, E., 2013. Using high resolution UAV thermal imagery to assess the variability in the water status of five fruit tree species within a commercial orchard. *Precis. Agric.* 14, 660–678. <https://doi.org/10.1007/s11119-013-9322-9>
- Hardin, P.J., Hardin, T.J., 2010. Small-scale remotely piloted vehicles in environmental *Research. Geogr. Compass* 4, 1297–1311. <https://doi.org/10.1111/j.1749-8198.2010.00381.x>
- Hernández, A.J., Lacasta, C., Pastor, J., 2000. Cubiertas vegetales para un viñedo ecológico en zonas semiáridas, in: Actas IV Congreso SEAE. Armonía entre Ecología y Economía. Córdoba, p. 11.
- Hunt, E.R., Daughtry, C.S.T., Mirsky, S.B., Hively, W.D., 2013. Remote sensing with unmanned aircraft systems for precision agriculture applications, in: 2013 Second International Conference on Agro-Geoinformatics (Agro-Geoinformatics). Presented at the 2013 Second International Conference on Agro-Geoinformatics (Agro-Geoinformatics), pp. 131–134. <https://doi.org/10.1109/Argo-Geoinformatics.2013.6621894>
- Ikerd, J.E., 1993. The need for a systems approach to sustainable agriculture, in: Edwards, C.A., Wali, M.K., Horn, D.J., Miller, F. (Eds.), Agriculture and the Environment. Elsevier, Amsterdam, pp. 147–160. <https://doi.org/10.1016/B978-0-444-89800-5.50014-2>
- Jensen, J.R., 2007. Remote sensing of the environment: an earth resource perspective, 2nd Edition.
- Johansen, K., Raharjo, T., McCabe, M.F., 2018. Using multi-spectral UAV imagery to extract tree crop structural properties and assess pruning effects. *Remote Sens.* 10, 854. <https://doi.org/10.3390/rs10060854>
- JRC-EC, 2014. Precision agriculture: an opportunity for eu-farmers – potential support with the cap 2014-2020 - think tank.
[http://www.europarl.europa.eu/thinktank/en/document.html?reference=IPOL-AGRI_NT\(2014\)529049](http://www.europarl.europa.eu/thinktank/en/document.html?reference=IPOL-AGRI_NT(2014)529049)
- Junta de Andalucía, 2016. Sistema de Indicadores Ambientales de la Red de Información Ambiental de Andalucía.
http://www.juntadeandalucia.es/medioambiente/portal_web/rediam/indicadores/2015/IA03_2015.pdf
- Jurado-Expósito, M., López-Granados, F., González-Andújar, J.L., García-Torres, L., 2004. Spatial and temporal analysis of *Convolvulus arvensis* L. populations over four

- growing seasons. *Eur. J. Agron.* 21, 287–296.
<https://doi.org/10.1016/j.eja.2003.10.001>
- Knowler, D., Bradshaw, B., 2007. Farmers' adoption of conservation agriculture: A review and synthesis of recent research. *Food Policy* 32, 25–48.
<https://doi.org/10.1016/j.foodpol.2006.01.003>
- Laliberte, A.S., Goforth, M.A., Steele, C.M., Rango, A., 2011. Multispectral remote sensing from unmanned aircraft: image processing workflows and applications for rangeland environments. *Remote Sens.* 3, 2529–2551. <https://doi.org/10.3390/rs3112529>
- Lark, T.J., Mueller, R.M., Johnson, D.M., Gibbs, H.K., 2017. Measuring land-use and land-cover change using the U.S. department of agriculture's cropland data layer: cautions and recommendations. *Int. J. Appl. Earth Obs. Geoinformation* 62, 224–235.
<https://doi.org/10.1016/j.jag.2017.06.007>
- Lausch, A., Salbach, C., Schmidt, A., Doktor, D., Merbach, I., Pause, M., 2015. Deriving phenology of barley with imaging hyperspectral remote sensing. *Ecol. Model.* 295, 123–135. <https://doi.org/10.1016/j.ecolmodel.2014.10.001>
- Lelong, C.C.D., Burger, P., Jubelin, G., Roux, B., Labbé, S., Baret, F., 2008. Assessment of unmanned aerial vehicles imagery for quantitative monitoring of wheat crop in small plots. *Sensors* 8, 3557–3585. <https://doi.org/10.3390/s8053557>
- Liaghate, S., Balasundram, S.K., 2010. A review: the role of remote sensing in precision agriculture. *Am. J. Agric. Biol. Sci.* 5, 50–55.
<https://doi.org/10.3844/ajabssp.2010.50.55>
- Lichtfouse, E., Navarrete, M., Debaeke, P., Souchère, V., Alberola, C., Ménassieu, J., 2009. Agronomy for Sustainable Agriculture: A Review, in: Lichtfouse, E., Navarrete, M., Debaeke, P., Véronique, S., Alberola, C. (Eds.), Sustainable Agriculture. Springer Netherlands, Dordrecht, pp. 1–7. https://doi.org/10.1007/978-90-481-2666-8_1
- Lindblom, J., Lundström, C., Ljung, M., Jonsson, A., 2017. Promoting sustainable intensification in precision agriculture: review of decision support systems development and strategies. *Precis. Agric.* 18, 309–331.
<https://doi.org/10.1007/s11119-016-9491-4>
- Llorens, J., Gil, E., Llop, J., Escolà, A., 2010. Variable rate dosing in precision viticulture: Use of electronic devices to improve application efficiency. *Crop Prot.* 29, 239–248.
<https://doi.org/10.1016/j.cropro.2009.12.022>
- López-Granados, F., 2011. Weed detection for site-specific weed management: mapping and real-time approaches. <http://onlinelibrary.wiley.com/doi/10.1111/j.1365-3180.2010.00829.x/full>

- López-Granados, F., Jurado-Expósito, M., Peña-Barragán, J.M., García-Torres, L., 2006. Using remote sensing for identification of late-season grass weed patches in wheat. *Weed Sci.* 54, 346–353.
- López-Granados, F., Torres-Sánchez, J., Castro, A.I. de, Serrano-Pérez, A., Mesas-Carrascosa, F.J., Peña, J.M., 2016a. Object-based early monitoring of a grass weed in a grass crop using high resolution UAV imagery. *Agron. Sustain. Dev.* 36, 67. <https://doi.org/10.1007/s13593-016-0405-7>
- López-Granados, F., Torres-Sánchez, J., Serrano-Pérez, A., Castro, A.I. de, Mesas-Carrascosa, F.J., Peña, J.M., 2016b. Early season weed mapping in sunflower using UAV technology: variability of herbicide treatment maps against weed thresholds. *Precis. Agric.* 17, 183–199. <https://doi.org/10.1007/s11119-015-9415-8>
- Lottes, P., Khanna, R., Pfeifer, J., Siegwart, R., Stachniss, C., 2017. UAV-based crop and weed classification for smart farming, in: 2017 IEEE International Conference on Robotics and Automation (ICRA). Presented at the 2017 IEEE International Conference on Robotics and Automation (ICRA), pp. 3024–3031. <https://doi.org/10.1109/ICRA.2017.7989347>
- Luo, L., Zhai, Q., Su, Y., Ma, Q., Kelly, M., Guo, Q., 2018. Simple method for direct crown base height estimation of individual conifer trees using airborne LiDAR data. *Opt. Express* 26, A562–A578. <https://doi.org/10.1364/OE.26.00A562>
- Maeder, P., Fliessbach, A., Dubois, D., Gunst, L., Fried, P., Niggli, U., 2002. Soil fertility and biodiversity in organic farming. *Science* 296, 1694–1697. <https://doi.org/10.1126/science.1071148>
- Marques, P., Pádua, L., Adão, T., Hruška, J., Peres, E., Sousa, A., Sousa, J.J., 2019. UAV-based automatic detection and monitoring of chestnut trees. *Remote Sens.* 11, 855. <https://doi.org/10.3390/rs11070855>
- Marshall, E.J.P., 1988. Field-scale estimates of grass weed populations in arable land. *Weed Res.* 28, 191–198. <https://doi.org/10.1111/j.1365-3180.1988.tb01606.x>
- Mathews, A.J., 2014. Object-based spatiotemporal analysis of vine canopy vigor using an inexpensive unmanned aerial vehicle remote sensing system. *J. Appl. Remote Sens.* 8, 085199. <https://doi.org/10.1117/1.JRS.8.085199>
- Matson, P.A., Parton, W.J., Power, A.G., Swift, M.J., 1997. Agricultural intensification and ecosystem properties. *Science* 277, 504–509. <https://doi.org/10.1126/science.277.5325.504>
- Mesas-Carrascosa, F.J., Rumbao, I.C., Torres-Sánchez, J., García-Ferrer, A., Peña, J.M., Granados, F.L., 2017. Accurate ortho-mosaicked six-band multispectral UAV images

- as affected by mission planning for precision agriculture proposes. *Int. J. Remote Sens.* 38, 2161–2176. <https://doi.org/10.1080/01431161.2016.1249311>
- Mesas-Carrascosa, F.J., Torres-Sánchez, J., Clavero-Rumbao, I., García-Ferrer, A., Peña, J.M., Borra-Serrano, I., López-Granados, F., 2015. Assessing optimal flight parameters for generating accurate multispectral orthomosaicks by UAV to support site-specific crop management. *Remote Sens.* 7, 12793–12814. <https://doi.org/10.3390/rs71012793>
- Miranda-Fuentes, A., Llorens, J., Gamarra-Diezma, J.L., Gil-Ribes, J.A., Gil, E., 2015. Towards an optimized method of olive tree crown volume measurement. *Sensors* 15, 3671–3687. <https://doi.org/10.3390/s150203671>
- Miranda-Fuentes, A., Llorens, J., Rodríguez-Lizana, A., Cuenca, A., Gil, E., Blanco-Roldán, G.L., Gil-Ribes, J.A., 2016. Assessing the optimal liquid volume to be sprayed on isolated olive trees according to their canopy volumes. *Sci. Total Environ.* 568, 296–305. <https://doi.org/10.1016/j.scitotenv.2016.06.013>
- Moffett, K.B., Gorelick, S.M., 2013. Distinguishing wetland vegetation and channel features with object-based image segmentation. *Int. J. Remote Sens.* 34, 1332–1354. <https://doi.org/10.1080/01431161.2012.718463>
- Mosleh, M.K., Hassan, Q.K., Chowdhury, E.H., 2015. Application of remote sensors in mapping rice area and forecasting its production: a review. *Sensors* 15, 769–791. <https://doi.org/10.3390/s150100769>
- Mulla, D.J., 2013. Twenty five years of remote sensing in precision agriculture: key advances and remaining knowledge gaps. *Biosyst. Eng.*, Special Issue: Sensing Technologies for Sustainable Agriculture 114, 358–371. <https://doi.org/10.1016/j.biosystemseng.2012.08.009>
- Nebiker, S., Annen, A., Scherrer, M., Oesch, D., 2008. A light-weight multispectral sensor for micro UAV – opportunities for very high resolution airborne remote sensing. *ISPRS J. Photogramm. Remote Sens.* <https://pdfs.semanticscholar.org/50e5/7e9c8dd7e8269d82949ca993bfcc2c822286.pdf>
- Nex, F., Remondino, F., 2014. UAV for 3D mapping applications: a review. *Appl. Geomat.* 6, 1–15. <https://doi.org/10.1007/s12518-013-0120-x>
- Oerke, E.-C., 2006. Crop losses to pests. *J. Agric. Sci.* 144, 31–43. <https://doi.org/10.1017/S0021859605005708>
- Ostos-Garrido, F.J., de Castro, A.I., Torres-Sánchez, J., Pistón, F., Peña, J.M., 2019. High-throughput phenotyping of bioethanol potential in cereals using UAV-based multi-spectral imagery. *Front. Plant Sci.* 10. <https://doi.org/10.3389/fpls.2019.00948>

- Paoletti, M.G., Pimentel, D., Stinner, B.R., Stinner, D., 1992. Agroecosystem biodiversity: matching production and conservation biology. *Agric. Ecosyst. Environ.* 40, 3–23. [https://doi.org/10.1016/0167-8809\(92\)90080-U](https://doi.org/10.1016/0167-8809(92)90080-U)
- Park, J.K., Park, J.H., 2015. Crops classification using imagery of unmanned aerial vehicle (UAV). *J. Korean Soc. Agric. Eng.* 57, 91–97. <https://doi.org/10.5389/KSAE.2015.57.6.091>
- Paustian, M., Theuvsen, L., 2017. Adoption of precision agriculture technologies by German crop farmers. *Precis. Agric.* 18, 701–716. <https://doi.org/10.1007/s11119-016-9482-5>
- Peña, J.M., Torres-Sánchez, J., Castro, A.I. de, Kelly, M., López-Granados, F., 2013. Weed mapping in early-season maize fields using object-based analysis of unmanned aerial vehicle (UAV) images. *PLoS ONE* 8, e77151. <https://doi.org/10.1371/journal.pone.0077151>
- Peña, J.M., Torres-Sánchez, J., Serrano-Pérez, A., De Castro, A.I., López-Granados, F., 2015. Quantifying efficacy and limits of unmanned aerial vehicle (UAV) technology for weed seedling detection as affected by sensor resolution. *Sensors* 15, 5609–5626. <https://doi.org/10.3390/s150305609>
- Peña-Barragán, J.M., López-Granados, F., Jurado-Expósito, M., García-Torres, L., 2007. Mapping *Ridolfia segetum* patches in sunflower crop using remote sensing. *Weed Res.* 47, 164–172. <https://doi.org/10.1111/j.1365-3180.2007.00553.x>
- Pérez-Ortiz, M., Gutiérrez, P.A., Peña, J.M., Torres-Sánchez, J., Hervás-Martínez, C., López-Granados, F., 2015. An experimental comparison for the identification of weeds in sunflower crops via unmanned aerial vehicles and object-based analysis, in: Rojas, I., Joya, G., Catala, A. (Eds.), *Advances in Computational Intelligence, Lecture Notes in Computer Science*. Springer International Publishing, pp. 252–262.
- Pérez-Ortiz, M., Peña, J.M., Gutiérrez, P.A., Torres-Sánchez, J., Hervás-Martínez, C., López-Granados, F., 2016. Selecting patterns and features for between- and within-crop-row weed mapping using UAV-imagery. *Expert Syst. Appl.* 47, 85–94. <https://doi.org/10.1016/j.eswa.2015.10.043>
- Pfeiffer, S.A., Guevara, J., Cheein, F.A., Sanz, R., 2018. Mechatronic terrestrial LiDAR for canopy porosity and crown surface estimation. *Comput. Electron. Agric.* 146, 104–113. <https://doi.org/10.1016/j.compag.2018.01.022>
- Pöölönen, I., Saari, H., Kaivosoja, J., Honkavaara, E., Pesonen, L., 2013. Hyperspectral imaging based biomass and nitrogen content estimations from light-weight UAV. Presented at the Remote Sensing for Agriculture, Ecosystems, and Hydrology XV, International Society for Optics and Photonics, p. 88870J. <https://doi.org/10.1117/12.2028624>

Rango, A., Laliberte, A., Herrick, J.E., Winters, C., Havstad, K.M., Steele, C., Browning, D.M., 2009. Unmanned aerial vehicle-based remote sensing for rangeland assessment, monitoring, and management. *J. Appl. Remote Sens.* 3, 033542. <https://doi.org/10.1117/1.3216822>

Real Decreto 1311, 2012. Real Decreto 1311/2012, de 14 de septiembre, por el que se establece el marco de actuación para conseguir un uso sostenible de los productos fitosanitarios. <https://www.boe.es/buscar/pdf/2012/BOE-A-2012-11605-consolidado.pdf>

Recasens, J., Cabrera, C., Valencia, F., De Castro, A.I., Royo, A., Torres-Sánchez, J., Civit, J., Jiménez-Brenes, F.M., López-Granados, F., 2019. Manejo, dinámica espacio-temporal y detección aérea de rodales de *Cynodon dactylon* en viñedos con cubierta vegetal. XVII Congreso de la Sociedad Española de Malherbología, Vigo.

Reganold, J.P., Elliott, L.F., Unger, Y.L., 1987. Long-term effects of organic and conventional farming on soil erosion. *Nature* 330, 370-372. <https://doi.org/10.1038/330370ao>

Reglamento 1107, 2009. Reglamento (CE) no 1107/2009 del Parlamento Europeo y del Consejo, de 21 de octubre de 2009, relativo a la comercialización de productos fitosanitarios y por el que se derogan las Directivas 79/117/CEE y 91/414/CEE del Consejo. <https://www.boe.es/doue/2009/309/L00001-00050.pdf>

Ribeiro, A., Bengochea-Guevara, J.M., Conesa-Muñoz, J., Nuñez, N., Cantuña, K., Andújar, D., 2017. 3D monitoring of woody crops using an unmanned ground vehicle. *Adv. Anim. Biosci.* 8, 210–215. <https://doi.org/10.1017/S2040470017001200>

Robert, P.C., 2002. Precision agriculture: a challenge for crop nutrition management. *Plant Soil* 247, 143–149. <https://doi.org/10.1023/A:1021171514148>

Roman, A., Ursu, T.M., 2016. Multispectral satellite imagery and airborne laser scanning techniques for the detection of archaeological vegetation marks. In book: Landscape archaeology on the northern frontier of the Roman Empire at Porolissum—an interdisciplinary research project.

https://www.researchgate.net/publication/315797574_Multispectral_satellite_image_ry_and_airborne_laser_scanning_techniques_for_the_detection_of_archaeological_vegetation_marks

Rosell, J.R., Sanz, R., 2012. A review of methods and applications of the geometric characterization of tree crops in agricultural activities. *Comput. Electron. Agric.* 81, 124–141. <https://doi.org/10.1016/j.compag.2011.09.007>

Rueda-Ayala, V.P., Peña, J.M., Höglind, M., Bengochea-Guevara, J.M., Andújar, D., 2019. Comparing UAV-based technologies and RGB-D reconstruction methods for plant

- height and biomass monitoring on grass ley. *Sensors* 19(3), 535. <https://doi.org/10.3390/s19030535>
- Santesteban, L.G., Di Gennaro, S.F., Herrero-Langreo, A., Miranda, C., Royo, J.B., Matese, A., 2017. High-resolution UAV-based thermal imaging to estimate the instantaneous and seasonal variability of plant water status within a vineyard. *Agric. Water Manag.*, Special Issue: Advances on ICTs for Water Management in Agriculture 183, 49–59. <https://doi.org/10.1016/j.agwat.2016.08.026>
- Sanz, R., Llorens, J., Escolà, A., Arnó, J., Planas, S., Román, C., Rosell-Polo, J.R., 2018. LIDAR and non-LIDAR-based canopy parameters to estimate the leaf area in fruit trees and vineyard. *Agric. For. Meteorol.* 260–261, 229–239. <https://doi.org/10.1016/j.agrformet.2018.06.017>
- Schmidt, K.S., Skidmore, A.K., 2003. Spectral discrimination of vegetation types in a coastal wetland. *Remote Sens. Environ.* 85, 92–108. [https://doi.org/10.1016/S0034-4257\(02\)00196-7](https://doi.org/10.1016/S0034-4257(02)00196-7)
- Seelan, S.K., Laguette, S., Casady, G.M., Seielstad, G.A., 2003. Remote sensing applications for precision agriculture: A learning community approach. *Remote Sens. Environ.*, IKONOS Fine Spatial Resolution Land Observation 88, 157–169. <https://doi.org/10.1016/j.rse.2003.04.007>
- Senthilnath, J., Dokania, A., Kandukuri, M., K.n., R., Anand, G., Omkar, S.N., 2016. Detection of tomatoes using spectral-spatial methods in remotely sensed RGB images captured by UAV. *Biosyst. Eng.*, Special issue: advances in robotic agriculture for crops 146, 16–32. <https://doi.org/10.1016/j.biosystemseng.2015.12.003>
- Shaner, D.L., Beckie, H.J., 2014. The future for weed control and technology. *Pest Manag. Sci.* 70, 1329–1339. <https://doi.org/10.1002/ps.3706>
- Shibusawa, S., 1998. Precision farming and terra-mechanics. Fifth ISTVS Asia-Pacific Regional Conference in Korea, October 20-22, 1998.
- Souza, C.H.W. de, Lamparelli, R.A.C., Rocha, J.V., Magalhães, P.S.G., 2017. Mapping skips in sugarcane fields using object-based analysis of unmanned aerial vehicle (UAV) images. *Comput. Electron. Agric.* 143, 49–56. <https://doi.org/10.1016/j.compag.2017.10.006>
- Srinivasan, A., 2006. Handbook of Precision Agriculture: Principles and Applications. Taylor & Francis. 683 pp.
- Tahmasebi, B.K., Alebrahim, M.T., Roldán-Gómez, R.A., Silveira, H.M. da, Carvalho, L.B. de, Alcántara-de la Cruz, R., De Prado, R., 2018. Effectiveness of alternative herbicides on three *Conyza* species from Europe with and without glyphosate resistance. *Crop Prot.* 112, 350–355. <https://doi.org/10.1016/j.cropro.2018.06.021>

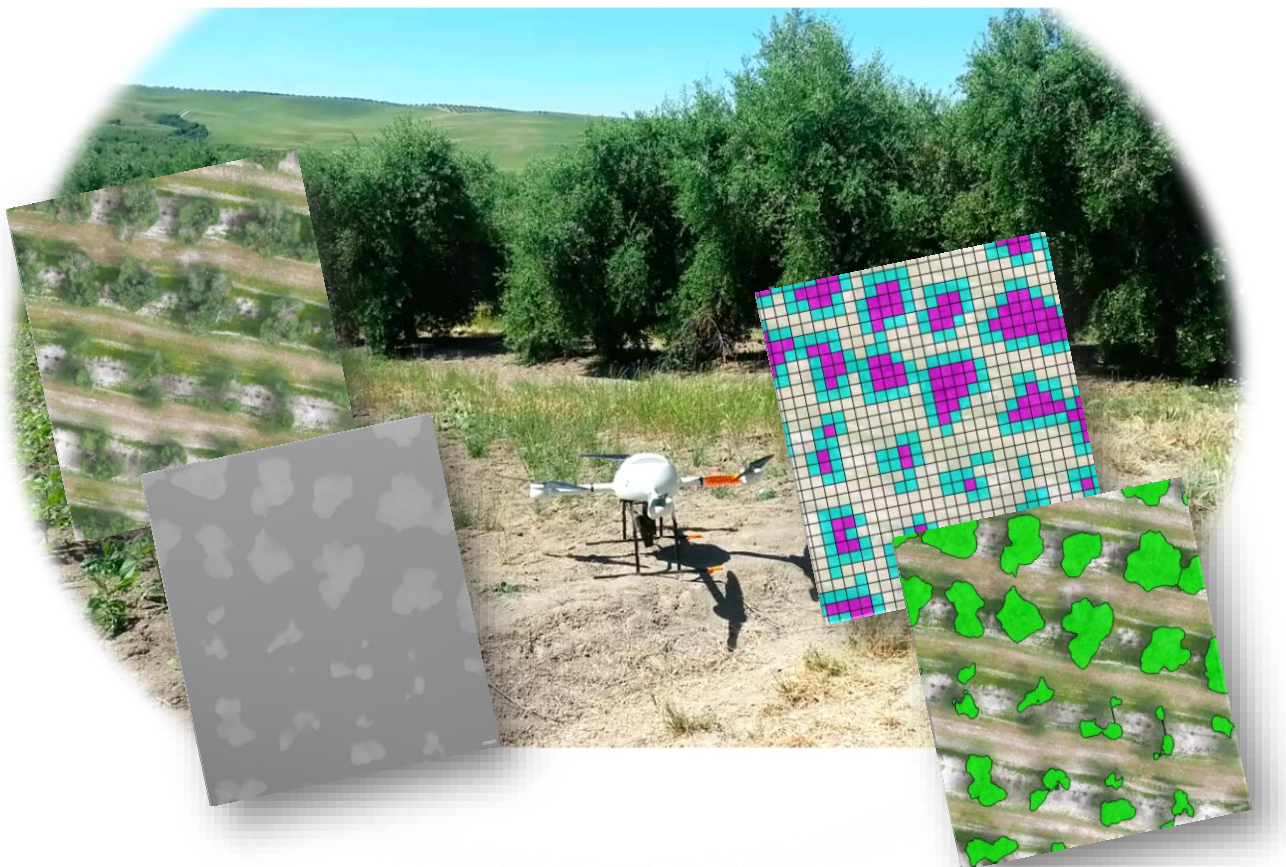
- Taylor, J., 2018. Capital growth: precision agriculture and vertical farming in the corporate food regime. Diss. Theses Capstone Proj.
https://academicworks.cuny.edu/cgi/viewcontent.cgi?article=3682&context=gc_etds
- Thorp, K.R., Tian, L.F., 2004. A review on remote sensing of weeds in agriculture. *Precis. Agric.* 5, 477–508. <https://doi.org/10.1007/s11119-004-5321-1>
- Tian, L., 2002. Development of a sensor-based precision herbicide application system. *Comput. Electron. Agric.* 36, 133–149. [https://doi.org/10.1016/S0168-1699\(02\)00097-2](https://doi.org/10.1016/S0168-1699(02)00097-2)
- Torres-Sánchez, J. 2017. Monitorización 3D de cultivos y cartografía de malas hierbas mediante vehículos aéreos no tripulados para un uso sostenible de fitosanitarios. Tesis Doctoral. Universidad de Córdoba.
- Torres-Sánchez, J., de Castro, A.I., Peña, J.M., Jiménez-Brenes, F.M., Arquero, O., Lovera, M., López-Granados, F., 2018. Mapping the 3D structure of almond trees using UAV acquired photogrammetric point clouds and object-based image analysis. *Biosyst. Eng.* 176, 172–184. <https://doi.org/10.1016/j.biosystemseng.2018.10.018>
- Torres-Sánchez, J., F. López-Granados, Serrano, N., Arquero, O., Peña, J.M., 2015. High-throughput 3-D monitoring of agricultural-tree plantations with unmanned aerial vehicle (UAV) Technology. *PLoS ONE* 10(6): e0130479.
<https://doi.org/10.1371/journal.pone.0130479>
- Torres-Sánchez, J., López-Granados, F., Castro, A.I.D., Peña-Barragán, J.M., 2013. Configuration and specifications of an unmanned aerial vehicle (UAV) for early site specific weed management. *PLoS ONE* 8(3): e58210.
<https://doi.org/10.1371/journal.pone.0058210>
- Torres-Sánchez, J., Peña, J.M., de Castro, A.I., López-Granados, F., 2014. Multi-temporal mapping of the vegetation fraction in early-season wheat fields using images from UAV. *Comput. Electron. Agric.* 103, 104–113.
<https://doi.org/10.1016/j.compag.2014.02.009>
- Underwood, J.P., Hung, C., Whelan, B., Sukkarieh, S., 2016. Mapping almond orchard canopy volume, flowers, fruit and yield using lidar and vision sensors. *Comput. Electron. Agric.* 130, 83–96. <https://doi.org/10.1016/j.compag.2016.09.014>
- Valencia, F., Mas, N., Recasens, J., 2017. El uso de cubiertas vegetales y sus labores de implantación en el manejo de *Cynodon dactylon* en viñedo. Actas XVI Congreso de la Sociedad Española de Malherbología. Universidad Pública de Navarra. pp 147-152.
- Vitousek, P.M., Aber, J.D., Howarth, R.W., Likens, G.E., Matson, P.A., Schindler, D.W., Schlesinger, W.H., Tilman, D.G., 1997. Human alteration of the global nitrogen cycle:

- sources and consequences. *Ecol. Appl.* 7, 737–750. [https://doi.org/10.1890/1051-0761\(1997\)007\[0737:HAOTGN\]2.0.CO;2](https://doi.org/10.1890/1051-0761(1997)007[0737:HAOTGN]2.0.CO;2)
- Wallace, L., Lucieer, A., Watson, C., Turner, D., 2012. Development of a UAV-LiDAR system with application to forest inventory. *Remote Sens.* 4, 1519–1543. <https://doi.org/10.3390/rs4061519>
- Wang, L., Zhou, X., Zhu, X., Dong, Z., Guo, W., 2016. Estimation of biomass in wheat using random forest regression algorithm and remote sensing data. *Crop J.* 4, 212–219. <https://doi.org/10.1016/j.cj.2016.01.008>
- West, P.W., 2009. Tree and forest measurement. Springer Berlin Heidelberg, Berlin, Heidelberg.
- Woodcock, C.E., Strahler, A.H., 1987. The factor of scale in remote sensing. *Remote Sens. Environ.* 21, 311–332. [https://doi.org/10.1016/0034-4257\(87\)90015-0](https://doi.org/10.1016/0034-4257(87)90015-0)
- WSSA, 2016. Do you have a weed, noxious weed, invasive weed or “superweed”? <http://wssa.net/wp-content/uploads/WSSA-Weed-Science-Definitions.pdf>
- Wu, X., Shen, X., Cao, L., Wang, G., Cao, F., 2019. Assessment of individual tree detection and canopy cover estimation using unmanned aerial vehicle based light detection and ranging (UAV-LiDAR) data in planted forests. *Remote Sens.* 11, 908. <https://doi.org/10.3390/rs11080908>
- Xiang, H., Tian, L., 2011. Method for automatic georeferencing aerial remote sensing (RS) images from an unmanned aerial vehicle (UAV) platform. *Biosyst. Eng.* 108, 104–113. <https://doi.org/10.1016/j.biosystemseng.2010.11.003>
- Yalew, S.G., van Griensven, A., Mul, M.L., van der Zaag, P., 2016. Land suitability analysis for agriculture in the Abbay basin using remote sensing, GIS and AHP techniques. *Model. Earth Syst. Environ.* 2, 101. <https://doi.org/10.1007/s40808-016-0167-x>
- Yang, G., Liu, J., Zhao, C., Li, Zhenhong, Huang, Y., Yu, H., Xu, B., Yang, X., Zhu, D., Zhang, X., Zhang, R., Feng, H., Zhao, X., Li, Zhenhai, Li, H., Yang, H., 2017. Unmanned aerial vehicle remote sensing for field-based crop phenotyping: current status and perspectives. *Front. Plant Sci.* 8. <https://doi.org/10.3389/fpls.2017.01111>
- You, J., Li, X., Low, M., Lobell, D., Ermon, S., 2017. Deep gaussian process for crop yield prediction based on remote sensing data, in: Thirty-First AAAI Conference on Artificial Intelligence. Presented at the Thirty-First AAAI Conference on Artificial Intelligence. <https://aaai.org/ocs/index.php/AAAI/AAAI17/paper/view/14435/14067>
- Yu, Q., Gong, P., Clinton, N., Biging, G., Kelly, M., Schirokauer, D., 2006. Object-based detailed vegetation classification with airborne high spatial resolution remote sensing

- imagery. *Photogramm. Eng. Remote Sens.* 72, 799–811.
<https://doi.org/10.14358/PERS.72.7.799>
- Yue, J., Lei, T., Li, C., Zhu, J., 2012. The application of unmanned aerial vehicle remote sensing in quickly monitoring crop pests. *Intell. Autom. Soft Comput.* 18, 1043–1052.
<https://doi.org/10.1080/10798587.2008.10643309>
- Zarco-Tejada, P.J., Díaz-Varela, R., Angileri, V., Loudjani, P., 2014. Tree height quantification using very high resolution imagery acquired from an unmanned aerial vehicle (UAV) and automatic 3D photo-reconstruction methods. *Eur. J. Agron.* 55, 89–99. <https://doi.org/10.1016/j.eja.2014.01.004>
- Zhang, C., Kovacs, J.M., 2012. The application of small unmanned aerial systems for precision agriculture: a review. *Precis. Agric.* 13, 693–712.
<https://doi.org/10.1007/s11119-012-9274-5>
- Zhang, J.-H., Wang, K., Bailey, J.S., Wang, R.-C., 2006. Predicting nitrogen status of rice using multispectral data at canopy scale project supported by the national natural science foundation of China (Nos. 30070444 and 40201021), the British Council (No. SHA/992/308), and the Doctor Foundation of Qingdao University of Science and Technology. *Pedosphere* 16, 108–117. [https://doi.org/10.1016/S1002-0160\(06\)60032-5](https://doi.org/10.1016/S1002-0160(06)60032-5)
- Zhu, J., Wang, K., Deng, J., Harmon, T., 2009. Quantifying nitrogen status of rice using low altitude UAV-mounted system and object-oriented segmentation methodology. *ASME* 3, 603–609. <https://doi.org/10.1115/DETC2009-87107>

Capítulo 2

Quantifying pruning impacts on olive tree architecture and annual canopy growth by using UAV-based 3D modelling



F.M. Jiménez-Brenes, F. López-Granados, A.I. de Castro, J. Torres-Sánchez, N. Serrano, J.M. Peña. (2017). Quantifying pruning impacts on olive tree architecture and annual canopy growth by using UAV-based 3D modelling. *Plant Methods*, 13:55.
<https://doi.org/10.1186/s13007-017-0205-3> (Open Access)

1. Resumen

Antecedentes

La poda es una práctica costosa con importantes implicaciones en la cosecha y nutrición de los cultivos, el control de plagas y enfermedades, la protección del suelo y las estrategias de riego. Las investigaciones sobre la poda suelen realizarse a través de tediosas mediciones en campo de las dimensiones primarias de las copas de los árboles, que también pueden generar resultados inconsistentes debido a la geometría irregular de los árboles. Como alternativa al trabajo de campo intensivo, este estudio muestra un procedimiento innovador basado en la combinación de la tecnología de vehículos aéreos no tripulados (UAV) y la metodología avanzada de análisis de imagen basado en objetos (OBIA) para la monitorización multitemporal tridimensional (3D) de cientos de olivos que fueron podados con tres estrategias diferentes (poda tradicional, adaptada y mecánica). Las imágenes UAV fueron adquiridas antes de la poda, después de la poda y un año después de la poda, siendo cuantificados y analizados los impactos de cada tratamiento de poda a lo largo del tiempo sobre el área proyectada, altura y volumen de copa de cada olivo.

Resultados

El procedimiento completo descrito aquí identificó automáticamente cada olivo de la parcela y calculó sus dimensiones primarias en 3D en las tres fechas del estudio con alta precisión en la mayoría de los casos. La poda adaptada fue, en general, el tratamiento más agresivo en términos de área proyectada y volumen (los árboles disminuyeron un 38,95 y un 42,05% de media, respectivamente), seguidos de los árboles de poda tradicional (33,02 y 35,72% de media, respectivamente). En cuanto a las alturas de los árboles, la poda mecánica produjo una mayor disminución (12,15%), siendo mínimos estos valores para los otros dos tratamientos. El crecimiento del árbol durante un año se vio afectado por la severidad de la poda y por el tipo de tratamiento de poda, es decir, los árboles de poda adaptada experimentaron un mayor crecimiento que los árboles de los otros dos tratamientos cuando la intensidad de poda era baja (<10%), similar a los árboles tradicionalmente podados con una intensidad moderada (10-30%), y más bajo que los otros árboles cuando la intensidad de poda era superior al 30% del volumen de la copa.

Conclusiones

La combinación de imágenes basadas en UAV con un procedimiento OBIA permitió medir las dimensiones de los árboles y cuantificar los impactos de tres diferentes tratamientos de poda sobre cientos de olivos con un mínimo trabajo de campo. Las pérdidas de follaje de los árboles y el crecimiento anual de la copa mostraron diferentes

tendencias según el tipo y la severidad de los tratamientos de poda. Además, esta tecnología ofrece información geoespacial muy valiosa para el diseño de estrategias de manejo de cultivos específicos en el contexto de la agricultura de precisión, con los consiguientes beneficios económicos y ambientales.

2. Abstract

Background

Tree pruning is a costly practice with important implications for crop harvest and nutrition, pest and disease control, soil protection and irrigation strategies. Investigations on tree pruning usually involve tedious on-ground measurements of the primary tree crown dimensions, which also might generate inconsistent results due to the irregular geometry of the trees. As an alternative to intensive field-work, this study shows an innovative procedure based on combining unmanned aerial vehicle (UAV) technology and advanced object-based image analysis (OBIA) methodology for multi-temporal three-dimensional (3D) monitoring of hundreds of olive trees that were pruned with three different strategies (traditional, adapted and mechanical pruning). The UAV images were collected before pruning, after pruning and a year after pruning, and the impacts of each pruning treatment on the projected canopy area, tree height and crown volume of every tree were quantified and analyzed over time.

Results

The full procedure described here automatically identified every olive tree on the orchard and computed their primary 3D dimensions on the three study dates with high accuracy in the most cases. Adapted pruning was generally the most aggressive treatment in terms of the area and volume (the trees decreased by 38.95 and 42.05% on average, respectively), followed by trees under traditional pruning (33.02 and 35.72% on average, respectively). Regarding the tree heights, mechanical pruning produced a greater decrease (12.15%), and these values were minimal for the other two treatments. The tree growth over one year was affected by the pruning severity and by the type of pruning treatment, i.e., the adapted-pruning trees experienced higher growth than the trees from the other two treatments when pruning intensity was low (<10%), similar to the traditionally pruned trees at moderate intensity (10–30%), and lower than the other trees when the pruning intensity was higher than 30% of the crown volume.

Conclusions

Combining UAV-based images and an OBIA procedure allowed measuring tree dimensions and quantifying the impacts of three different pruning treatments on hundreds of trees with minimal field work. Tree foliage losses and annual canopy growth showed different trends as affected by the type and severity of the pruning treatments. Additionally, this technology offers valuable geo-spatial information for designing site-specific crop management strategies in the context of precision agriculture, with the consequent economic and environmental benefits.

3. Introduction

Crop viability essentially relies on the management strategy adopted by the farmer. Among the tasks that impact orchard production, tree pruning remains as a costly practice with important implications for harvest (Ferguson et al., 2012), nutrition, pest and disease control, and irrigation strategies (Connor et al., 2014). The pruning type and its intensity modify the tree crown to differing degrees of severity, which notably affects the tree physiology and, consequently, the fruit quantity and quality (Castillo-Ruiz et al., 2015; Villalobos et al., 2006). Investigations on tree pruning usually involve the characterization of the tree architecture by measuring several geometric features of the crown. The conventional method consists in using a ruler to measure the primary dimensions of the tree (e.g., the tree height and its primary axis) and, next, estimating the canopy area and the crown volume either by applying equations that treat the trees as regular polygons or by applying empirical models (Miranda-Fuentes et al., 2015). Obviously, this task is very tedious; it requires intensive fieldwork and usually generates inconsistent results due to the irregular geometry of the tree crown (West, 2009).

Current advances in sensors and geo-spatial technologies offer an alternative to hands-on measurement tasks. Rosell and Sanz (2012) described the following techniques: ultrasound, digital photographic techniques, light sensors, high-resolution radar images, high-resolution X-ray computed tomography, stereovision and LiDAR sensors. However, although some of these techniques, primarily terrestrial LiDAR laser scanning and stereovision systems, are very precise at measuring crop architecture (Friedli et al., 2016; Rovira-Más et al., 2008), they still pose some limitations under real agricultural scenarios that are usually characterized by large spaces and rugged areas. In these cases, Unmanned Aerial Vehicles (UAVs) or drones have become a cost-effective tool for collecting continuous crop information at the field scale. The advantages of the UAVs in comparison to the traditional remote-sensing platforms are attributed to their lower cost, greater flexibility in

flight scheduling and their capacity to collect remote images with much higher spatial resolution (Torres-Sánchez et al., 2014; Xiang and Tian, 2011; Zhang and Kovacs, 2012). In addition, because the UAVs can fly at low altitude and acquire images with high overlaps, these images can be processed with automatic photo-reconstruction software and be used to produce a Digital Surface Model (DSM) of the flight area, i.e., the three dimensions (3D) of the topography and all the elements (e.g., trees) over the surface (Nex and Remondino, 2014). As a consequence, recent investigations have focused on evaluating the quality of UAV-based 3D models of tree plantations, and they have reported satisfactory results for olive trees (Díaz-Varela et al., 2015; Torres-Sánchez et al., 2015; Zarco-Tejada et al., 2014), palm trees (Kattenborn et al., 2014) and *Pinus pinea* (Guerra-Hernández et al., 2016). For example, by comparing UAV-based estimations of olive trees to on-ground measurements, Torres-Sánchez et al. (2015) obtained coefficients of determination (R^2) of 0.94, 0.90 and 0.65 for projected canopy area, tree height and crown volume, respectively.

To seize on all the benefits of the UAV capacity for collecting detailed information over large areas at a spatial resolution of a few centimeters, it is essential to develop and apply robust and automatic image analysis tools that are capable of computing a huge amount of crop data to produce useful maps for crop monitoring or other agronomic objectives. The Object-Based Image Analysis (OBIA) paradigm includes a wide array of techniques that offer a high level of automation and adaptability, improving on some of the limitations of pixel-based methods (Castillejo-González et al., 2014). OBIA is based on two primary stages, called segmentation and classification. In the first stage, adjacent pixels with homogenous digital values are grouped as “objects”, which are used as the basic elements of analysis and classification (Blaschke et al., 2014). In the second stage, OBIA combines the spectral, topological and contextual features of these objects to successfully address complicated classification issues, e.g., in rangelands (López-Granados et al., 2016; Peña et al., 2013), or urban areas (Qin, 2014).

The combined use of UAV images, 3D models and OBIA procedures offers new opportunities for the high-throughput monitoring of crop conditions at the level of individual plants or trees (Rousseau et al., 2015). Therefore, this study takes advantage of this geo-spatial technology to compute the 3D geometric features of hundreds of olive trees with the ultimate objective of quantifying the pruning impact on the tree architecture and tree growth. Three different pruning treatments were evaluated by comparing a multi-temporal UAV-based dataset that was collected before tree pruning, after tree pruning and one year after tree pruning. The specific objectives of this research were separated in two linked sections (Figure 1) as follows: a) technological objectives, which involved the description and evaluation of the full procedure to acquire remote images with the UAV and to generate the image-based 3D tree models. These objectives included the development and implementation of an innovative OBIA algorithm with the capacity to automatically

classify and identify every tree of the olive grove and to compute their position, projected area, height, and volume; and b) agronomic objectives, which aimed to explore and interpret the temporal variability that was measured within the olive grove as affected by every applied pruning treatment. Additionally, the potential uses of the valuable dataset and maps obtained with this technology were also discussed, including applications for physiological and agronomical studies as well for designing site-specific crop management strategies in the context of precision agriculture.

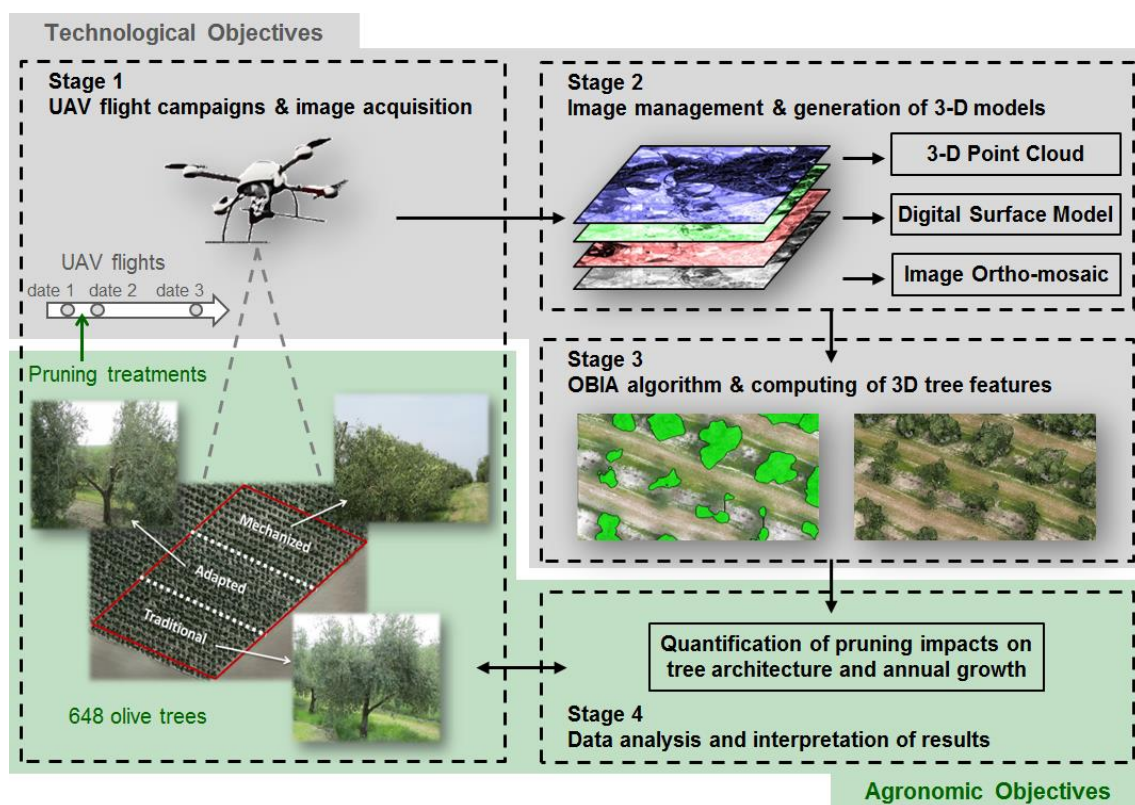


Figure 1. Graphical scheme of the stages and specific technological and agronomic objectives of this investigation.

4. Results

4.1. Technological objectives: multi-temporal quantification of the tree 3D features (location, projected canopy area, tree height and crown volume) at the field scale

The OBIA algorithm that was developed for this investigation automatically identified all the olive trees and reported their geographic coordinates, projected areas, heights and volumes on the three study dates (Table 1). The algorithm also accounted for the relative position of the trees, i.e. their row number (from 1 to 27) and their order in the row (from 1 to 24), which facilitated their localization within the field.

Table 1. A sample of the output dataset delivered by the customized OBIA algorithm.

Tree ID	Row	Column	Central Coordinates*		Pruning Treatment	Projected Canopy Area (m ²)			Tree Height (m)			Crown Volume (m ³)		
			X	Y		Date 1	Date 2	Date 3	Date 1	Date 2	Date 3	Date 1	Date 2	Date 3
1	1	1	485726	4217762	Traditional	15.38	12.44	17.24	3.81	3.72	3.75	44.09	34.74	43.16
2	1	2	485732	4217760	Traditional	15.88	9.61	16.69	4.10	4.01	4.14	47.75	27.52	44.68
3	1	3	485738	4217757	Traditional	13.98	10.77	14.58	3.91	3.62	3.70	35.42	26.68	34.68
...
217	10	1	485786	4217808	Adapted	15.34	5.16	11.13	4.37	4.04	4.43	43.81	13.28	31.43
218	10	2	485789	4217806	Adapted	14.96	5.46	12.26	3.81	3.80	3.97	43.81	15.15	35.45
219	10	3	485795	4217803	Adapted	12.64	7.62	13.02	4.53	3.77	3.45	31.73	18.99	27.43
...
433	19	1	485840	4217852	Mechanical	7.00	5.75	7.20	3.85	3.48	3.83	18.78	15.67	17.68
434	19	2	485846	4217851	Mechanical	10.11	10.00	13.64	4.31	3.58	3.79	27.28	26.73	31.97
435	19	3	485850	4217848	Mechanical	13.55	13.46	14.93	4.17	3.54	3.61	43.87	39.38	42.49
...
648	27	24	486017	4217841	Mechanical	6.06	5.93	6.30	3.48	3.34	3.54	15.27	14.52	15.46

* Coordinate system: UTM, zone 30N, datum WGS84.

The computed values were generally consistent on the three dates, decreasing from date 1 to date 2 as a result of the pruning operation, and increasing from date 2 to date 3 due to the tree development that occurred over one year. On average, the projected canopy areas varied from a range of 11.6-14.7 m² on date 1 (before pruning) to 8.4-10.7 m² on date 2 (after pruning) and to 13.7-15.1 m² on date 3 (1-year after pruning). Similarly, the tree heights varied over a range from 3.9-4.1 m (on date 1) to 3.4-4.1 m (on date 2) and to 3.3-4.2 m (on date 3), and the crown volumes varied over a range from 31.9-42.7 m³ (on date 1) to 22.7-28.1 m³ (on date 2) and to 32.8-41.0 m³ (on date 3).

However, detailed observations of the full dataset revealed incorrect dimensions for some trees, which could be attributed to errors that occurred during the DSM generation. Therefore, the quality of the DSM created on the three dates was evaluated by visually comparing every tree perimeter that was defined by the OBIA algorithm (which was based on the DSM information) and the real tree perimeter observed in the orthomosaicked image. The accuracy that was achieved for the full 3D tree photo-reconstruction procedure varied as affected by the type of pruning treatment and the flight date (Table 2).

Table 2. Number and percentage of trees correctly photo-reconstructed on one of the three study dates (columns Date 1, Date 2 and Date 3) and on all the three study dates (column 1-2-3).

Pruning Treatment	Number of trees	Date 1	Date 2	Date 3	Dates 1-2-3
Mechanical	216	185 (85.7 %)	208 (96.3 %)	191 (88.4 %)	177 (81.9 %)
Adapted	216	200 (92.6 %)	163 (75.5 %)	177 (81.9 %)	161 (74.5 %)
Traditional	216	200 (92.6 %)	180 (83.3 %)	190 (88.0 %)	174 (80.6 %)

Flight dates: Date 1 (Before pruning); Date 2 (After pruning); Date 3 (1-year after pruning).

When the three dates were jointly considered, the most accurate olive tree photo-reconstruction was obtained for mechanical pruning (MP). However, for individual dates, the worst and best results for the three treatments were all obtained on date 2, after pruning. These values varied from 75.5% at the adapted pruning (AP) parcel, to 83.3% at the traditional pruning (TP) parcel and to 96.3% at the MP parcel. This finding could be due to the specific characteristics of each treatment. The MP removed protruding branches, which produced a tree shape that was more uniform than that of the other pruning treatments, thus facilitating the task of building the 3D point cloud field geometry and consequently, the correct definition and photo-reconstruction of the MP tree edges. In the AP treatment, pruning drastically cut back the crown biomass of the trees, which increased the overall tree shape heterogeneity. As a result, the accuracy of the photo-reconstruction of some of the trees decreased. These results indicate that the pruning treatment affected the tree architecture and crown size, and it might have also positively or negatively affected the quality of the UAV-based 3D geo-spatial products. Additionally, no correlation between every tree location and photo-reconstruction errors was found at the orchard scale, which also indicates that other factors with respect to the weather conditions (e.g., wind or clouds) or operational issues (e.g., flight altitude, orientation of sensor axes or UAV velocity) could apparently produce slight random changes at the moment of image shooting. As a result of this evaluation, 512 trees (approximately 80 % of the total) that were correctly photo-reconstructed on the three dates were studied in the subsequent analysis, and the rest of the

trees were discarded to avoid imprecise conclusions in the context of the agronomic objectives proposed in this investigation.

The detailed information reported in Table 1 was ranked as four levels of projected canopy area (Figure 2), tree height (Figure 3) and crown volume (Figure 4), which allowed for the observation of all the tree variability at the orchard scale.

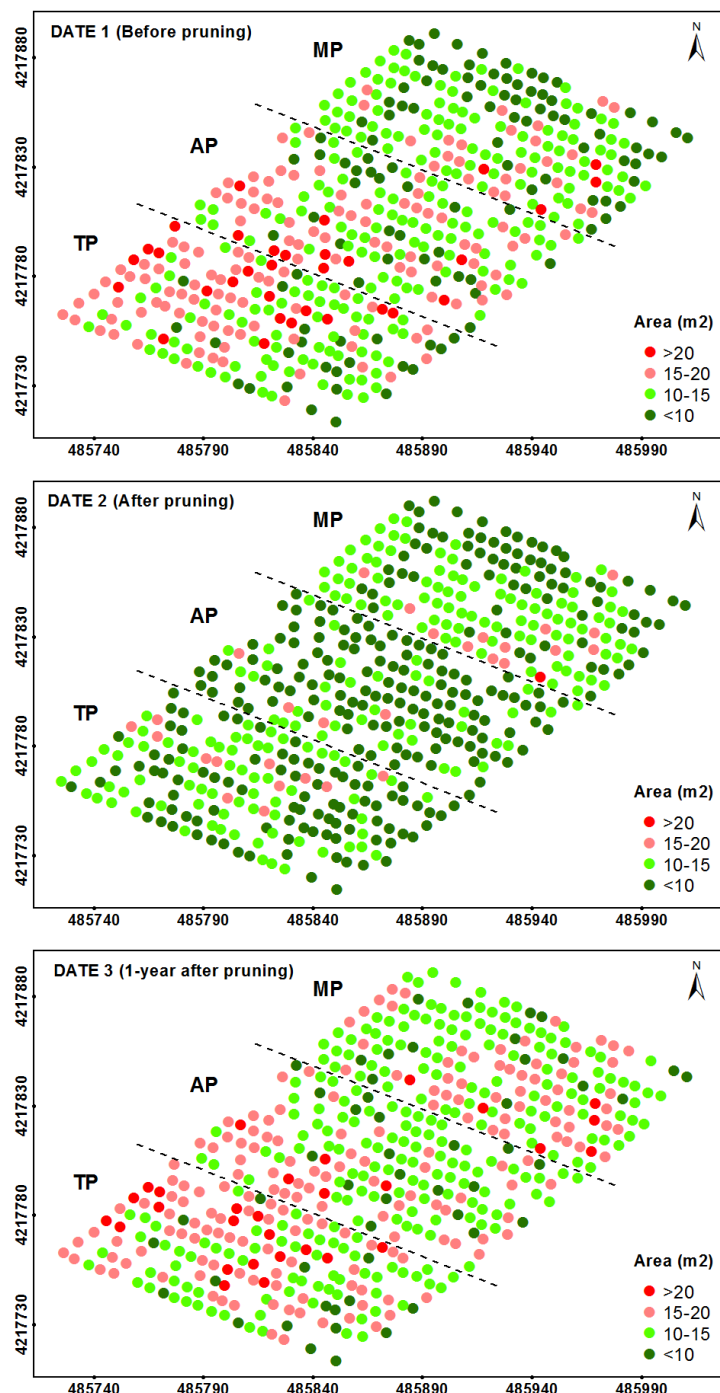


Figure 2. Four-level representation of the projected tree canopy areas as computed on the three study dates. The letters indicate the pruning treatments as follows: TP (traditional), AP (adapted), and MP (mechanical). In the axes, coordinate system UTM zone 30N, datum WGS84.

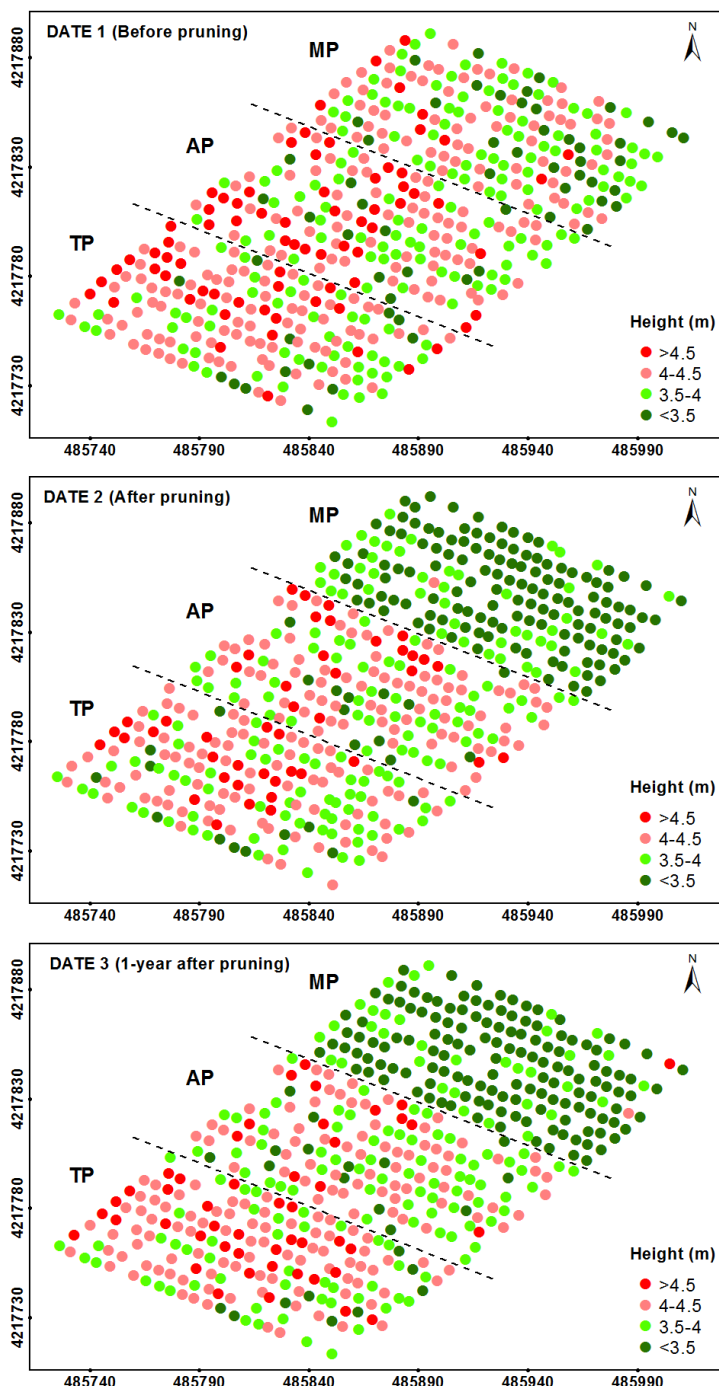


Figure 3. Four-level representation of the tree heights as computed on the three study dates. The letters indicate the pruning treatments as follows: TP (traditional), AP (adapted), and MP (mechanical). In the axes, coordinate system UTM zone 30N, datum WGS84.

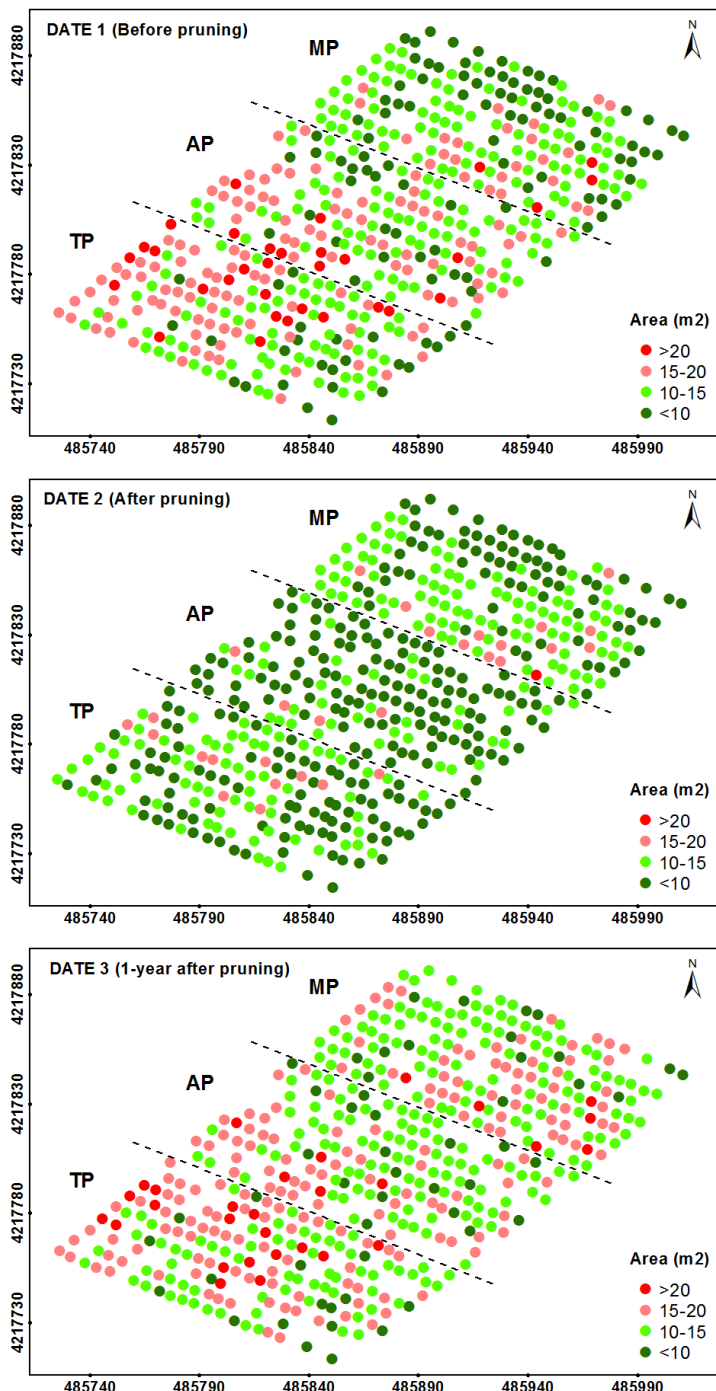


Figure 4. Four-level representation of the tree crown volumes as computed on the three study dates. The letters indicate the pruning treatments as follows: TP (traditional), AP (adapted), and MP (mechanical). In the axes, coordinate system UTM zone 30N, datum WGS84.

A view of these figures on date 1 (before pruning) revealed the distribution of the tree sizes throughout the orchard, showing a higher number of small trees located at the three upper rows of the graph, which corresponded to the top zone of the field. On date 2 (after pruning), the homogeneity of the tree heights was clearly notable at the MP parcel (Figure 3), as shown by a coefficient of variation (CV) of only 6%. On this date, a severe reduction of

the projected canopy areas and crown volumes was also observed on the trees located at the AP and TP zones. Next, the geometric features on date 3 (1-year after pruning) of a majority of the trees showed similar values to the one observed on date 1 for the projected areas and crown volumes (Figures 2 and 4, respectively) and on date 2 for the tree heights (Figure 3). This finding indicates that the olive trees grew in area and volume over the duration of this experiment, but not in height.

4.2. Agronomic objectives: impact of every pruning treatment on the tree architecture, annual tree growth and tree restoration

The impact of the pruning treatments on the tree architecture was evaluated by comparing tree dimensions on date 2 (after pruning) and date 1 (before pruning) (Figure 5, Table 3). The AP treatment was generally the most aggressive for the olive trees, producing an average decrease of approximately 40% in canopy area and crown volume. However, the heights of the AP trees only decreased by an average of 0.05 m. These values were slightly greater than the ones obtained for the TP treatment. Regarding the MP treatment, the heights of these trees decreased 0.51 m on average, being up to ten times the overall decrease relative to the other two treatments, although the average reductions in the projected canopy area and crown volume were approximately five and four times lower than they were for the AP trees, respectively.

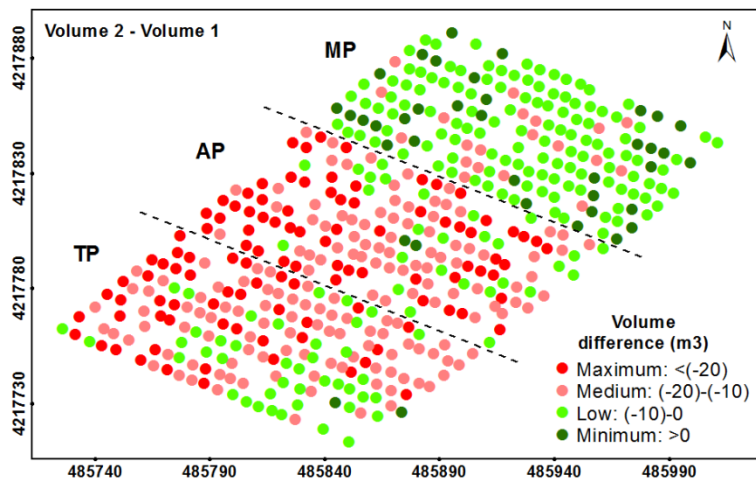


Figure 5. Four-level representation of the pruning impact on tree volume (differences in tree volume between dates 2 and 1). The letters indicate the pruning treatments as follows: TP (traditional), AP (adapted), and MP (mechanical). In the axes, coordinate system UTM zone 30N, datum WGS84.

Table 3. Impact of tree pruning treatment on the tree architecture, when computed as the differences in the projected canopy area, tree height, and crown volume between dates 2 (after pruning) and 1 (before pruning).

Pruning Treatments	Area		Height		Volume	
	(Date 2 – Date 1)		(Date 2 – Date 1)		(Date 2 – Date 1)	
	Mean±SD (m ²)	%*	Mean±SD (m)	%*	Mean±SD (m ³)	%*
Mechanical	-0.89 ± 1.40	-6.97	-0.51 ± 0.40	-12.15	-3.79 ± 4.93	-9.89
Adapted	-5.56 ± 2.68	-38.95	-0.05 ± 0.38	-0.65	-17.46 ± 8.73	-42.05
Traditional	-5.00 ± 2.87	-33.02	-0.03 ± 0.31	-0.37	-15.58 ± 8.19	-35.72

* Average percentage of increase (+) or decrease (-) of each tree geometric feature between the date 2 and the date 1, as follow: % = (feature_date2 – feature_date1)/(feature_date1)

Regarding the impact of the pruning treatments on the annual tree growth (date 3 – date 2), the type of pruning treatment might have a major influence on the vegetative response of the trees over time, mostly with respect to the crown volume growth (Figure 6, Table 4). In comparing the tree data computed on date 2 and date 3 (after 1 year), the TP trees showed the greatest growth rates in projected canopy area (5.39 m², 64.27%), tree height (0.06 cm, 1.66%), and crown volume (13.90 m³, 61.49%), although the projected canopy area of the AP trees showed higher growth in their percentage values (5.34 m², or 71.14%). By contrast, the MP showed the lowest growth rates for the three variables (3.25 m², -0.08 m and 4.66 m³, respectively).

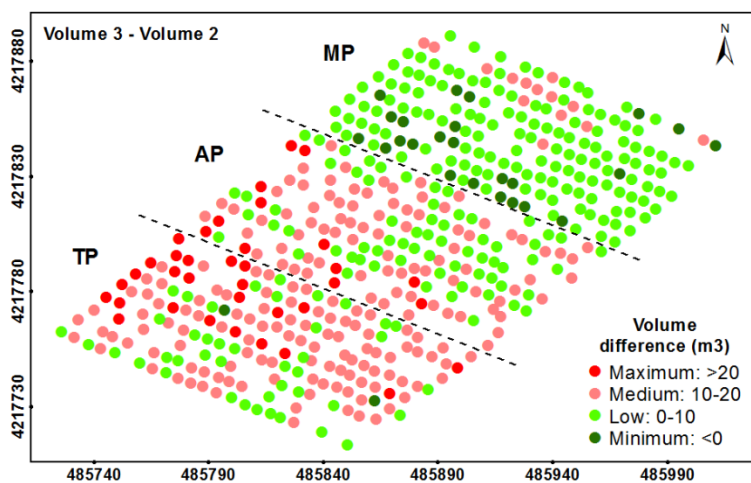


Figure 6. Four-level representation of the annual growth on tree volume after the pruning task (differences in tree volume between dates 3 and 2). The letters indicate the pruning treatments as follows: TP (traditional), AP (adapted), and MP (mechanical). In the axes, coordinate system UTM zone 30N, datum WGS84.

Table 4. Impact of tree pruning treatment on annual tree growth, computed as the differences of projected canopy area, tree height, and crown volume between the date 3 (1-year after pruning) and the date 2 (after pruning).

Pruning Treatments	Area		Height		Volume	
	(Date 3 – Date 2)		(Date 3 – Date 2)		(Date 3 – Date 2)	
	Mean±SD (m ²)	%*	Mean±SD (m)	%*	Mean±SD (m ³)	%*
Mechanical	3.25 ± 1.50	37.37	-0.08 ± 0.19	-2.32	4.66 ± 4.60	23.65
Adapted	5.34 ± 1.71	71.14	-0.05 ± 0.24	-1.14	11.58 ± 4.98	58.51
Traditional	5.39 ± 2.03	64.27	0.06 ± 0.20	1.66	13.90 ± 6.06	61.49

* Average percentage of increase (+) or decrease (-) of each tree geometric feature between the date 3 and the date 2, as follow: % = (feature_date3 – feature_date2)/(feature_date2)

These results are linked to the ability of the trees to return to their initial dimensions from before the pruning task (Figure 7, Table 5). Of the three treatments applied here, most MP trees were totally restored in terms of canopy area and volume in comparison to the original tree dimensions before the pruning task (date 1), but not in terms of the tree height. On average, the trees exceeded the canopy area and crown volume by 2.35 m² and by 0.87 m³, respectively, although these trees were 0.59 m smaller in comparison to their heights on date 1. In the case of TP, these trees generally grew back to their original dimensions regarding the canopy area (0.39 m² of average excess) and height (0.03 m of average excess), but not in terms of crown volume (1.68 m³ of average shortage). Finally, the AP trees did not generally reach their initial canopy area, tree height or crown volume in most of the trees.

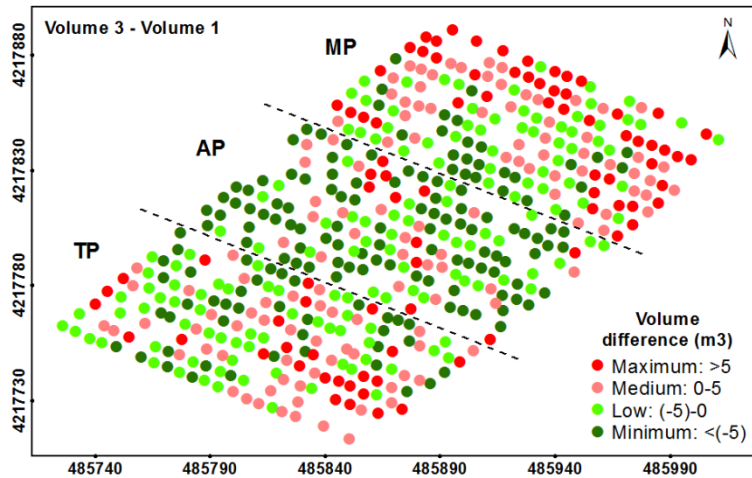


Figure 7. Four-level representation of the tree restoration in terms of volume (differences in tree volume between dates 3 and 1). The letters indicate the pruning treatments as follows: TP (traditional), AP (adapted), and MP (mechanical). In the axes, coordinate system UTM zone 30N, datum WGS84.

Table 5. Impact of the tree pruning treatment on tree restoration, when computed as the differences in the canopy area, tree height, and crown volume between date 3 (1-year after pruning) and date 1 (before pruning).

Pruning Treatments	Area		Height		Volume	
	(Date 3 – Date 1)		(Date 3 – Date 1)		(Date 3 – Date 1)	
	Mean \pm SD (m²)	%*	Mean \pm SD (m)	%*	Mean \pm SD (m³)	%*
Mechanical	2.35 \pm 1.76	26.14	-0.59 \pm 0.42	- 14.26	0.87 \pm 6.47	10.26
Adapted	-0.23 \pm 2.50	1.95	-0.10 \pm 0.36	- 1.99	-5.88 \pm 7.81	-10.76
Traditional	0.39 \pm 2.32	6.68	0.03 \pm 0.28	1.01	-1.68 \pm 6.80	0.29

* Average percentage of increase (+) or decrease (-) of each tree geometric feature between the date 3 and the date 1, as follow: % = (feature_date3 - feature_date1)/(feature_date1)

A detailed analysis of the data by grouping the trees according to pruning intensity revealed that tree restoration might be affected not only by the pruning severity but also by the type of pruning treatment (Figure 8). In general, the trees that were subjected to more aggressive pruning experienced much more vegetative development for the three studied treatments. Moreover, it was determined that the trees that were pruned to less than 30%

of their crown volume grew approximately 20-40% over one year, while the trees that were pruned by up to 50% of their crown volume grew more than 75% for the same period. However, differences in tree growth were also observed among pruning treatments. Our results showed that the AP trees were relatively more productive in terms of vegetative growth than the other two treatments when the pruning intensity was low (<10%) and similar to that of the TP trees when the intensity was moderate (10-30%). By contrast, the TP generated more vegetative growth when the pruning intensity was very high (>50%), and similar to the MP when the intensity was high (30-50%).

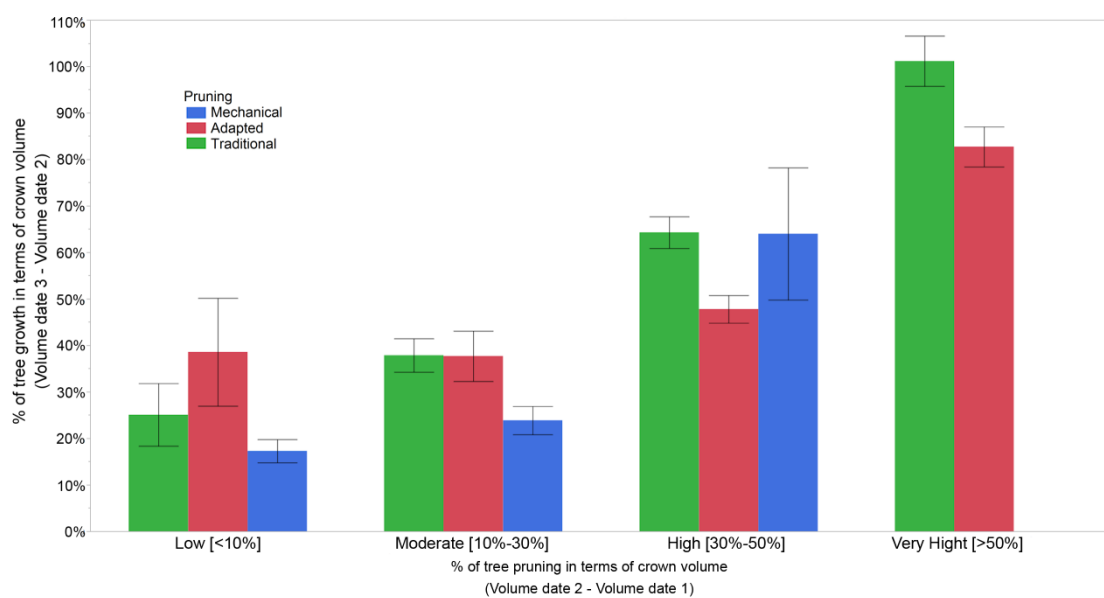


Figure 8. Percentage of annual tree growth after pruning as affected by the pruning severity and type of pruning treatment. Lines over the columns indicate the standard deviations.

5. Discussion

The direct assessment of the primary dimensions and certain geometric features of the olive trees such as the projected canopy area, height and crown volume is currently possible with the combined use of UAV imagery and advanced image processing and analysis procedures. This technology opens new opportunities to monitor tree status and progress at the field scale, as an efficient, objective and accurate alternative to the arduous and frequently inconsistent manual measurements on the ground (Miranda-Fuentes et al., 2015). This investigation takes advantage of this innovative UAV-based technology to evaluate the impact of pruning treatments in an olive plantation, reporting quantitative data for an unprecedented number of trees.

From the multi-temporal analysis of the location and the 3D models of every tree in the olive orchard, the effect of the pruning intensity on the tree architecture and annual tree growth after pruning was quantified. AP and TP reduced the crown volume by approximately 42% and 36% on average, respectively, which is 4 and 5-fold more compared to that of MP (approximately 10% on average). However, the trees that were subjected to TP grew slightly more than the AP trees, accounting for crown volume increases of approximately 62% and 59% on average, respectively. Regarding the effect of pruning on tree heights, important differences were only reported in the MP trees, which were homogenously cut to 3.5 to 4 meters over the surface, as observed in Figure 3. The data observed in this figure also confirmed the capacity of this UAV-based technology to accurately measure the tree heights. The trees also experienced minimum changes in terms of vertical growth after the pruning treatments, suggesting that the tree primarily grew along the horizontal axes. As expected, the trees that were subjected to more severe pruning generally experienced higher growth over time, although the magnitude of this event was affected by the given pruning treatment. In comparing the three pruning treatments, it was observed that AP benefitted tree development if the pruning intensity was lower than 10% of the crown volume, although this treatment was relatively worse in terms of tree growth when the pruning intensity was higher than 30%. These overall results were obtained in adult irrigated trees, so further analysis are needed to support such agronomic conclusions in other scenarios, e.g., under rain-fed conditions or with younger plantations.

Together with the evaluation of the pruning treatments, remote sensed information about the tree architecture at the orchard scale also has multiple implications for tree physiology, agronomy and field management (Usha and Singh, 2013) with potential applications for investigations about tree growth and yield (Villalobos et al., 2006), crown porosity (Castillo-Ruiz et al., 2016), or the interception of solar irradiation (Cherbiy-Hoffmann et al., 2012; Mariscal et al., 2000), among others. For example, the results presented here would improve the prediction models that connect the tree crown volume and tree canopy density with the tree yields, which is a complex issue since these models depend on a large number of factors (Álamo et al., 2012). Some investigations have also addressed the relationship of pruning treatments to tree productivity and mechanical harvesting (Farinelli et al., 2011). Tombesi et al. (2002) studied the influence of the canopy density on the efficiency of a trunk shaker after applying several pruning intensities, and they concluded that moderate and heavy annual pruning assisted mechanical harvesting. By contrast, a lack of pruning caused the crown to grow upward and away from the primary branches which resulted in defoliation due to a lack of light and from parasitic attack.

Additionally, quantifying the impact of pruning on the tree volume gives an estimated value of the available residual biomass (Velázquez-Martí et al., 2011), which could serve to calculate the potential energy from this raw material (Bilanzdija et al., 2012) or,

furthermore, to evaluate the site-specific effects of the application of these by-products on the soil in no-till systems to prevent land degradation and improve the organic matter content (Gómez-Muñoz et al., 2016; Repullo et al., 2012; Rodríguez-Lizana et al., 2017). The use of pruned residues as mulch is growing (Calatrava and Franco, 2011) and can help prevent pollutant dispersion in olive groves (Rodríguez-Lizana et al., 2008).

Geo-referenced maps with the locations and dimensions of every tree could also be the basis for designing a programme for a variable rate application of plant protection products (Miranda-Fuentes et al., 2016), and in combination with on-ground equipment (Pérez-Ruiz et al., 2015; Rosell-Polo et al., 2015), contribute to help fulfill the requirements of the European Directive for a Sustainable Use of Pesticides (European Commision, 2009).

6. Conclusions

This investigation combined aerial images that were collected with an UAV on three different dates (before pruning, after pruning and 1-year after pruning), 3D models of the olive tree field that were created by photo-reconstruction procedures and an original OBIA algorithm to evaluate the impacts of three different pruning treatments (traditional, adapted and mechanical) on hundreds of irrigated trees. The projected canopy area, tree height and crown volume were quantified and compared among pruning treatments and flight dates.

The full procedure had high accuracy, and it correctly identified and measured every olive tree on the three dates with the exception of some cases when the 3D point cloud was incorrectly generated. As a general trend, the trees that were subjected to AP showed the highest foliage losses after pruning, followed by trees under TP. However, trees under TP experienced higher growths than the other trees for the quantification of this vegetative response one year after pruning. Due to the typical MP typology, the trees under this treatment maintained a more constant vegetative growth during this study.

This research offers valuable information for designing site-specific olive tree management strategies in the context of precision agriculture, which allows for the optimized application of agronomic tasks such as pruning, fertilization, pesticide use or irrigation, with the consequent economic and environmental benefits. The technology presented here can be made adaptable and transferable with corresponding adjustments to other woody crops such as vineyards or fruit orchards.

7. Methods

7.1. Study area and description of the pruning treatments

This research was performed in a commercial 20-year-old olive grove located in Villacarrillo, in the province of Jaen (southern Spain, central coordinates 485885 m X, 4217810 m Y, system UTM zone 30N, datum WGS84). A rectangular field of approximately 3 hectares that was under drip-irrigation was selected for the experiment. This field was made up of 648 olive trees of the Arbequina variety, and it was laid out as 27 trees long and 24 across the field, with an intensive single-tree pattern of 8x4 m tree spacing. The field soil was loamy and silty clay loam, with at least 1.5 m deep without stoniness, and no limitations for crop production. The irrigation was controlled at a dose of approximately 800 m³ per hectare, which corresponded to 3200 l per tree. A natural cover crop, 1.5 m wide and composed of grass and legume species, covered the soil among the tree lines. The cover crop was controlled with a brush-cutter, meanwhile herbicides were applied in early autumn and spring to control weeds under the olive trees. Fertigation was applied at 100 units of fertilizer per hectare.

The pruning strategy was part of a broader research program with the aim of studying the efficiency of different olive pruning and mechanical harvesting systems. Therefore, a simple demonstration strip design was selected in order to prioritize viability of mechanical pruning, which relies on continuous work at large areas, instead of designing a complex field experiment. The study field was divided in three sub-plots of 9x24 trees each, in which traditional, adapted and mechanical pruning treatments were separately performed on March 4th and 5th, 2015 (Figure 9). In the TP, the highest branches, the crossed ones, and the ones below the base of the canopy and established at 60 centimeters over the soil were pruned. In the AP, the inner branches were totally removed, plus the crossed and low branches as described in the previous treatment. Thus, a large number of trees under this treatment presented a sizeable gap in the central crown part. The AP mainly aimed to adapt the olive architecture for canopy shaker harvesting. Finally, in the MP, a tractor with opposite mechanical cuts at a 30° angle removed the branches from 3.5 to 4 meters above the terrain. This tractor also used a horizontal mechanical cut to remove the branches at less than 70 centimeters above the terrain.

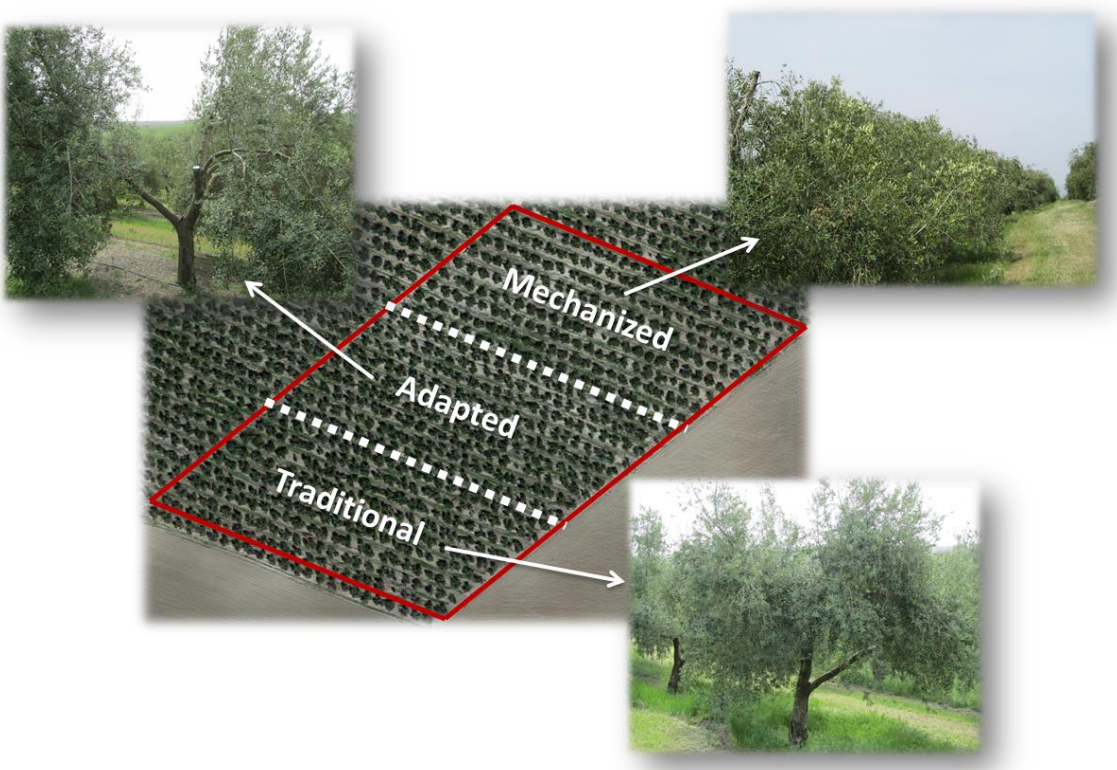


Figure 9. Description of the three pruning treatments evaluated in this investigation.

7.2. Multi-temporal UAV flights and the generation of geo-spatial products

A set of remote images of the experimental field were acquired through UAV flights that were performed on the following three dates: 1) before tree pruning (date 1: December 9th, 2014), 2) a short time after tree pruning (date 2: April 14th, 2015), and 3) almost a year after tree pruning (date 3: February 1st, 2016). The flight equipment was a quadcopter UAV with vertical take-off and landing model MD4-1000 (Microdrones GmbH, Siegen, Germany), with a still point-and-shoot camera of model Olympus PEN E-PM1 (Olympus Corporation, Tokyo, Japan) (Figure 10). This camera took 12.2 megapixel images in true color (Red, R; Green, G; and Blue, B, bands) with 8-bit radiometric resolution and at a 14 mm focal length. The camera's sensor size was 17.3 x 13.0 mm and the pixel size was 0.0043 mm. These parameters are needed to calculate the image resolution on the ground or, i.e., the ground sample distance as affected by the flight altitude.



Figure 10. The quadcopter UAV and the Red-Green-Blue (RGB) camera used to acquire the remote images of the olive trees.

During each flight, the UAV route was designed to take photos continuously at 1-second intervals, resulting in a forward lap of at least 90%. In addition, a side lap of 60% was programmed. The flight speed was 3 m/s and the flight altitudes were 100 meters on the first and third dates and 50 meters on the second date. Due to the strong windy conditions, the 100-m flight was aborted on the second date. The UAV used a total of 24 and 15 minutes to fly the experiment field at 50 and 100 meters altitude, respectively. The area covered in each flight was 3.5 hectares. To fully cover the experimental field, the camera collected 840 and 420 RGB images at ground sample distances of 1.90 and 3.81 cm/pixel for 50-m and 100-m flight altitudes, respectively. The flight operations fulfilled the list of requirements established by the Spanish National Agency of Aerial Security, including the pilot license, safety regulations and limited flight distance (AESPA, 2017). The UAV flights were authorized by the person in charge of the olive grove as well.

In processing the set of UAV aerial images, the following three geo-spatial products of the olive grove were produced: 1) the 3D point cloud file, by applying the structure-from-motion technique (Figure 11), 2) the DSM, with height information, which was created from the 3D point cloud, and 3) the ortho-mosaicked image, with RGB information on every pixel. In this research, Agisoft PhotoScan Professional software, version 1.2.4 build 2399 (Agisoft LLC, St. Petersburg, Russia) was used for this task. The mosaicking process was fully automatic with the exception of the manual localization of six ground control points

that were used to georeference the products. These ground control points were located in the corners and the center of the olive orchard, and their coordinates were taken with a GPS device after the flight operations. The automatic process involved the following three phases: 1) aligning images, 2) building field geometry, and 3) ortho-photo generation. The common points and the camera position for each image were located and matched, which facilitated the refinement of the camera calibration parameters. Once the images were aligned, the point cloud was generated. Next, the DSM was built on the basis of the estimated camera position and the images themselves. This process requires high computational resources and it can usually take approximately 5 to 6 hours due to the use of many high-resolution images. Finally, the images were projected over the DSM, and the ortho-mosaicked image was generated. The DSM is a 3D polygon mesh that represents the overflowed area and reflects the irregular geometry of the ground and the tree crowns. The DSM was joined to the ortho-mosaic in the form of TIFF files, which produced a 4-band multi-layer file (Red, Green, Blue and DSM). More information about the PhotoScan function is described in Dandois and Ellis (2013).



Figure 11. A partial view of the 3-D point cloud for the olive grove studied in this investigation, which was produced by the photogrammetric processing of the remote images taken with the UAV.

7.3. Object-based image analysis algorithm for computing the 3D tree features

An innovative algorithm based on the OBIA paradigm was applied to the 4-band multi-layer file that was created during the previous stage to classify and identify every individual tree in the olive grove and to compute the tree geographic position and primary 3D geometric features, including the projected canopy area, the tree height and the crown volume. The OBIA algorithm was developed using eCognition Developer 9 software (Trimble GeoSpatial, Munich, Germany) and it was adapted from the basic version described in Torres-Sánchez et al. (2015).

However, the procedure presented here was original and included improvements and variations related to the specifications of this research (Figure 12).

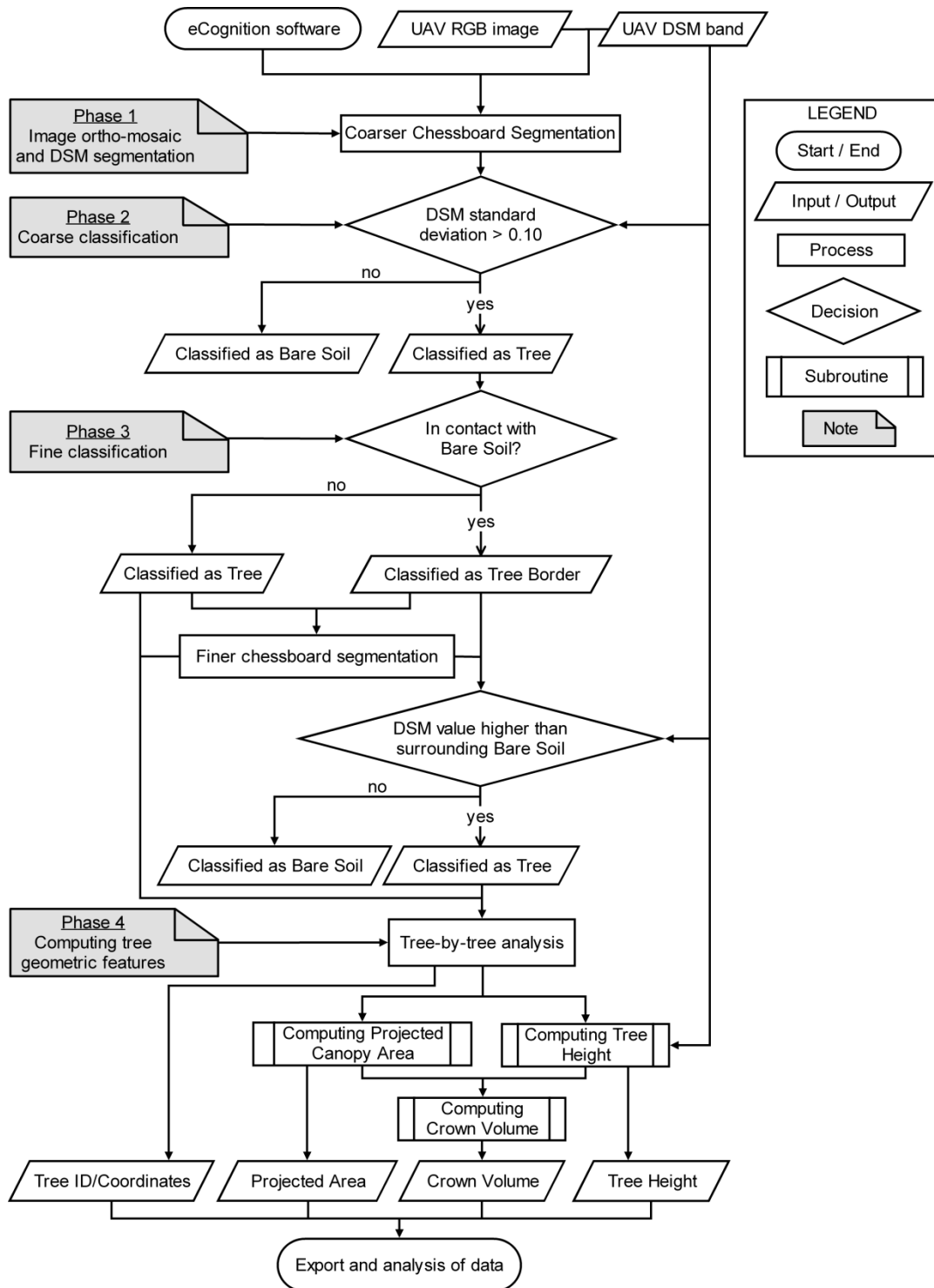


Figure 12. Flowchart of the OBIA algorithm developed in this investigation.

The algorithm was specifically programmed to run in a fully automatic manner without the need for user intervention, and with the ability to be auto-adaptive to any olive grove, independent of the plantation pattern and of the given pruning treatment. The full procedure was composed of a sequence of phases (Figure 13), which is described as follows:

Phase 1, image ortho-mosaic and DSM segmentation: The 4-band (B, G, R, and DSM) multi-layer file (Figures 13a1-a2) was segmented into 1-m² square objects by using the chessboard segmentation process (Figure 13b). Because segmentation is by far the slowest task of the full OBIA procedure, the algorithm used chessboard segmentation instead of the multi-resolution option. In addition, it was programmed to only use the DSM band as the reference for the segmentation, which weighted the variable “height” instead of the spectral information. This configuration produced a notable decrease in computational demand, and consequently, an increase in the processing speed, without penalizing the segmentation accuracy.

Phase 2, coarse classification of trees and bare soil: The segmented objects, whose standard deviation (SD) value of the DSM (height) layer was greater than 0.10 m, were classified as trees. The remaining objects were classified as bare soil (Figure 13c).

Phase 3, fine classification of trees: To refine the tree delineation, the tree objects were analyzed at the pixel level. Firstly, the tree objects that were in contact with bare soil were classified as tree border objects (Figure 13d), and next, they were segmented at the pixel size (Figure 13e). Then, the algorithm classified every tree border object as a tree or bare soil by comparing their DSM value to the surrounding bare soil and tree DSM values (Figure 13f). Finally, the objects classified as trees were joined into single objects and identified as individual trees (Figure 13g).

Phase 4, computing the tree geometric features: The algorithm automatically calculated the geometric features (projected canopy area, tree height and crown volume) of all the tree objects by applying a looping process in which every tree was individually identified and analyzed. During this sequential process, the height of every tree was obtained by comparing its maximum DSM value to the average DSM values of a bare soil area with a 1 m buffer surrounding each tree. Simultaneously, the crown volume was calculated by adding up the volumes (by multiplying the pixel areas and heights) of all the pixels corresponding to every tree. Finally, the OBIA algorithm automatically exported the identification, location and the three primary geometric features of every tree as vector (e.g., shapefile format) and table (e.g., Excel or ASCII format) files for further analysis.

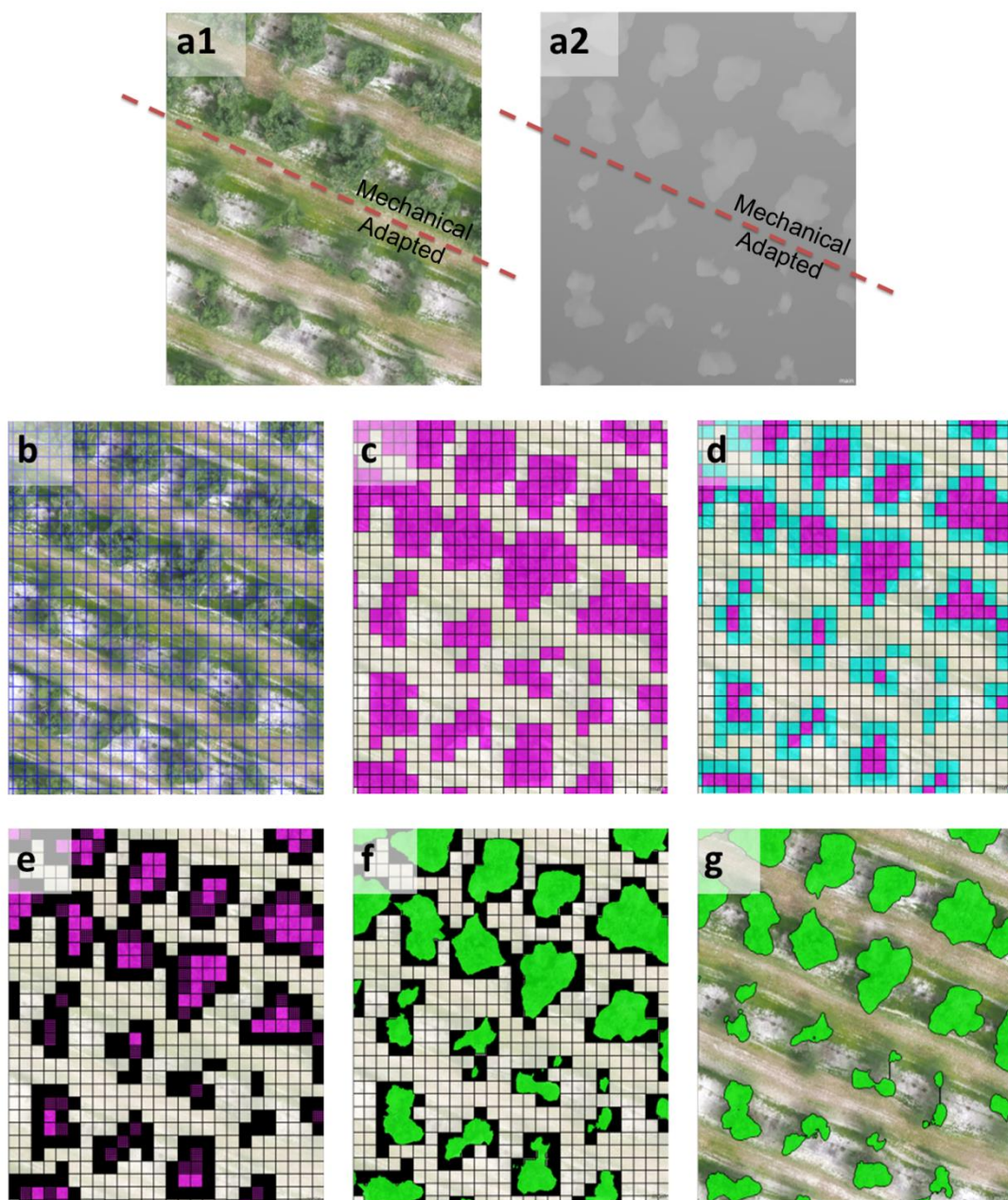


Figure 13. Partial views of the primary OBIA algorithm outputs: a) the 4-band multi-layer file with the RGB (a1) and the DSM (a2) layers, showing the results of mechanical and adapted pruning as applied to the trees on the two top and bottom rows, respectively; b) chessboard segmentation output; c) the coarse classification of the tree (pink colour) and bare soil (white colour) objects based on the difference in DSM (height) values; d) the coarse classification of the tree borders (blue color); e) pixel-based segmentation of the tree borders; f) the fine classification of the tree (green colour) objects; and g) the tree and the bare-soil objects were joined with separately. As a result of the whole procedure, the algorithm computed the 3D tree geometric features (projected area, height and volume) and exported the values as vector and table files for further analysis.

7.4. Data analysis

The outputs delivered by the OBIA algorithm for the three study dates were subjected to descriptive analysis with JMP version 10 software (SAS Institute Inc., Cary, NC, USA). The impacts of pruning on the tree architecture and annual tree growth was separately evaluated at each pruning zone by analyzing tree-by-tree variability over time, i.e., by quantifying the differences in the three primary dimensions (projected area, tree height and crown volume) between dates 1 and 2 (the impact on the tree architecture) and between dates 2 and 3 (the impact on the annual tree growth). In addition, the ability of the trees to return to their original dimensions before the pruning task was quantified by comparing the data on dates 1 and 3. The field experimental design, which prioritized mechanical pruning viability rather than testing statistical hypothesis, allowed for ranking pruning treatments according to averaged values obtained in every study date and to trends observed over time.

8. Acknowledgements

The authors thank Ms. Irene Borrà-Serrano and Mr. Juan José Caballero-Novella for their very helpful assistance during the field work.

9. References

- AESA, 2017. URL:
http://www.seguridadaerea.gob.es/LANG_EN/cias_empresas/trabajos/rpas/marco/default.aspx (accessed 6.2.17).
- Bilanzdija, N., Voca, N., Kricka, T., Matin, A., Jurisic, V., 2012. Energy potential of fruit tree pruned biomass in Croatia. *Span. J. Agric. Res.* 10, 292–298.
<https://doi.org/10.5424/sjar/2012102-126-11>
- Blaschke, T., Hay, G.J., Kelly, M., Lang, S., Hofmann, P., Addink, E., Queiroz Feitosa, R., van der Meer, F., van der Werff, H., van Coillie, F., Tiede, D., 2014. Geographic object-based image analysis – towards a new paradigm. *Isprs J. Photogramm. Remote Sens.* 87, 180–191. <https://doi.org/10.1016/j.isprsjprs.2013.09.014>
- Calatrava, J., Franco, J.A., 2011. Using pruning residues as mulch: Analysis of its adoption and process of diffusion in Southern Spain olive orchards. *J. Environ. Manage.* 92, 620–629. <https://doi.org/10.1016/j.jenvman.2010.09.023>
- Castillejo-González, I.L., Peña-Barragán, J.M., Jurado-Expósito, M., Mesas-Carrascosa, F.J., López-Granados, F., 2014. Evaluation of pixel- and object-based approaches for

- mapping wild oat (*Avena sterilis*) weed patches in wheat fields using QuickBird imagery for site-specific management. *Eur. J. Agron.* 59, 57–66.
<https://doi.org/10.1016/j.eja.2014.05.009>
- Castillo-Ruiz, F.J., Castro-García, S., Blanco-Roldán, G.L., Sola-Guirado, R.R., Gil-Ribes, J.A., 2016. Olive crown porosity measurement based on radiation transmittance: an assessment of pruning effect. *Sensors* 16. <https://doi.org/10.3390/s16050723>
- Castillo-Ruiz, F.J., Jiménez-Jiménez, F., Blanco-Roldán, G.L., Sola-Guirado, R.R., Agüera-Vega, J., Castro-García, S., 2015. Analysis of fruit and oil quantity and quality distribution in high-density olive trees in order to improve the mechanical harvesting process. *Span. J. Agric. Res.* 13, 0209.
- Cherbiy-Hoffmann, S.U., Searles, P.S., Hall, A.J., Rousseaux, M.C., 2012. Influence of light environment on yield determinants and components in large olive hedgerows following mechanical pruning in the subtropics of the Southern Hemisphere. *Sci. Hortic.* 137, 36–42. <https://doi.org/10.1016/j.scienta.2012.01.019>
- Connor, D.J., Gómez-del-Campo, M., Rousseaux, M.C., Searles, P.S., 2014. Structure, management and productivity of hedgerow olive orchards: A review. *Sci. Hortic.* 169, 71–93. <https://doi.org/10.1016/j.scienta.2014.02.010>
- Dandois, J.P., Ellis, E.C., 2013. High spatial resolution three-dimensional mapping of vegetation spectral dynamics using computer vision. *Remote Sens. Environ.* 136, 259–276. <https://doi.org/10.1016/j.rse.2013.04.005>
- Díaz-Varela, R.A., de la Rosa, R., León, L., Zarco-Tejada, P.J., 2015. High-resolution airborne UAV imagery to assess olive tree crown parameters using 3D photo reconstruction: application in breeding trials. *Remote Sens.* 7, 4213–4232.
<https://doi.org/10.3390/rs70404213>
- European Commision, 2009. Directive 2009/128/EC of the european parliament and of the council of 21 October 2009- establishing a framework for community action to achieve the sustainable use of pesticides.
- Farinelli, D., Onorati, L., Ruffolo, M., Tombesi, A., 2011. Mechanical pruning of adult olive trees and influence on yield and on efficiency of mechanical harvesting. *Acta Hortic.* 203–209. <https://doi.org/10.17660/ActaHortic.2011.924.25>
- Ferguson, L., Glozer, K., Crisosto, C., Rosa, U.A., Castro-García, S., Fichtner, E.J., Guinard, J.X., Lee, S.M., Krueger, W.H., Miles, J.A., Burns, J.K., 2012. Improving canopy contact olive harvester efficiency with mechanical pruning. *Acta Hortic.* 83–87.
<https://doi.org/10.17660/ActaHortic.2012.965.8>
- Friedli, M., Kirchgessner, N., Grieder, C., Liebisch, F., Mannale, M., Walter, A., 2016. Terrestrial 3D laser scanning to track the increase in canopy height of both monocot

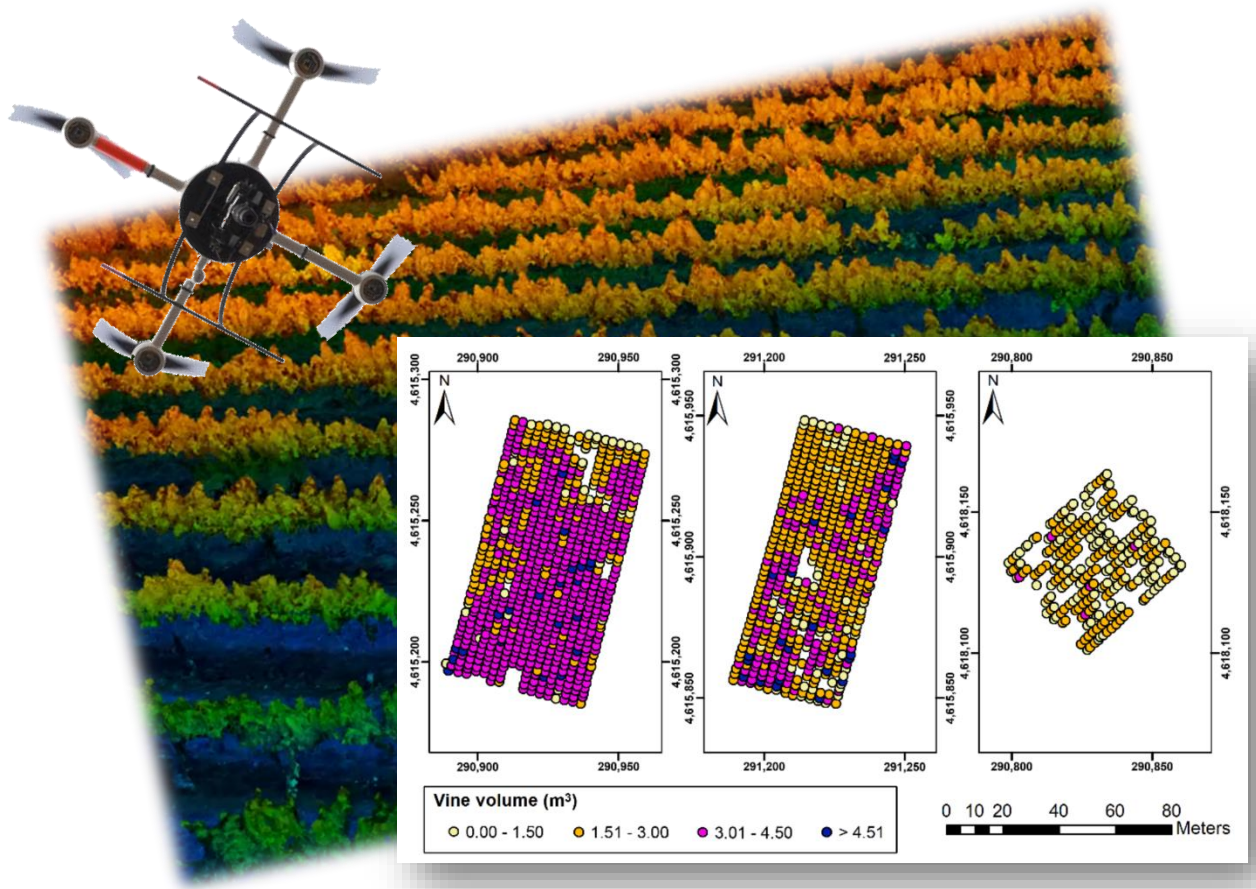
- and dicot crop species under field conditions. *Plant Methods* 12, 9.
<https://doi.org/10.1186/s13007-016-0109-7>
- Gómez-Muñoz, B., Valero-Valenzuela, J.D., Hinojosa, M.B., García-Ruiz, R., 2016. Management of tree pruning residues to improve soil organic carbon in olive groves. *Eur. J. Soil Biol.* 74, 104–113. <https://doi.org/10.1016/j.ejsobi.2016.03.010>
- Guerra-Hernández, J.G., González-Ferreiro, E., Sarmento, A., Silva, J., Nunes, A., Correia, A.C., Fontes, L., Tomé, M., Díaz-Varela, R., 2016. Short Communication. Using high resolution UAV imagery to estimate tree variables in *Pinus pinea* plantation in Portugal. *For. Syst.* 25, 09. <https://doi.org/10.5424/fs/2016252-08895>
- Kattenborn, T., Sperlich, M., Bataua, K., Koch, B., 2014. Automatic single tree detection in plantations using UAV-based photogrammetric point clouds, in: ISPRS - international archives of the photogrammetry, remote sensing and spatial information sciences. Presented at the *ISPRS Technical Commission III Symposium* (Volume XL-3); 5-7 September 2014, Zurich, Switzerland, Copernicus GmbH, pp. 139–144. <https://doi.org/10.5194/isprsarchives-XL-3-139-2014>
- López-Granados, F., Torres-Sánchez, J., Castro, A.I. de, Serrano-Pérez, A., Mesas-Carrascosa, F.J., Peña, J.M., 2016. Object-based early monitoring of a grass weed in a grass crop using high resolution UAV imagery. *Agron. Sustain. Dev.* 36, 67. <https://doi.org/10.1007/s13593-016-0405-7>
- Mariscal, M.J., Orgaz, F., Villalobos, F.J., 2000. Modelling and measurement of radiation interception by olive canopies. *Agric. For. Meteorol.* 100, 183–197. [https://doi.org/10.1016/S0168-1923\(99\)00137-9](https://doi.org/10.1016/S0168-1923(99)00137-9)
- Miranda-Fuentes, A., Llorens, J., Gamarra-Diezma, J.L., Gil-Ribes, J.A., Gil, E., 2015. Towards an optimized method of olive tree crown volume measurement. *Sensors* 15, 3671–3687. <https://doi.org/10.3390/s150203671>
- Miranda-Fuentes, A., Llorens, J., Rodríguez-Lizana, A., Cuenca, A., Gil, E., Blanco-Roldán, G.L., Gil-Ribes, J.A., 2016. Assessing the optimal liquid volume to be sprayed on isolated olive trees according to their canopy volumes. *Sci. Total Environ.* 568, 296–305. <https://doi.org/10.1016/j.scitotenv.2016.06.013>
- Nex, F., Remondino, F., 2014. UAV for 3D mapping applications: a review. *Appl. Geomat.* 6, 1–15. <https://doi.org/10.1007/s12518-013-0120-x>
- Peña, J.M., Torres-Sánchez, J., Castro, A.I. de, Kelly, M., López-Granados, F., 2013. Weed mapping in early-season maize fields using object-based analysis of unmanned aerial vehicle (UAV) images. *PLoS ONE* 8, e77151. <https://doi.org/10.1371/journal.pone.0077151>

- Pérez-Ruiz, M., González-de-Santos, P., Ribeiro, A., Fernández-Quintanilla, C., Peruzzi, A., Vieri, M., Tomic, S., Agüera, J., 2015. Highlights and preliminary results for autonomous crop protection. *Comput. Electron. Agric.* 110, 150–161.
<https://doi.org/10.1016/j.compag.2014.11.010>
- Qin, R., 2014. An object-based hierarchical method for change detection using unmanned aerial vehicle images. *Remote Sens.* 6, 7911–7932.
<https://doi.org/10.3390/rs6097911>
- Repullo, M.A., Carbonell, R., Hidalgo, J., Rodríguez-Lizana, A., Ordóñez, R., 2012. Using olive pruning residues to cover soil and improve fertility. *Soil Tillage Res.* 124, 36–46. <https://doi.org/10.1016/j.still.2012.04.003>
- Rodríguez-Lizana, A., Espejo-Pérez, A.J., González-Fernández, P., Ordóñez-Fernández, R., 2008. Pruning residues as an alternative to traditional tillage to reduce erosion and pollutant dispersion in olive groves. *Water. Air. Soil Pollut.* 193, 165–173.
<https://doi.org/10.1007/s11270-008-9680-5>
- Rodríguez-Lizana, A., Pereira, M.J., Ribeiro, M.C., Soares, A., Márquez-García, F., Ramos, A., Gil-Ribes, J., 2017. Assessing local uncertainty of soil protection in an olive grove area with pruning residues cover: a geostatistical cosimulation approach. *Land Degrad. Dev.* <https://doi.org/10.1002/ldr.2734>
- Rosell, J.R., Sanz, R., 2012. A review of methods and applications of the geometric characterization of tree crops in agricultural activities. *Comput. Electron. Agric.* 81, 124–141. <https://doi.org/10.1016/j.compag.2011.09.007>
- Rosell-Polo, J.R., Auat Cheein, F., Gregorio, E., Andújar, D., Puigdomènech, L., Masip, J., Escolà, A., 2015. Chapter three - advances in structured light sensors applications in precision agriculture and livestock farming, in: Sparks, D.L. (Ed.), Advances in Agronomy. Academic Press, pp. 71–112.
<https://doi.org/10.1016/bs.agron.2015.05.002>
- Rousseau, D., Chéné, Y., Belin, E., Semaan, G., Trigui, G., Boudehri, K., Franconi, F., Chapeau-Blondeau, F., 2015. Multiscale imaging of plants: current approaches and challenges. *Plant Methods* 11, 6. <https://doi.org/10.1186/s13007-015-0050-1>
- Rovira-Más, F., Zhang, Q., Reid, J.F., 2008. Stereo vision three-dimensional terrain maps for precision agriculture. *Comput. Electron. Agric.* 60, 133–143.
<https://doi.org/10.1016/j.compag.2007.07.007>
- Tombesi, A., Boco, M., Pilli, M., Farinelli, D., 2002. Influence of canopy density on efficiency of trunk shaker on olive mechanical harvesting. *Acta Hortic.* 291–294.
<https://doi.org/10.17660/ActaHortic.2002.586.56>

- Torres-Sánchez, J., López-Granados, F., Serrano, N., Arquero, O., Peña, J.M., 2015. High-throughput 3-D monitoring of agricultural-tree plantations with unmanned aerial vehicle (UAV) technology. *PLoS ONE* 10, e0130479.
<https://doi.org/10.1371/journal.pone.0130479>
- Torres-Sánchez, J., Peña, J.M., de Castro, A.I., López-Granados, F., 2014. Multi-temporal mapping of the vegetation fraction in early-season wheat fields using images from UAV. *Comput. Electron. Agric.* 103, 104–113.
<https://doi.org/10.1016/j.compag.2014.02.009>
- Usha, K., Singh, B., 2013. Potential applications of remote sensing in horticulture—A review. *Sci. Hortic.* 153, 71–83. <https://doi.org/10.1016/j.scienta.2013.01.008>
- Velázquez-Martí, B., Fernández-González, E., López-Cortés, I., Salazar-Hernández, D.M., 2011. Quantification of the residual biomass obtained from pruning of trees in Mediterranean olive groves. *Biomass Bioenergy* 35, 3208–3217.
<https://doi.org/10.1016/j.biombioe.2011.04.042>
- Villalobos, F.J., Testi, L., Hidalgo, J., Pastor, M., Orgaz, F., 2006. Modelling potential growth and yield of olive (*Olea europaea* L.) canopies. *Eur. J. Agron.* 24, 296–303.
<https://doi.org/10.1016/j.eja.2005.10.008>
- West, P.W., 2009. Tree and Forest Measurement. Springer Berlin Heidelberg, Berlin, Heidelberg.
- Xiang, H., Tian, L., 2011. Development of a low-cost agricultural remote sensing system based on an autonomous unmanned aerial vehicle (UAV). *Biosyst. Eng.* 108, 174–190. <https://doi.org/10.1016/j.biosystemseng.2010.11.010>
- Zarco-Tejada, P.J., Díaz-Varela, R., Angileri, V., Loudjani, P., 2014. Tree height quantification using very high resolution imagery acquired from an unmanned aerial vehicle (UAV) and automatic 3D photo-reconstruction methods. *Eur. J. Agron.* 55, 89–99. <https://doi.org/10.1016/j.eja.2014.01.004>
- Zhang, C., Kovacs, J.M., 2012. The application of small unmanned aerial systems for precision agriculture: A review. *Precis. Agric.* 13, 693–712.
<https://doi.org/10.1007/s11119-012-9274-5>

Capítulo 3

3-D characterization of vineyard using a novel UAV imagery-based OBIA procedure for precision viticulture applications



A.I. de Castro, F.M. Jiménez-Brenes, J. Torres-Sánchez, J.M. Peña, I. Borrà-Serrano, F. López-Granados. (2018). 3-D characterization of vineyard using a novel UAV imagery-based OBIA procedure for precision viticulture applications. *Remote Sensing*, 10(4), 584. <https://doi.org/10.3390/rs10040584> (Open Access)

1. Resumen

La viticultura de precisión ha surgido en los últimos años como un nuevo enfoque en la producción vitivinícola y se basa en la evaluación de la variabilidad espacial sobre el terreno y en la aplicación de estrategias de manejo localizado, lo que puede requerir información georreferenciada del dosel tridimensional (3D) de la vid como uno de los datos de entrada. La estructura 3D de los campos de viñedo puede ser generada aplicando técnicas fotogramétricas a las imágenes aéreas adquiridas con vehículos aéreos no tripulados (UAV), aunque el procesamiento de la gran cantidad de datos correspondientes a dichos modelos 3D es actualmente el cuello de botella de esta tecnología. Para resolver esta limitación, se desarrolló un novedoso y robusto análisis de imágenes basado en objetos (OBIA) basado en el Modelo Digital de Superficie (DSM). La importancia de este trabajo se basa en el algoritmo OBIA desarrollado, que es completamente automático y autoadaptable a las diferentes condiciones de los cultivos en campo, clasificando las vides y los espacios libres dentro de la hilera de viña (huecos), y el cálculo de las dimensiones de la vid sin intervención del usuario. Los resultados obtenidos en tres campos y dos fechas diferentes mostraron una gran precisión en la clasificación del área de las vides y de los huecos dentro de la hilera, así como errores menores en las estimaciones de la altura de las vides. Además, el algoritmo calculó la posición, el área proyectada y el volumen de cada cepa en el campo, lo que aumenta el potencial de esta tecnología basada en UAV y OBIA como una herramienta a implementar en aplicaciones de manejo localizado de cultivos.

2. Abstract

Precision viticulture has arisen in recent years as a new approach in grape production. It is based on assessing field spatial variability and implementing site-specific management strategies, which can require georeferenced information of the three dimensional (3D) grapevine canopy structure as one of the input data. The 3D structure of vineyard fields can be generated applying photogrammetric techniques to aerial images collected with Unmanned Aerial Vehicles (UAVs), although processing the large amount of crop data embedded in 3D models is currently a bottleneck of this technology. To solve this limitation, a novel and robust object-based image analysis (OBIA) procedure based on Digital Surface Model (DSM) was developed for 3D grapevine characterization. The significance of this work relies on the developed OBIA algorithm which is fully automatic and self-adaptive to different crop-field conditions, classifying grapevines, and row gap (missing vine plants), and computing vine dimensions without any user intervention. The results obtained in three testing fields on two different dates showed high accuracy in the

classification of grapevine area and row gaps, as well as minor errors in the estimates of grapevine height. In addition, this algorithm computed the position, projected area, and volume of every grapevine in the field, which increases the potential of this UAV- and OBIA-based technology as a tool for site-specific crop management applications.

3. Introduction

Vineyard yield and grape quality are variable and depend on several field and crop-related factors, so that studying the influence and spatial distribution of these factors allows grape growers to improve vineyard management according to quality and productivity parameters (Bramley and Hamilton, 2004). In this context, precision viticulture (PV) has arisen in recent years as a new approach in grape production, which is based on assessing intra- and inter- crop-field spatial variability and implementing site-specific crop management systems (Arnó Satorra et al., 2009). Its ultimate objective is to optimize crop production and profitability through a reduction in production inputs (e.g., pesticides, fertilizers, machinery, fuel, water, etc.) and, consequently, diminish potential damage to the environment due to the over-application of inputs (Schieffer and Dillon, 2015; Tey and Brindal, 2012). To design site-specific management strategies, georeferenced information of the grapevine canopy structure and its variability at the field scale are required as input data, since plant architecture is one of the most important traits for the characterization and monitoring of fruit trees (Ballesteros et al., 2015). As an alternative to time-consuming on-ground methods traditionally used to collect crop data, remote sensing offers the possibility of a rapid assessment of large vineyard areas (Hall et al., 2002; Johnson et al., 2003). Within the PV context, aerial remote sensing in the optical domain offers a potential way to map crop structure, such as vegetation cover fraction, row orientation, or leaf area index. This information can be registered in a non-destructive way and can be later used in decision support tools (Weiss et al., 2017). Among the remote sensing platforms, Unmanned Aerial Vehicles (UAVs) stand out because of their unprecedented high spatial resolution and flexibility of flight scheduling, which are essential for the accurate and timely monitoring of the crop. To date, UAVs have been used for a wide range of purposes in PV, such as the assessment of water status (Baluja et al., 2012), disease detection (Albetis et al., 2017), vine canopy characterization (Ballesteros et al., 2015; Mathews and Jensen, 2013; Poblete-Echeverría et al., 2017; Weiss et al., 2017), and the study of spatial variability in yield and berry composition (Rey-Caramés et al., 2015). The development of new techniques based on UAV imagery is therefore a required target for PV, since UAVs are rapidly replacing other platforms for vineyard monitoring (Poblete-Echeverría et al., 2017).

In addition to the aforementioned advantages, UAVs are able to fly at low altitudes with high image overlap, which permits the generation of Digital Surface Models (DSMs) using photo-reconstruction techniques or artificial vision (Geipel et al., 2014; Mancini et al., 2013; Nex and Remondino, 2014; Rosnell and Honkavaara, 2012). The UAV-based DSMs have recently been used in agricultural applications, for example to discriminate weeds in herbaceous crops at early stage (Bendig et al., 2014; de Castro et al., 2018); to calculate tree area, height, and crown volume in olive orchards and to quantify the impact of different pruning treatments (Jiménez-Brenes et al., 2017; Torres-Sánchez et al., 2015); to isolate vine pixel as intermediate stage and to assess biomass volume (Matese et al., 2017). Processing the large amount of detailed crop data embedded in UAV images and DSMs requires the implementation of robust and automatic image analysis procedures. In the last few years, object-based image analysis (OBIA) techniques have reached high levels of automation and adaptability to ultra-high spatial resolution images and provide better solutions to the problem of pixel heterogeneity in comparison with conventional pixel-based methods (Blaschke et al., 2014). The elemental analysis unit of OBIA is the “object”, which groups adjacent pixels with homogenous spectral values. Then, OBIA combines the spectral, topological, and contextual information of these objects to address complicated classification issues. Successful examples of OBIA applications include agricultural (Castillejo-González et al., 2014; López-Granados et al., 2016; Mathews, 2014; Peña et al., 2013; Souza et al., 2017), grassland (Laliberte et al., 2011, 2007), and forest scenarios (Franklin and Ahmed, 2018; Hellesen and Matikainen, 2013; Van Den Eeckhaut et al., 2012). Therefore, the combination of UAV-based DSM and OBIA enables to tackle the significant challenge of automating image analysis (de Castro et al., 2018), which represents a relevant advance in agronomy science.

In this investigation, a novel OBIA procedure was developed to characterize the 3D structure of the grapevines without any user intervention. The 3D information was generated by combining aerial images collected with a low-cost camera attached to an UAV and photo-reconstructed digital surface models (DSMs). Specific objectives included: (1) automatic classification of grapevines and row gaps (missing vine plants) without user intervention, overcoming the problem of spectral similarity with inter-row vegetation (cover-crop or weeds) and (2) automatic estimation of individual grapevines position (geographic coordinates) and dimensions (projected area, height, and volume). In addition, the potential applications of the outputs obtained with this methodology were discussed, including agronomical studies as well as for designing site-specific management strategies in the context of precision viticulture.

4. Materials and Methods

4.1. Study fields and UAV flights

The experiment was carried out in three different commercial vineyards located in the province of Lleida, Northeastern Spain (Table 1). The private company Raimat owner of the fields authorized this investigation and the UAV flights with an agreement in written. Vines were drip-irrigated and trellis-trained in all the vineyards, with the rows separated by 3 m and vine spacing of 2 m, and inter-row cover crops (Figure 1a), which has been reported in previous studies as a complex scenario due to the spectral similarity between vines and green cover crops (Baluja et al., 2012; Poblete-Echeverría et al., 2017). Vines management was mainly focused on wine production. The rows were north-south generally oriented for field A and B, and northwest-southeast for field C.

Table 1. Main characteristics of the studied fields. Coordinates are in the WGS84, UTM zone 31N reference system.

Field	Grape variety	Studied Area (m ²)	Central Coordinates (X, Y)
A	Merlot	4,925	291,009 E; 4,613,392 N
B	Albariño	4,415	291,303 E; 4,614,055 N
C	Chardonnay	2,035	290,910 E; 4,616,282 N



Figure 1. Images of the studied fields at different growth stages: a) inter-row cover crop growing in Field C in July; b) the UAV flying over Field B; c) and d) comparison between the field situations (green cover crops, vines and bare soil) between July and September in Field B.

The remote images were acquired with a low-cost RGB (R: red; G: green; B: blue) commercial off-the-shelf camera, model Olympus PEN E-PM1 (Olympus Corporation, Tokyo, Japan) mounted in a quadcopter model MD4-1000 (microdrones GmbH, Siegen, Germany) (Figure 1b). Technical specifications of the sensor are given in Table 2. The UAV can fly either manually by radio control (1000 m control range) or autonomously, with the aid of its Global Navigation Satellite System (GNSS) receiver and its waypoint navigation system. The UAV is battery powered and can load any sensor weighing up to 1.25 kg.

Table 2. Technical specifications of the imaging sensor on board the Unmanned Aerial Vehicle (UAV).

Sensor Size (mm)	Pixel Size (mm)	Sensor Resolution (pixels)	Focal Length (mm)	Radiometric Resolution (bit)	Image Format
17.3 × 13.0	0.0043	4,032 × 3,024	14	8	JPEG

Two flights were performed in each field, the first one on 29 July 2015 and the second one on 16 September 2015, depicting two different crop stages. In late July, the grapevine canopy was fully developed, with most of berries beginning to touch or touching, corresponding to 77 and 79 growth stage of the BBCH (Biologische Bundesanstalt,

Bundessortenamt, and Chemische Industrie) scale (Meier, 1997) (Figure 1c); while in September, the grapes had been machine-harvested (being at 91 growth stage of the BBCH scale), and consequently, the grapevine canopy was less dense (Figure 1d).

This approach, consisting of three fields at two crop stages, made it possible to analyze a wide range of situations to ensure the robustness of the OBIA procedure. The flights were performed at 30 m flight altitude, with a resulting spatial resolution of 1 cm pixel size and a ground image dimension of 37×28 m. The UAV route was programmed to take images continuously at 1-second intervals, thus resulting in a 93% of forward lap, and to produce a side lap of 60%. These overlaps were high enough to achieve the 3D reconstruction of woody crops according to previous investigations (Torres-Sánchez et al., 2015). The flight operations fulfilled the list of requirements established by the Spanish National Agency of Aerial Security, including the pilot license, safety regulations, and limited flight distance (AESPA, 2017).

4.2. DSM and orthomosaic generation

The DSM with height information and orthomosaic were generated using the Agisoft PhotoScan Professional Edition software (Agisoft LLC, St. Petersburg, Russia) version 1.2.4 build 1874. The mosaicking process was fully automatic, with the exception of the manual localization of 5 ground control points in the corners and in the center of each field with a Trimble GeoXH 2008 Series (Trimble, Sunnyvale, CA, USA) to georeference the DSM and orthomosaic. The whole automatic process involved three principal stages: (1) aligning images; (2) building field geometry; and (3) ortho-photo generation. First, the camera position for each image and common points in the images were located and matched, which facilitated the refinement of camera calibration parameters. Next, the software searched for more common points in the images to create a dense 3D point cloud (Figure 2) that was used as basis to generate the DSM, which was saved in greyscale tiff format. Finally, the individual images were projected over the DSM, and the orthomosaic was generated (Figure 3). The methodology to build these accurate geomatic products has been validated in previous research (Torres-Sánchez et al., 2018, 2015). The orthomosaics were only employed for validation purposes. More details about the Photoscan functioning are given in Dandois and Ellis (2013), and information about the processing parameters of the software are shown in Table 3. Radiometric corrections were not applied to the images as the proposed algorithm uses only DSM values, with independence of the spectral information of the images, which reduces time and optimizes the procedure.



Figure 2. A partial view of the 3-D point cloud for the vineyard field A in July, which was produced by the photogrammetric processing of the remote images taken with the UAV.

Table 3. Processing parameters selected for Digital Surface Model (DSM) and orthomosaic generation procedure by Agisoft Photoscan software.

Preference Setting	Control Parameter	Selected Setting
Alignment parameters	Accuracy	High
	pair preselection	Disabled
Dense point cloud	Quality	High
	depth filtering	Mild
DSM	Coordinate system	WGS84 / UTM zone 31 N
	source data	Dense cloud
Orthomosaic	Blending mode	Mosaic

4.3. OBIA algorithm

The OBIA algorithm for the detection and characterization of grapevines was developed using Cognition Network programming language with the eCognition Developer 9 software (Trimble GeoSpatial, Munich, Germany). The algorithm is fully automatic, it therefore requires no user intervention, and also has the benefit of self-adapting to the

different crop-field conditions, such as row-orientation, row and vine spacing, field slope, inter-row cover crops or grapevine dimensions.

The algorithm consisted of a sequence of phases (Figure 3), using only the DSM image as input, which are described as follows:

1. **Vine classification:** A chessboard segmentation algorithm was used to segment the DSM in square objects of 0.5 m side size (Figure 3). The grid size was based on the common vine row width for trellis system that is around 0.7 m. Most of the objects that covered vine regions also included pixels of bare soil, making the DSM standard deviation (SD_{DSM}) within those objects very large. Thus, the objects with a SD_{DSM} greater than 0.15 m were classified as “vine candidates”. The 0.15 SD_{DSM} value was selected to be well suited for vine detection based on previous studies. The remaining objects were pre-classified as bare soil (Figure 3).

The square objects that covered only vine regions had a low SD_{DSM} . To correctly classify them as “vine candidates”, the fact that they were surrounded by “vine candidates” was taken into account and implemented in the OBIA algorithm.

Each individual “vine candidates” was automatically analyzed at the pixel level to refine the vine classification. Firstly, the “vine candidates” objects were segmented at the pixel size objects by using the chessboard segmentation process. Next, the algorithm classified every pixel as vineyard or bare soil by comparing their DSM value with that of the surrounding bare soil square (Figure 3). The 0.8 m value was used as suited threshold to accurately classify actual vine objects, based on previous studies, which also avoided misclassification of cover green as vine.

The individual analysis of each “vine candidate” showed to be very suitable for vine classification, as only the surrounding soil altitude was taken into account for the discrimination, which could prevent errors due to field slope if the average soil altitude is considered instead. Moreover, using chessboard segmentation instead of the any other segmentation option, such as multi-resolution algorithm, decreases the computational time of the full process, because segmentation is by far the slowest task of the full OBIA procedure (Jiménez-Brenes et al., 2017). Thus, this configuration consisting of selecting DMS band as the reference for the segmentation instead of the spectral information, and the chessboard segmentation produced a notable increase in the processing speed without penalizing the segmentation accuracy (Jiménez-Brenes et al., 2017).

2. **Gap detection in vine rows:** Once the vines were classified, the gaps into the rows were detected by following four steps: (1) estimation of row orientation; (2) image

gridding based on strips following the row orientation; (3) strip classification; and (4) detection of gaps. Firstly, a new level was created above the previous one to calculate the main orientation of the vines and then to generate a mesh of strips of 0.5 width size with the same orientation as the vine row. Then, a looping process was performed until all the strips were analyzed: the strip in the upper level with the higher percentage of vine objects in the lower one, as well as its neighbors strips, were classified as “vine row”; and continuously, the adjacent strips were classified as “no row” to simplify the process.

Finally, the strips classified as “vine row” in the upper level were segmented into 0.5 m length segments and compared to the lower level for gap detection, so that these segments were recognized as “gap” if no vine objects were placed in the lower level.

3. Computing the vine geometric features: once the gaps into the row were identified, the vine rows were divided into 2 m length objects, which corresponded to each vine based on vine spacing. This parameter is user configurable to adapt the algorithm to different vine spacing. Before vine geometric feature calculation, the height of every pixel was individually obtained by comparing its DSM value (pixel height) to the average DSM value of the surrounding bare soil area. Then, the algorithm automatically calculated the geometric features (width, length and projected area, height and volume) of each vine, as follows: the highest height value of the pixels that composed the vine was selected as the vine height; and the volume was calculated by adding up the volumes (by multiplying the pixel areas and heights) of all the pixels corresponding to the vine. Finally, the geometric features of each vine, as well the identification and location, were automatically exported as vector (e.g., shapefile format) and table (e.g., Excel or ASCII format) files.

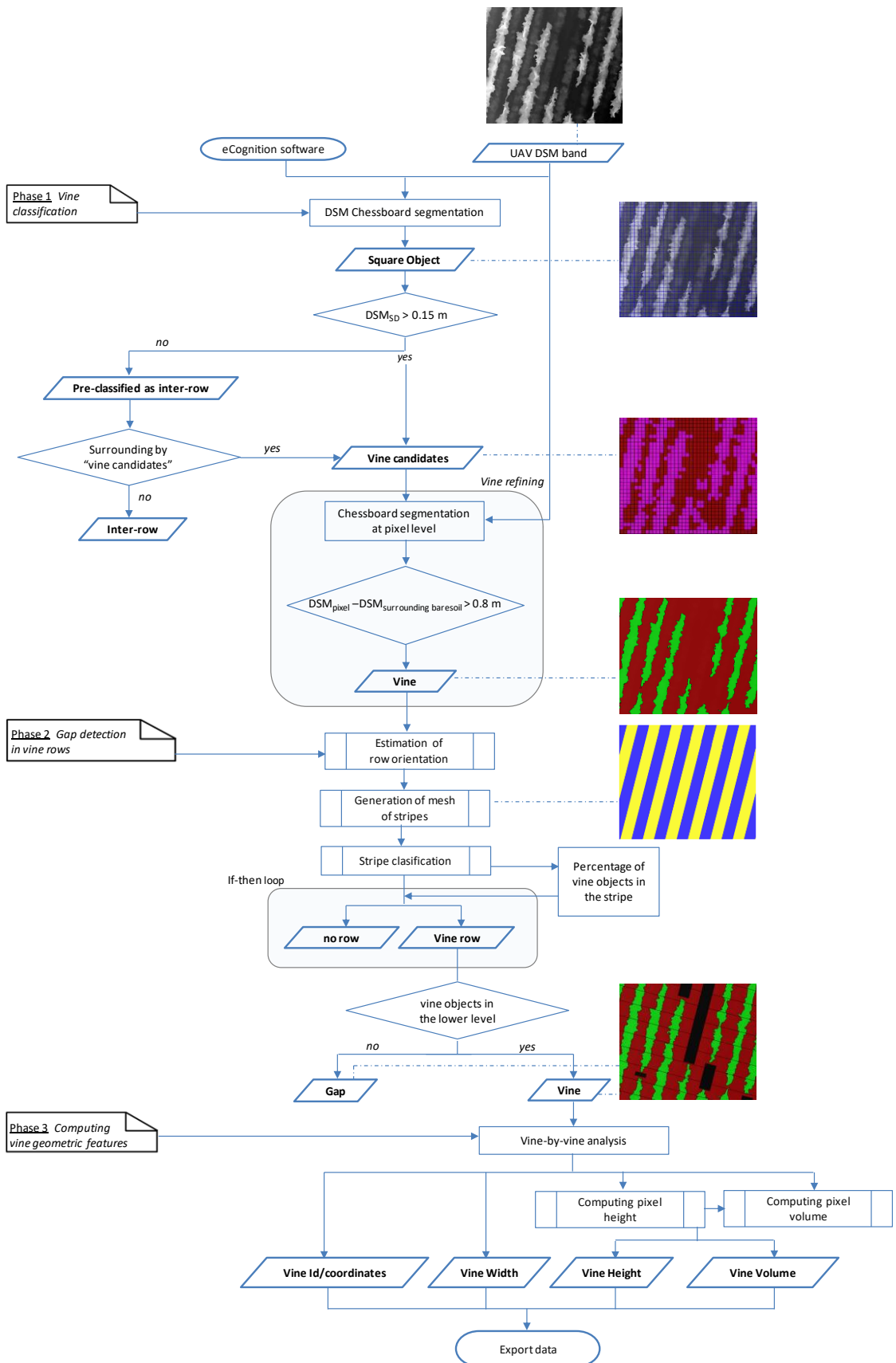


Figure 3. Flowchart and graphical examples of the Object Based Image Analysis (OBIA) procedure outputs for automatic vine characterization.

4.4. Validation

The validation of the vine classification and height estimation was carried out on the basis of a grid over the study fields, where 20 validation points were distributed and georeferenced during the flights in each field and year (Figure 4a,b).

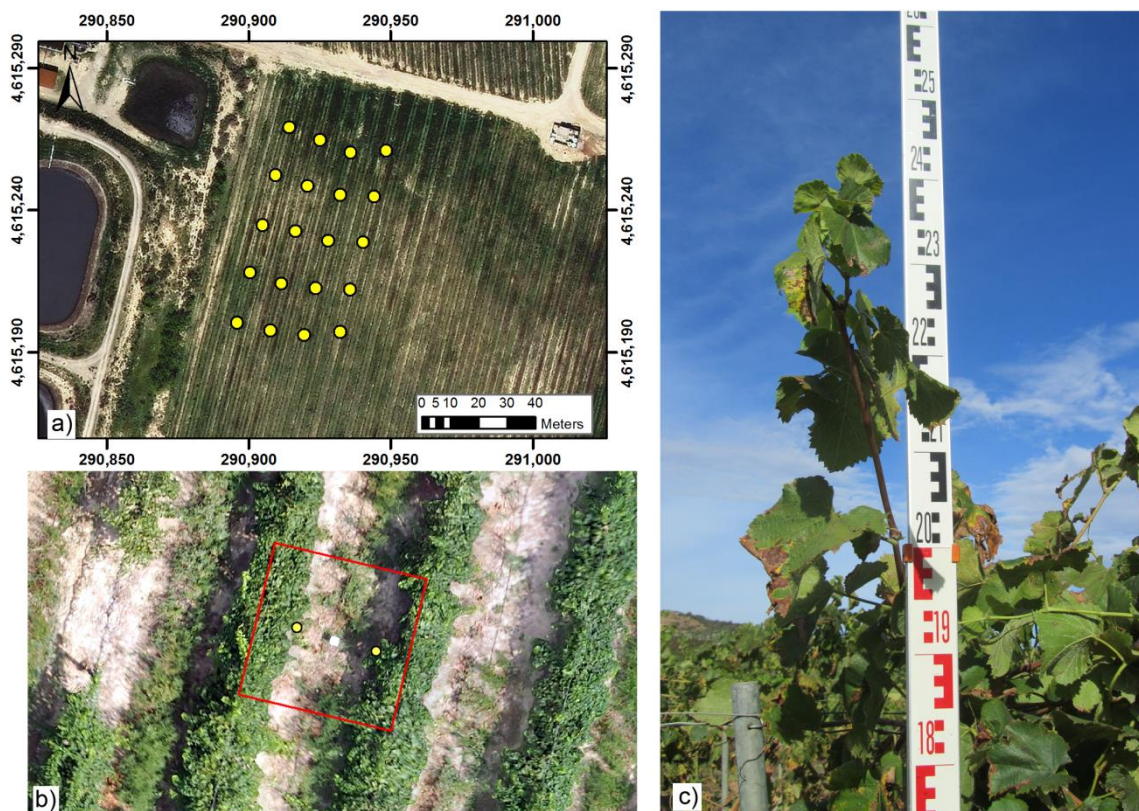


Figure 4. Experimental set for validating the results: a) validation point grid in Field A on July; b) a vector squares used for classification validation (yellow points indicate the positions of 40 true height data, and the white square is the artificial target placed in the field); c) measurement of the vine height.

4.4.1 Grapevine classification and gap detection

A 2×2 m validation square was designed in every validation point, previously described, with the same orientation as the vine rows using ArcGis 10.0 (ESRI, Redlands, CA, USA) shapefiles to evaluate the performance of the grapevine classification. The very high spatial resolution of the orthomosaicked made possible to visually identify and manually classify the vine plants and soil in every designed square.

A confusion matrix was created to quantify the accuracy of the method by comparing the manual classification with the output of the automatic classification algorithm. The confusion matrix provided the overall accuracy (OA) of the classification (Equation (1)), which indicates the percentage of correctly classified area, and thus, the overall success of classification; and the Cohen's Kappa index (Kc) (Equation (2)) that takes into account the possibility of the agreement occurring by chance. Information about the confusion matrix is shown in Table 4.

Table 4. Error matrix schema for validation of vineyard classification.

Classified Data				
		Vineyard	No vineyard	
Manual	Vineyard	%V _V	%V _{NV}	T _{R1}
classification	No vineyard	%NV _V	%NV _{NV}	T _{R2}
		T _{C1}	T _{C2}	T _{R1} + T _{R2} = T _{C1} + T _{C2} = 100%

where: %V_V: percentage of data correctly classified as vineyard; %V_{NV}: percentage of data corresponding to vineyard wrongly classified as No vineyard; %NV_V: percentage of data wrongly classified as vineyard; %NV_{NV}: percentage of data correctly classified as No vineyard; TR₁, TR₂, TC₁, and TC₂ are the totals of row 1, row 2, column 1, and column 2, respectively.

$$\text{Overall Accuracy} \quad \text{OA} = \%V_V + \%NV_{NV} \quad (\text{Eq. 1})$$

$$\text{Kappa} \quad kc = \frac{p_o - p_c}{1 - p_c} \quad (\text{Eq. 2})$$

where: P_c is the *Proportion of chance agreement*, $p_c = \frac{T_{C1}}{100} \times \frac{T_{R1}}{100} + \frac{T_{C2}}{100} \times \frac{T_{R2}}{100}$

and P_o is the *Actual proportion of agreement*, $p_o = \frac{\%V_V + \%NV_{NV}}{100}$

For the validation of the gap detection, manual digitalization and length measurement of gaps were carried out in the orthomosaic. Thus, the on-ground gaps (real gap) were compared to the image OBIA process output, and the accuracy was measured by calculating true positive defined as real gaps correctly classified as gap; false positive refers to real vines wrongly classified as gaps; and false negative refers to real gaps wrongly classified as vines.

4.4.2 Grapevine height

For height quantification, 40 true height data resulting of measuring on both sides of every validation point were taken in every field and date (Figure 4a,b). Each true data corresponding to grapevine height was photographed with the branch of the vine in front and the ruler included (Figure 4c). Then, the measured vine heights were compared to the height estimated by the OBIA algorithm. The coefficient of determination (R^2) derived from a linear regression model and the root mean square error (RMSE) of this comparison were calculated using JMP software (SAS, Cary, NC, USA).

5. Results and Discussion

5.1. Vine classification

The classification statistics obtained in the confusion matrix (OA and K_c) for every field and year are shown in Table 5. Overall Accuracy assessments varied slightly according to the location and year, providing OA values higher than 93.6% in all classifications, e.g., 95.5% in field A-July, and 96.0% and 96.1 in field B and field C in September, respectively. Therefore, OA values much greater than 85% -the minimum accepted value according to Foody (2002)- were recorded at all six cases analyzed, which indicated that the algorithm was able to accurately classify vines at different growth stages. An example of a validation frame is shown in Figure 5.

Table 5. Classification statistics (Overall accuracy and Kappa index) obtained in confusion matrix at every location and date.

Field	Date	Overall Accuracy (%)	Kappa
A	July	95.5	0.9
	September	95.4	0.9
B	July	95.2	0.9
	September	96.0	0.9
C	July	93.6	0.8
	September	96.1	0.7

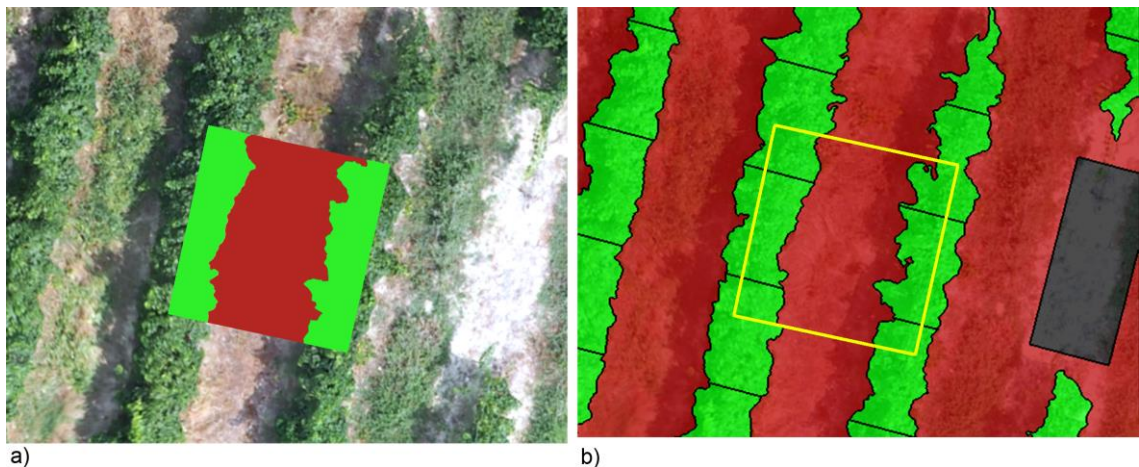


Figure 5. Example of 2 x 2 validation frame in field A-July: (a) manually classified orthomosaicked image (R-G-B composition); (b) DSM-OBIA-based classification.

Regarding Kappa coefficient, values over 0.8 were achieved in most of the studied cases (e.g., 0.9 in field A-July and field B-September, and 0.8 in field C-July), which strongly indicates that these classifications are unlikely to have been obtained by chance alone (Landis and Koch, 1977). Although the classification of field C-September did not achieve that high accurate value, the obtained kappa result of 0.7 pointed out a substantial classification agreement according to Landis and Koch (1977). The lower Kappa results obtained in Field C could be due to irregular growth of vines, with many thin branches containing few leaves, which made the 3D canopy modelling more difficult. In fact, the low yield and irregular growth obtained last years in field C led the owner to uproot the entire field in winter 2015. Therefore, this fact highlights how crucial the accurate definition of DSM is for this procedure. Alternatively, the high accuracy obtained in this field based on OA contrasted with those lower Kappa values and might be related to the fact that the Kappa statistic is more sensible to unbalanced classes, as the soil covered a greater portion of image than vines in this field.

Previous investigations have attempted to isolate vines using a spectral approach, for example Baluja et al. (2012) used thresholding techniques to an inverse NDVI (Normalized Difference Vegetation Index) compute image to extract pure vine pixel. However, they detected problems with the inclusion of soil information or large loss of information, since determining the optimal threshold involved a compromise between retaining non-vine NDVI values and losing vine NDVI values. Similarly, Smit et al. (2010) reported that achieving the optimal balance was a very difficult and inaccurate task and, consequently, thresholding on its own was not suitable for vine row classification. Comparatively, our results proved that less than 6.5% of soil was misclassified as vine (data not shown) using the DSM-based OBIA algorithm developed in this paper. Moreover, using those thresholding techniques for vine classification might generate inconsistent results due to shadows and inter-row cover crops. Puletti et al. (2014) used the Red channel for

identification of grapevine rows achieving acceptable accuracy values (lower than 87% of OA), however the inter-row spaces were not vegetation-covered. Therefore, the use of DSM in the vine classification is shown to be as a more accurate and efficient alternative to spectral approach, especially in the challenging spectral similarity scenario due to cover crops growing in the inter-rows.

In addition to the above, the OBIA algorithm developed was fully automatic compared to other approaches for vine classification that needed a manual touch-up to remove non-vine objects (Laliberte et al., 2011); previous training of the classifier (Albetis et al., 2017; Poblete-Echeverría et al., 2017); or manual delineation of vines (Matese et al., 2015). Although some of these approaches achieved high level of accuracy, not much greater than that obtained in our work, they required user intervention and/or carried out the experiments in vineyard without cover crops growing in the inter-rows. In this way, the DSM-OBIA method offered a significant improvement compared to conventional classifiers, since it does not require any user intervention that makes the classification process time-efficient, reliable, and more accurate, removing errors from a subjective manual process (de Castro et al., 2018).

5.2. Vine gap detection

Table 6 shows the classification results of gap detection obtained from the DSM-OBIA algorithm. The correct classification percentage (true positive) for each field and growth stage analyses was 100% except for field A-September, where the accuracy achieved was 96.8%. False negative that indicated wrongly classified gaps as vines only occurred in field A-September with a value of 3.2%, which proved the efficiency of the OBIA algorithm. Moreover, rates lower than 6% of vines were misclassified as gaps in fields A and B for both dates, and field C in July. However, higher rates of false positives were detected in field C-September due to the lower accuracy of vine 3D reconstruction, as explained in the previous section, which was even more prominent in September because of the harvest machinery activity.

Table 6. Results of the gap detection in vine rows. Percentages were calculated over the total length of gaps in the field.

Field	Date	True Positive (%)	False Positive (%)	False Negative (%)
A	July	100.0	1.12	0.0
	September	96.8	0.0	3.2
B	July	100.0	1.0	0.0
	September	100.0	6.0	0.0
C	July	100.0	0.0	0.0
	September	100.0	46.8	0.0

This kind of information can be used for vineyard management, e.g., to target areas that need more specific attention (Delenne et al., 2010). Thus, false negatives might be more risky than false positives, as a problem that causes missing vine plants would be not detected. Delenne et al. (2010) used images acquired from a manned ultra-light aircraft for vineyard delineation by using spectral approach, and they concluded that non-detection of missing vine plants could be due the spectral similarity of the grass under the row. According to our findings, the use of accurate DSM in the algorithm is crucial for gap detection, which was feasible using high UAV-imagery overlap and photogrammetric techniques.

5.3. Vine height quantification

Accuracy and graphical comparisons between the manually acquired and DSM-OBIA estimated vine heights for all fields and years are shown in Figure 6. The OBIA algorithm accurately estimated the plant height from the DSM of the vineyards achieving a very high correlation ($R^2 = 0.78$). A low RMSE of 0.19 was reported for this comparison, similar magnitude to that obtained in the detection of olive height using a visible-light camera attached to an UAV (Torres-Sánchez et al., 2015). Moreover, most of the points were close to the 1:1 line with the points evenly scattered on either side of the line, which indicated an excellent fit of OBIA-estimated and measured height.

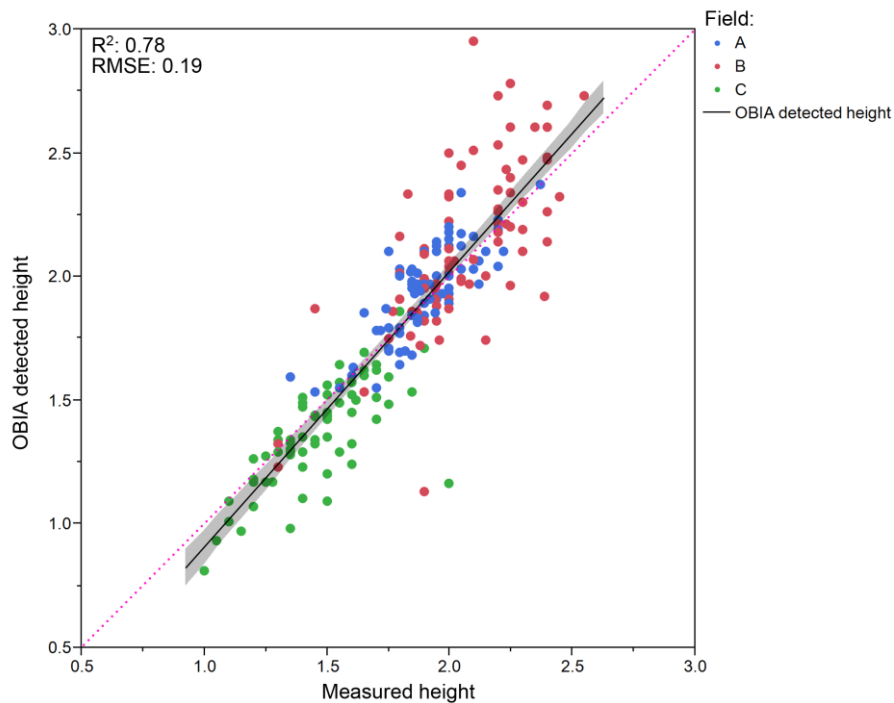


Figure 6. Graphic comparing DSM-OBIA estimated and vine height for all data corresponding to the three fields and both dates (July and September). The root mean square error (RMSE) and correlation coefficient (R^2) derived from the regression fit are included ($p < 0.0001$). The solid line is the fitted linear function and the pink dashed line represents the 1:1 line.

Analyzing the data by field and date (Figure 7), a better fit was obtained for each case reaching lower RMSE values for each one (<0.16), with the exception of field B-July, with independence of the growth stages, which demonstrated algorithm robustness. In a previous investigation, Burgos et al. (2015) obtained similar results using image-based UAV technology for vine height detection, although an exhaustive validation was not carried out because of the lack of individual vine height, using average height of polygons instead, so this methodology remained non-validated at the individual vine level. In addition, Burgos et al. (2015) performed a flight plan with higher cost in time, consisting of perpendicular directions, which implies reducing the area analyzed due to the limited UAV autonomy; and generated a digital terrain model as well, thus increasing the computational time. Furthermore, Matese et al. (2017) reported quite a discordance (0.50 m) between actual height and estimated height vines from UAV-based crop surface models due to the low resolution sensor used (1.3 MP), which caused a smoothing effect in the DSM generation. Accordingly, this issue could be solved employing higher spatial resolution images.

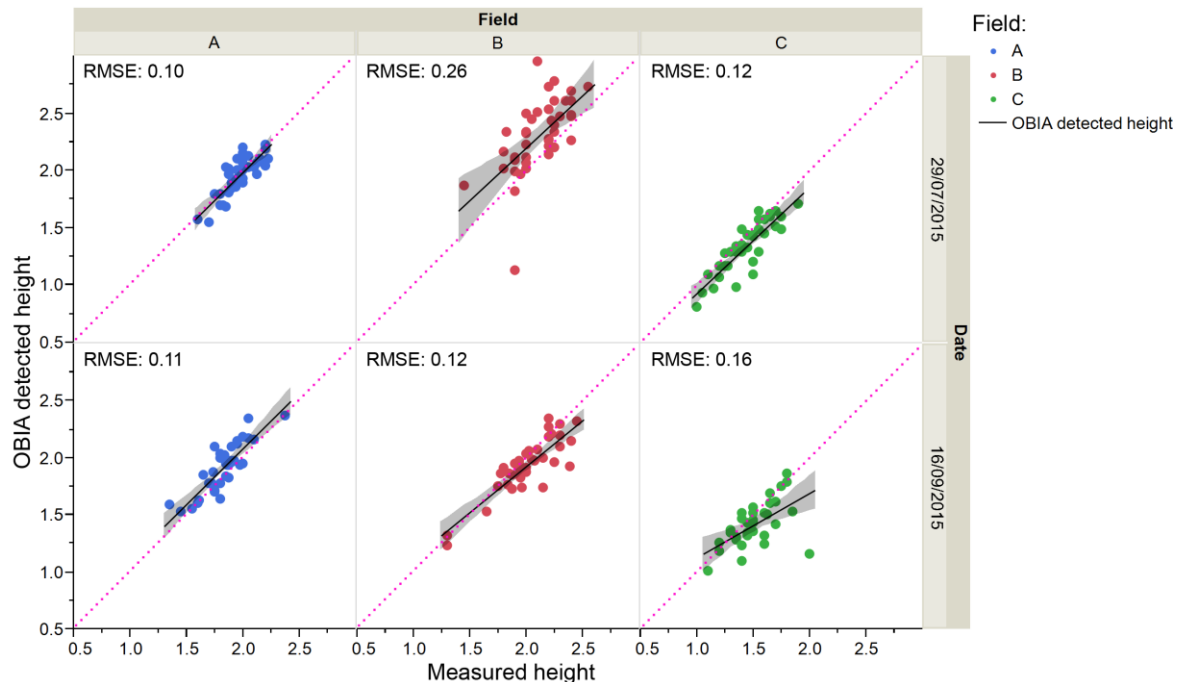


Figure 7. DSM-OBIA detected height vs. measured vine height divided by field and date. The root mean square error (RMSE) derived from the regression fit are included ($p < 0.0001$). The solid line is the fitted linear function and the pink dashed lines represent the 1:1 line.

The lower accuracy observed for gap detection in field C-September contrasted with the accurate vine height detection (Table 6 and Figure 7, respectively). Despite limitations in the bottom of the vine canopy 3D reconstruction due to the weak canopy with sparse leaves, the top of them were correctly identified so that the OBIA algorithm was able to accurately detect the height of every vine. Consequently, the vine height detection is even effective when the 3D reconstruction of the bottom of the canopy is not very precise.

Based on our finding, the use of a DSM in the OBIA algorithm enabled the efficient assessment of vine height, and the development of DSM was feasible due to the high overlap and spatial resolution of UAV-imagery. To the best of our knowledge, OBIA-based technology has not yet been applied to automatically estimate vine height, and subsequently, to validate the procedure using individual ground truth data. In this context, some authors have estimated vine height by using photogrammetric point clouds from UAV imagery, such as Ballesteros et al. (2015) and Weiss et al. (2017). However manual intervention was needed in both approaches, which would make the process less time-efficient and less accurate due to errors from a subjective manual process (de Castro et al., 2018). Moreover, they pointed out that no exhaustive validation was carried out, which was a pending challenge. Therefore, the experiments carried out in this paper overcame both limitations of manual intervention and precise validation.

The DSM-OBIA process hence developed is useful for trellis system, one of the most widely used training systems around the word. However, more training systems are routinely employed in vineyard fields depending on the production objective (wine quality, yield), the cost of the system, climate, topography, vine vigour, vine variety, and mechanization requirements, among others. Thereby, the OBIA algorithm could be adapted to those training system characteristics. In addition, this approach was based on the DSM, which allowed for isolation of the vine from the bare soil and cover crops, which is considered a major issue in vineyard characterization (Weiss et al., 2017). Cover crops are a common practice widely used in vineyard as a management tool to maintain the optimal vine growth and fruit development, as well as controlling the excess grapevine shoot vigour. For these purposes, cover crops are kept at low height. Although it hardly ever occurs, the cover crops could achieve a higher altitude than the vines, making it difficult to isolate the vine. Accordingly, it could be solved by adding the orthomosaic to the OBIA algorithm, and thus combining textural, spectral, topological, or contextual information to separate vine and cover crops.

5.4. Potential algorithm result applications

The technological combination of UAV imagery and the DSM-OBIA algorithm herein developed enables the rapid and accurate vineyard characterization by identifying, isolating, and extracting geometric features of every vine at several growth stages. This accurate methodology has multiple implications for PV purposes, for example, it could be used to automatically mask soil and cover crops pixels and extract information of every vine from multispectral imagery for disease detection (Albetis et al., 2017); or thermal imagery for assessment the vineyard water status (Santesteban et al., 2017), as requested by Baluja et al. (2012) and Espinoza et al. (2017).

Vine volume could be efficiently estimated from the accurate area classification and vine height detection, by multiplying the height and area of every pixel that compose the vine canopy. This approach would leave those few leaves bellow the basal level of the vineyard canopy without computing, since they are difficult to identify. Alternatively, on-the-go soil sensing systems, as a terrestrial laser scanner, have shown potential to estimate vine volume for precision applications, as spraying application (Llorens et al., 2010). However, these systems are slower than UAV technology and enable one to only take one vineyard side information. Therefore, a combination of mobile terrestrial sensors and OBIA-UAV technology could be conducted in further research to evaluate the performance of both approaches in vine volume quantification.

The algorithm output can be automatically exported both as table files (Table 7) and vector files, i.e., geo-referenced maps with the locations and dimensions of every vine (Figure 8), thus showing the spatial variability of the vineyard, a crucial key for precision viticulture (Bramley and Hamilton, 2004). These geo-referenced maps with the dimensions of every vine could be useful to identify less vigour or size areas that require special attention, as well as being the basis for designing a site-specific management program (Albetis et al., 2017; Hall et al., 2011). For example, Figure 8 showed that vines in field C had much lower volume than fields A and B, which was indicative of the low vigour that led growers to uproot the field.

Table 7. A sample of the output data file delivered by the OBIA algorithm for vine of field A-September.

X Center	Y Center	Length (m)	Width (m)	Area (m ²)	Vine Max Height (m)	Vine Mean Height (m)	Vine Volume (m ³)
290,909.63	4,615,191.17	1.36	0.48	0.51	2.02	1.49	0.76
290,909.85	4,615,192.23	2.06	1.41	1.93	2.13	1.33	2.56
...
290,910.55	4,615,194.39	2.05	1.21	1.32	2.22	1.53	2.02
290,918.60	4,615,225.30	2.06	1.74	2.35	2.22	1.72	4.05
290,919.09	4,615,227.23	2.14	1.65	2.15	2.18	1.54	3.31
290,919.60	4,615,229.19	2.03	1.37	1.46	2.00	1.41	2.06
290,920.12	4,615,231.14	2.19	1.63	2.13	2.00	1.40	2.99

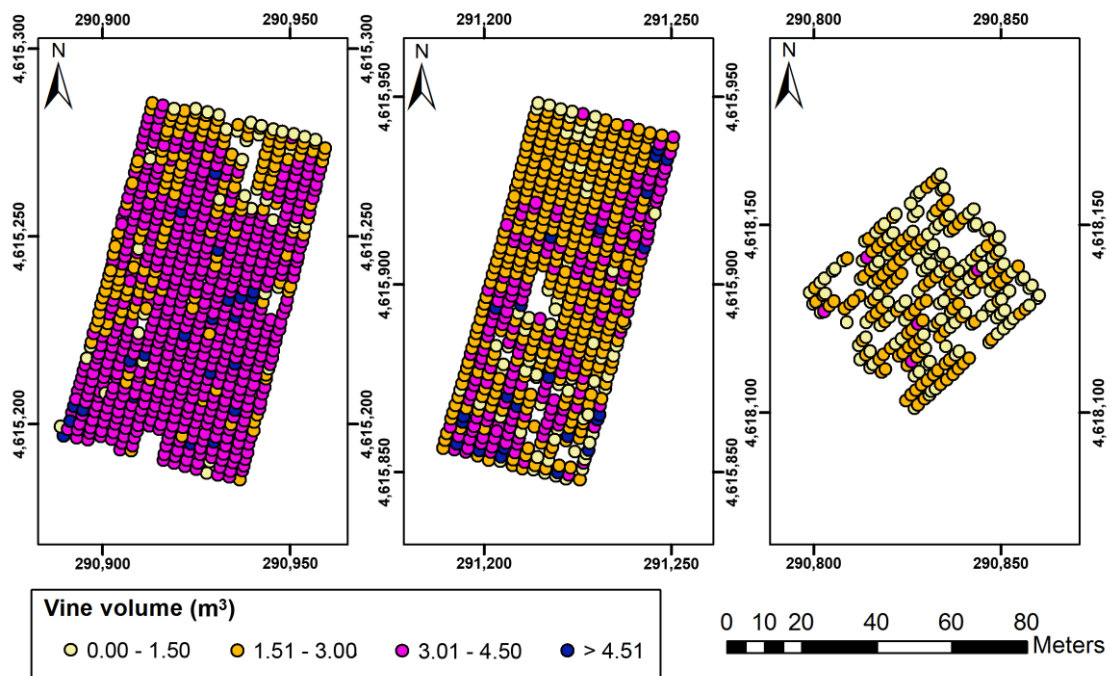


Figure 8. Four-level representation of the estimated vine canopy volume as computed on the three fields in July, from left to right: From left to right: Field A, Field B and Field C. In the axes, coordinate system UTM zone 31 N, datum WGS84.

This technology has been proven at two growth stages, and its use in a multi-temporal approach could open new opportunities to monitor vine status and progress at the field scale, as an efficient and accurate alternative to the arduous and inconsistent manual measurements on the ground. For example, Figure 9 shows the distribution of height, area, and volume of a vine row at the two dates studied (July and September) that corresponded to different growth stages. Segment length is a user-configurable parameter for the algorithm output, and for this example 0.10 m was selected to catch in detail the impact of the harvesting machinery. Specifically, this Figure showed that vine area decreased from July to September in a higher range, around 40%, than that of the other geometric characteristics, which could be directly due to the harvest, as the machinery activity causes the berries to fall off the stem, as well as leaves and other debris that may have fallen from the vines along with the fruit. The height parameter showed a slight decrease of around 6%, since the machinery affects the upper part of the vines much less. As the volume is calculated directly from the area and height of the vine, it decreased in an intermediate range of 30%. Canopy monitoring throughout the growing cycle could help growers with multiple purposes, such as identifying biotic stress, irrigation deficit or nutrient status. In addition, this approach would help to address the goal of improving prediction models that

connect the vine geometric characteristics with the vineyard yield, which is a complex issue that depends on a large number of factors (Jiménez-Brenes et al., 2017).

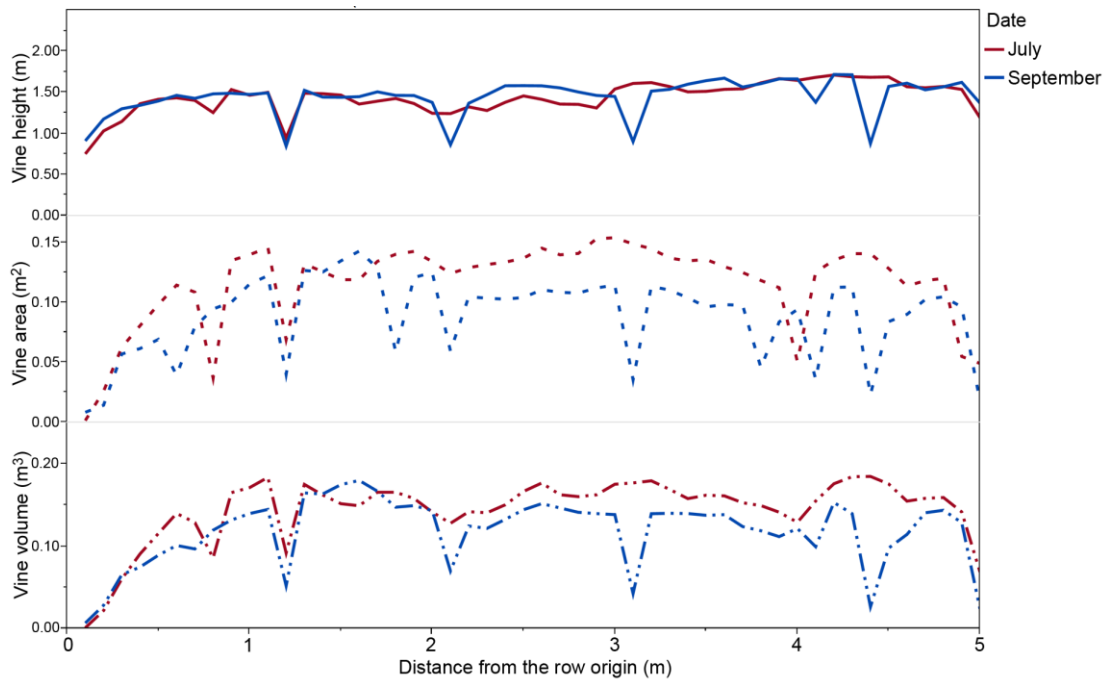


Figure 9. Height, area and volume values in two dates (July and September, corresponding to different growth stages) from the left side to the row. Every data corresponded to 0.10 m length segments of the vine row.

6. Conclusions

A robust and fully automatic OBIA algorithm was developed for the 3D characterization of the vineyard fields, including vine classification, height estimation, and gap detection, from UAV-imagery. Using photogrammetric-based DSM as input in the algorithm, the misclassification due to spectral similarity between vines and green-cover growing in the inter-rows was avoided. The DSM-OBIA model was tested in three commercial vineyards at two different growth stages using images acquired with a low-cost camera onboard an UAV. The algorithm accurately detected the area and height of the vines, and the existence of gaps. Moreover, the developed OBIA algorithm is self-adaptive to different crop-field conditions, as row orientation, row and vine spacing, field slope, inter-row cover crops, or grapevine dimensions. This fully automatic process, without previous training or user intervention, is an important asset that makes this procedure time-efficient, reliable and more accurate, removing the potential errors inherent to a manual process.

In addition, the algorithm output can be exported as geo-referenced maps with the locations and dimensions of every vine, thus showing the spatial variability of the vineyard, a crucial key for precision management. Volume of the vine canopy can be estimated from the area and height of vines, which could be considered another potentiality of this methodology. Thereby, the procedure developed, based on ultra-high-spatial resolution DSMs and the OBIA algorithm, has shown to be a valuable tool for the accurate characterization of the vines that has important implications for the adoption of Precision Viticulture. Thus, for instance, it could help growers to identify less vigor or size areas that require special attention, monitor the vine growth, determine the proper moment to harvest, or to evaluate the effect different trimming treatments in the grapevine canopy structure.

7. Acknowledgments

The authors thank RAIMAT S.A. for allowing developing the field work and UAV flights in its vineyards. This research was funded by the AGL2017-83325-C4-4R project (Spanish Ministry of Economy, Industry and Competitiveness FEDER Funds: Fondo Europeo de Desarrollo Regional). Research of A. I. de Castro and J. M. Peña was financed by the Juan de la Cierva Incorporación and Ramon y Cajal (RYC-2013-14874) Programs, respectively. We acknowledge support of the publication fee by the CSIC Open Access Publication Support Initiative through its Unit of Information Resources for Research (URICI).

8. References

AESA, 2017. URL

http://www.seguridadaerea.gob.es/LANG_EN/cias_empresas/trabajos/rpas/marco/default.aspx (accessed 6.2.17).

Albetis, J., Duthoit, S., Guttler, F., Jacquin, A., Goulard, M., Poilv , H., F ret, J.-B., Dedieu, G., 2017. Detection of flavescence dor e grapevine disease using unmanned aerial vehicle (UAV) multispectral imagery. *Remote Sens.* 9, 308.

<https://doi.org/10.3390/rs9040308>

Arn  Satorra, J., Casasnovas, M., Antonio, J., Ribes Dasi, M., Polo, R., Ram n, J., 2009.

Review. Precision viticulture. Research topics, challenges and opportunities in site-specific vineyard management. *Span. J. Agric. Res.* 7(4): 779-790.

<https://doi.org/10.5424/sjar/2009074-1092>

- Ballesteros, R., Ortega, J.F., Hernández, D., Moreno, M.Á., 2015. Characterization of *Vitis vinifera* L. canopy using unmanned aerial vehicle-based remote sensing and photogrammetry techniques. *Am. J. Enol. Vitic.* ajev.2014.14070. <https://doi.org/10.5344/ajev.2014.14070>
- Baluja, J., Diago, M.P., Balda, P., Zorer, R., Meggio, F., Morales, F., Tardaguila, J., 2012. Assessment of vineyard water status variability by thermal and multispectral imagery using an unmanned aerial vehicle (UAV). *Irrig. Sci.* 30, 511–522. <https://doi.org/10.1007/s00271-012-0382-9>
- Bendig, J., Bolten, A., Bennertz, S., Broscheit, J., Eichfuss, S., Bareth, G., 2014. Estimating biomass of barley using crop surface models (CSMs) derived from UAV-based RGB imaging. *Remote Sens.* 6, 10395–10412. <https://doi.org/10.3390/rs6110395>
- Blaschke, T., Hay, G.J., Kelly, M., Lang, S., Hofmann, P., Addink, E., Queiroz Feitosa, R., van der Meer, F., van der Werff, H., van Coillie, F., Tiede, D., 2014. Geographic object-based image analysis – towards a new paradigm. *Isprs J. Photogramm. Remote Sens.* 87, 180–191. <https://doi.org/10.1016/j.isprsjprs.2013.09.014>
- Bramley, R. g. v., Hamilton, R. p., 2004. Understanding variability in winegrape production systems. *Aust. J. Grape Wine Res.* 10, 32–45. <https://doi.org/10.1111/j.1755-0238.2004.tb00006.x>
- Burgos, S., Mota, M., Noll, D., Cannelle, B., 2015. Use of very high-resolution airborne images to analyse 3D canopy architecture of a vineyard. *ISPRS - Int. Arch. Photogramm. Remote Sens. Spat. Inf. Sci.* 3, 399–403. <https://doi.org/10.5194/isprsarchives-XL-3-W3-399-2015>
- Castillejo-González, I.L., Peña-Barragán, J.M., Jurado-Expósito, M., Mesas-Carrascosa, F.J., López-Granados, F., 2014. Evaluation of pixel- and object-based approaches for mapping wild oat (*Avena sterilis*) weed patches in wheat fields using QuickBird imagery for site-specific management. *Eur. J. Agron.* 59, 57–66. <https://doi.org/10.1016/j.eja.2014.05.009>
- Dandois, J.P., Ellis, E.C., 2013. High spatial resolution three-dimensional mapping of vegetation spectral dynamics using computer vision. *Remote Sens. Environ.* 136, 259–276. <https://doi.org/10.1016/j.rse.2013.04.005>
- de Castro, A.I., Torres-Sánchez, J., Peña, J.M., Jiménez-Brenes, F.M., Csillik, O., López-Granados, F., 2018. An automatic random forest-OBIA algorithm for early weed mapping between and within crop rows using UAV imagery. *Remote Sens.* 10, 285. <https://doi.org/10.3390/rs10020285>
- Delenne, C., Durrieu, S., Rabatel, G., Deshayes, M., 2010. From pixel to vine parcel: A complete methodology for vineyard delineation and characterization using remote-

- sensing data. *Comput. Electron. Agric.* 70, 78–83.
<https://doi.org/10.1016/j.compag.2009.09.012>
- Espinoza, C.Z., Khot, L.R., Sankaran, S., Jacoby, P.W., 2017. High resolution multispectral and thermal remote sensing-based water stress assessment in subsurface irrigated grapevines. *Remote Sens.* 9, 961. <https://doi.org/10.3390/rs9090961>
- Foody, G.M., 2002. Status of land cover classification accuracy assessment. *Remote Sens. Environ.* 80, 185–201. [https://doi.org/10.1016/S0034-4257\(01\)00295-4](https://doi.org/10.1016/S0034-4257(01)00295-4)
- Franklin, S.E., Ahmed, O.S., 2018. Deciduous tree species classification using object-based analysis and machine learning with unmanned aerial vehicle multispectral data. *Int. J. Remote Sens.* 39, 5236–5245. <https://doi.org/10.1080/01431161.2017.1363442>
- Geipel, J., Link, J., Claupein, W., 2014. Combined spectral and spatial modeling of corn yield based on aerial images and crop surface models acquired with an unmanned aircraft system. *Remote Sens.* 6, 10335–10355. <https://doi.org/10.3390/rs6110335>
- Hall, A., Lamb, D.W., Holzapfel, B., Louis, J., 2002. Optical remote sensing applications in viticulture - a review. *Aust. J. Grape Wine Res.* 8, 36–47.
<https://doi.org/10.1111/j.1755-0238.2002.tb00209.x>
- Hall, A., Lamb, D.W., Holzapfel, B.P., Louis, J.P., 2011. Within-season temporal variation in correlations between vineyard canopy and winegrape composition and yield. *Precis. Agric.* 12, 103–117. <https://doi.org/10.1007/s11119-010-9159-4>
- Hellesen, T., Matikainen, L., 2013. An object-based approach for mapping shrub and tree cover on grassland habitats by use of LiDAR and CIR orthoimages. *Remote Sens.* 5, 558–583. <https://doi.org/10.3390/rs5020558>
- Jiménez-Brenes, F.M., López-Granados, F., de Castro, A.I., Torres-Sánchez, J., Serrano, N., Peña, J.M., 2017. Quantifying pruning impacts on olive tree architecture and annual canopy growth by using UAV-based 3D modelling. *Plant Methods* 13, 55.
<https://doi.org/10.1186/s13007-017-0205-3>
- Johnson, L.F., Roczen, D.E., Youkhana, S.K., Nemani, R.R., Bosch, D.F., 2003. Mapping vineyard leaf area with multispectral satellite imagery. *Comput. Electron. Agric.* 38, 33–44. [https://doi.org/10.1016/S0168-1699\(02\)00106-0](https://doi.org/10.1016/S0168-1699(02)00106-0)
- Laliberte, A.S., Goforth, M.A., Steele, C.M., Rango, A., 2011. Multispectral remote sensing from unmanned aircraft: image processing workflows and applications for rangeland environments. *Remote Sens.* 3, 2529–2551. <https://doi.org/10.3390/rs3112529>
- Laliberte, A.S., Rango, A., Herrick, J.E., Fredrickson, E.L., Burkett, L., 2007. An object-based image analysis approach for determining fractional cover of senescent and

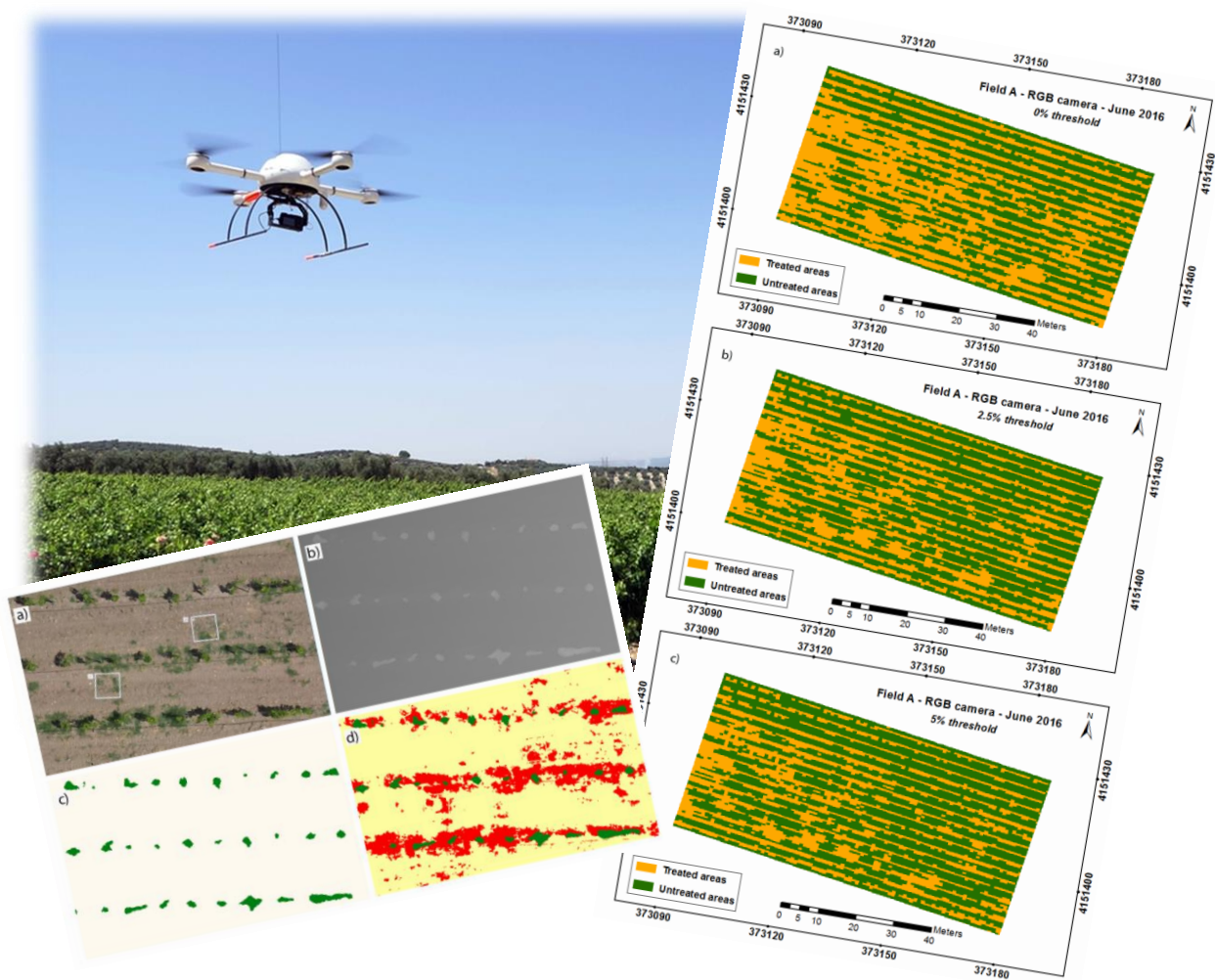
- green vegetation with digital plot photography. *J. Arid Environ.* 69, 1–14.
<https://doi.org/10.1016/j.jaridenv.2006.08.016>
- Landis, J.R., Koch, G.G., 1977. The measurement of observer agreement for categorical data. *Biometrics* 33, 159–174.
- Llorens, J., Gil, E., Llop, J., Escolà, A., 2010. Variable rate dosing in precision viticulture: use of electronic devices to improve application efficiency. *Crop Prot.* 29, 239–248.
<https://doi.org/10.1016/j.cropro.2009.12.022>
- López-Granados, F., Torres-Sánchez, J., Castro, A.I. de, Serrano-Pérez, A., Mesas-Carrascosa, F.J., Peña, J.-M., 2016. Object-based early monitoring of a grass weed in a grass crop using high resolution UAV imagery. *Agron. Sustain. Dev.* 36, 67.
<https://doi.org/10.1007/s13593-016-0405-7>
- Mancini, F., Dubbini, M., Gattelli, M., Stecchi, F., Fabbri, S., Gabbianelli, G., 2013. Using unmanned aerial vehicles (UAV) for high-resolution reconstruction of topography: the structure from motion approach on coastal environments. *Remote Sens.* 5, 6880–6898. <https://doi.org/10.3390/rs5126880>
- Matese, A., Gennaro, S.F.D., Berton, A., 2017. Assessment of a canopy height model (CHM) in a vineyard using UAV-based multispectral imaging. *Int. J. Remote Sens.* 38, 2150–2160. <https://doi.org/10.1080/01431161.2016.1226002>
- Matese, A., Toscano, P., Di Gennaro, S.F., Genesio, L., Vaccari, F.P., Primicerio, J., Belli, C., Zaldei, A., Bianconi, R., Gioli, B., 2015. Intercomparison of UAV, aircraft and satellite remote sensing platforms for precision viticulture. *Remote Sens.* 7, 2971–2990.
<https://doi.org/10.3390/rs70302971>
- Mathews, A.J., 2014. Object-based spatiotemporal analysis of vine canopy vigor using an inexpensive unmanned aerial vehicle remote sensing system. *J. Appl. Remote Sens.* 8, 085199. <https://doi.org/10.1117/1.JRS.8.085199>
- Mathews, A.J., Jensen, J.L.R., 2013. Visualizing and quantifying vineyard canopy lai using an unmanned aerial vehicle (UAV) collected high density structure from motion point cloud. *Remote Sens.* 5, 2164–2183. <https://doi.org/10.3390/rs5052164>
- Meier, U. (Ed.), 1997. Growth stages of mono- and dicotyledonous plants: BBCH-Monograph, Blackwell Wissenschaft. Blackwell Wissenschafts-Verlag, Berlin; Boston.
- Nex, F., Remondino, F., 2014. UAV for 3D mapping applications: A review. *Appl. Geomat.* 6, 1–15. <https://doi.org/10.1007/s12518-013-0120-x>
- Peña, J.M., Torres-Sánchez, J., Castro, A.I. de, Kelly, M., López-Granados, F., 2013. Weed mapping in early-season maize fields using object-based analysis of unmanned aerial

- vehicle (UAV) images. *PLoS ONE* 8, e77151.
<https://doi.org/10.1371/journal.pone.0077151>
- Poblete-Echeverría, C., Olmedo, G.F., Ingram, B., Bardeen, M., 2017. Detection and segmentation of vine canopy in ultra-high spatial resolution RGB imagery obtained from unmanned aerial vehicle (UAV): A case study in a commercial vineyard. *Remote Sens.* 9, 268. <https://doi.org/10.3390/rs9030268>
- Puletti, N., Perria, R., Storchi, P., 2014. Unsupervised classification of very high remotely sensed images for grapevine rows detection. *Eur. J. Remote Sens.* 47, 45–54.
<https://doi.org/10.5721/EuJRS20144704>
- Rey-Caramés, C., Diago, M.P., Martín, M.P., Lobo, A., Tardaguila, J., 2015. Using RPAS multi-spectral imagery to characterise vigour, leaf development, yield components and berry composition variability within a vineyard. *Remote Sens.* 7, 14458–14481.
<https://doi.org/10.3390/rs71114458>
- Rosnell, T., Honkavaara, E., 2012. Point cloud generation from aerial image data acquired by a quadrocopter type micro unmanned aerial vehicle and a digital still camera. *Sensors* 12, 453–480. <https://doi.org/10.3390/s120100453>
- Santesteban, L.G., Di Gennaro, S.F., Herrero-Langreo, A., Miranda, C., Royo, J.B., Matese, A., 2017. High-resolution UAV-based thermal imaging to estimate the instantaneous and seasonal variability of plant water status within a vineyard. *Agric. Water Manag.*, Special Issue: Advances on ICTs for Water Management in Agriculture 183, 49–59. <https://doi.org/10.1016/j.agwat.2016.08.026>
- Schieffer, J., Dillon, C., 2015. The economic and environmental impacts of precision agriculture and interactions with agro-environmental policy. *Precis. Agric.* 16, 46–61.
<https://doi.org/10.1007/s11119-014-9382-5>
- Smit, J.L., Sithole, G., Strever, A.E., 2010. Vine signal extraction – an application of remote sensing in precision viticulture. *South Afr. J. Enol. Vitic.* 31, 65–74.
<https://doi.org/10.21548/31-2-1402>
- Souza, C.H.W. de, Lamparelli, R.A.C., Rocha, J.V., Magalhães, P.S.G., 2017. Mapping skips in sugarcane fields using object-based analysis of unmanned aerial vehicle (UAV) images. *Comput. Electron. Agric.* 143, 49–56.
<https://doi.org/10.1016/j.compag.2017.10.006>
- Tey, Y.S., Brindal, M., 2012. Factors influencing the adoption of precision agricultural technologies: a review for policy implications. *Precis. Agric.* 13, 713–730.
<https://doi.org/10.1007/s11119-012-9273-6>
- Torres-Sánchez, J., López-Granados, F., Borrà-Serrano, I., Peña, J.M., 2018. Assessing UAV-collected image overlap influence on computation time and digital surface

- model accuracy in olive orchards. *Precis. Agric.* 19, 115–133.
<https://doi.org/10.1007/s11119-017-9502-0>
- Torres-Sánchez, J., López-Granados, F., Serrano, N., Arquero, O., Peña, J.M., 2015. High-throughput 3-D monitoring of agricultural-tree plantations with unmanned aerial vehicle (UAV) technology. *PLoS ONE* 10, e0130479.
<https://doi.org/10.1371/journal.pone.0130479>
- Van Den Eeckhaut, M., Kerle, N., Poesen, J., Hervás, J., 2012. Object-oriented identification of forested landslides with derivatives of single pulse LiDAR data. *Geomorphology* 173–174, 30–42. <https://doi.org/10.1016/j.geomorph.2012.05.024>
- Weiss, M., Baret, F., Weiss, M., Baret, F., 2017. Using 3D point clouds derived from UAV RGB imagery to describe vineyard 3D macro-structure. *Remote Sens.* 9, 111.
<https://doi.org/10.3390/rs9020111>

Capítulo 4

Automatic UAV-based detection of *Cynodon dactylon* for site-specific vineyard management



F.M. Jiménez-Brenes, F. López-Granados, J. Torres-Sánchez, J.M. Peña, P. Ramírez, I.L. Castillejo-González, A.I. de Castro. (2019) Automatic UAV-based detection of *Cynodon dactylon* for site-specific vineyard management. *PLoS ONE* 14(6): e0218132. <https://doi.org/10.1371/journal.pone.0218132> (Open Access)

1. Resumen

La mala hierba perenne y estolonífera, *Cynodon dactylon* (L.) Pers. (bermudagrass), constituye un grave problema en los viñedos. La similitud espectral entre la grama y el dosel de las cepas hace inviable la discriminación de las dos especies si el estudio se basa únicamente en la información espectral de las imágenes adquiridas por un sensor multiespectral. Sin embargo, ese desafío puede superarse mediante el uso de análisis de imágenes basados en objetos (OBIA) e imágenes de vehículos aéreos no tripulados (UAV) de ultra alta resolución espacial. El objetivo de esta investigación fue cartografiar de forma automática, precisa y rápida los rodales de grama y diseñar mapas para su manejo. Las imágenes aéreas de dos viñedos fueron capturadas usando dos cámaras multiespectrales (RGB y RGNIR) acopladas a un UAV. En primer lugar, se realizó un análisis espectral con el objeto de seleccionar el índice óptimo de vegetación (VI, en inglés) en la discriminación de grama y suelo desnudo. Seguidamente, el algoritmo OBIA basado en el VI seleccionado para cada cámara cartografió automáticamente cada una de las cepas del viñedo, la grama y el suelo desnudo (precisiones mayores al 97,7%). Finalmente, se generaron mapas de manejo localizado de grama para cada cámara y parcela analizadas. La combinación de imágenes de UAV y un algoritmo OBIA robusto hizo posible la cartografía automática de grama. El análisis del área clasificada permitió cuantificar el crecimiento de la vid y reveló la expansión de las áreas infestadas de grama. Los mapas generados podrían ayudar a los agricultores a mejorar el control de esta mala hierba a través de una estrategia bien programada. Por lo tanto, el algoritmo OBIA desarrollado ofrece información geoespacial valiosa para el diseño de estrategias de manejo localizado de grama, lo que conduciría a una reducción potencial del uso de herbicidas, así como a optimizar el combustible, tiempo empleado en las labores agrícolas asociadas y otros costes.

2. Abstract

The perennial and stoloniferous weed, *Cynodon dactylon* (L.) Pers. (bermudagrass), is a serious problem in vineyards. The spectral similarity between bermudagrass and grapevines makes discrimination of the two species, based solely on spectral information from multi-band imaging sensor, unfeasible. However, that challenge can be overcome by use of object-based image analysis (OBIA) and ultra-high spatial resolution Unmanned Aerial Vehicle (UAV) images. This research aimed to automatically, accurately, and rapidly map bermudagrass and design maps for its management. Aerial images of two vineyards were captured using two multispectral cameras (RGB and RGNIR) attached to a UAV. First, spectral analysis was performed to select the optimum vegetation index (VI) for

bermudagrass discrimination from bare soil. Then, the VI-based OBIA algorithm developed for each camera automatically mapped the grapevines, bermudagrass, and bare soil (accuracies greater than 97.7%). Finally, site-specific management maps were generated. Combining UAV imagery and a robust OBIA algorithm allowed the automatic mapping of bermudagrass. Analysis of the classified area made it possible to quantify grapevine growth and revealed expansion of bermudagrass infested areas. The generated bermudagrass maps could help farmers improve weed control through a well-programmed strategy. Therefore, the developed OBIA algorithm offers valuable geo-spatial information for designing site-specific bermudagrass management strategies leading farmers to potentially reduce herbicide use as well as optimize fuel, field operating time, and costs.

3. Introduction

Vineyard yield and grape quality are variable as a consequence of intrinsic factors related to the crop and the field (Hall et al., 2002). However, most vineyards have been managed as homogenous parcels of land due to the absence of methods that accurately analyze variability (Bramley and Hamilton, 2004). Therefore, analysis of the influence and spatial distribution of variability will allow grape growers to manage vineyards more efficiently for production and grape quality (de Castro et al., 2018a). This approach is the agronomic basis of precision viticulture (PV), which assesses within-field spatial variability (e.g., soil characteristics, weed patches, fungi infection, insect pest attack, grape quality or maturation, production, balance between vegetative growth, and reproductive growth, among others) (Arnó Satorra et al., 2009). Implementation of PV, for either targeted management of inputs and/or selective harvesting at vintage, begins with monitoring vineyard performance and associated attributes, followed by interpretation and evaluation of the collected data (Bramley et al., 2003). PV is mainly focused on optimizing crop production and profitability by reducing production inputs; therefore, its main objective is to diminish the potential damage to the environment and unnecessary costs due to over-application of inputs. Besides these economic and environmental benefits, PV practices comply with the European Policy to regulate a sustainable and rational use of agricultural products and pesticides at a farm level to lead current climatic, socio-economic, and environmental changes while ensuring feasibility and profitability (Schieffer and Dillon, 2015).

Remote sensing has been widely used to characterize vineyards and their associated attributes to be used in site-specific management. For example, Cunha et al. (2010) and Johnson et al. (2003) explored satellite images to predict wine yield and map vineyard leaf area, respectively; Puletti et al. (2014) used images taken by piloted aircrafts to estimate the

grapevine canopy density and identify the grapevine rows. Currently, Unmanned Aerial Vehicles (UAVs) stand out among the other remote sensing platforms because they can fly at low altitudes, capture images with ultra-high spatial resolution (millimetric accuracy) (de Castro et al., 2018a; Matese et al., 2015; Poblete-Echeverría et al., 2017), and, on demand in critical moments, which are not feasible with airborne or satellite platforms. Therefore, the use of UAVs has been proven to be a crucial remote sensing tool to address PV objectives (Rey et al., 2013; Romboli et al., 2017; Santesteban et al., 2017).

Weeds are known to be a major problem in agriculture, leading to a 32% worldwide reduction in crop yields (Mahlein et al., 2012). Recently, *Cynodon dactylon* (L.) Pers. (bermudagrass) has been reported to infest vineyards (Hernández et al., 2000; Valencia et al., 2017), causing competition for nutrients and water, especially in summer when irrigation is needed (Monteiro et al., 2013). This perennial summer grass is widely adapted to a range of climates and soils, propagates mainly vegetatively through stolons and rhizome fragmentation, and is considered a serious problem in cultivated crops worldwide. In addition, weed management strategies in vineyards such as tillage, herbicides, or cover crops have strong implications for wine quality (FAO, 2016; Guerra and Steenwerth, 2012; Håkansson, 1982).

The spectral similarity between bermudagrass and grapevines in summer just, when competition for water is maximum and weeds must be controlled, makes discrimination using pixel-based image analysis almost unfeasible, as this approach focuses solely on spectral information (Weiss et al., 2017). Alternatively, the use of UAV-based Digital Surface Models (DSMs) has been shown to be an efficient alternative to isolate and classify woody crop plants (de Castro et al., 2018a; Matese et al., 2017; Torres-Sánchez et al., 2015b). Nevertheless, computing the large amount of data embedded in UAV images and DSMs requires the implementation of robust and automatic image analysis procedures. In this sense, object-based image analysis techniques (OBIA) have reached high levels of automation and adaptability to ultra-high spatial resolution images, typical of UAV images (Laliberte and Rango, 2011; Peña et al., 2013). Compared to pixel-based methods, the application of object-based approach offers the possibility of evaluating spectral and textural, contextual, and hierarchical features (Blaschke et al., 2014), addressing challenging spectral similarity scenarios related to the design of site-specific weed management (Peña et al., 2013). However, to the best of our knowledge, the UAV-based DSM and OBIA combination has not yet been applied to map bermudagrass in vineyards.

Therefore, the goal of this research was automatic, accurate, and rapid mapping of bermudagrass and designing management maps using UAV-imagery and OBIA techniques. The specific objectives included: (1) selection of the optimum spectral vegetation indices that best discriminated bermudagrass from bare soil as affected by sensors separately

attached to the UAV (spectral analysis); (2) development of an automatic and robust OBIA algorithm for each camera, using those selected vegetation indices, for classifying bermudagrass, bare soil, and grapevines and evaluating the accuracy of the procedure (image analysis); and (3) design of site-specific management maps according to weed infestation level. It is important to highlight that the full protocol established in this paper is composed of a novel OBIA algorithm that does not require user intervention.

4. Materials and methods

4.1. Study sites description and UAV flights

This research was conducted in two experimental drip-irrigated organic vineyards, fields A and B, located in Cabra (Córdoba, Southern Spain). Each site was approximately 0.5 hectares. Both vineyards were planted with cv. Pedro Ximénez in 2013 with rows oriented east–west and trained as a vertical shoot positioned bilateral cordon. Plant spacing was 2.5 m (inter-rows) x 1.3 m (intra-row). Inter-row spaces were uniformly managed by biannual tillage and manual mowing using a brush cutter, which effectively controlled all weed species except bermudagrass, resulting in clean inter-row spacing without cover green and only with the presence of bermudagrass patches.

A quadcopter model MD4-1000 (microdrones GmbH, Siegen, Germany) with vertical take-off and landing (Fig 1a) was used as the platform for image acquisition. This model with four brushless motors was battery-powered and could either be manually operated by radio control or autonomously with the aid of its Global Position System (GPS) receiver and its waypoint navigation system. The imagery were acquired with two still point-and-shoot cameras that were separately mounted in the UAV: (1) a visible-light (RGB: Red (R), Green (G) and Blue (B)) camera, model Olympus PEN E-PM1 (Olympus Corporation, Tokyo, Japan) with a sensor size of 17.3 x 13.0 mm and 12.2 megapixels (4,032 x 3,024 pixels); and (2) a modified (RGNIR: Red (R), Green (G) and NIR) camera, model SONY ILCE-6000 (Sony Corporation, Tokyo, Japan) composed of a 23.5 x 15.6 mm APS-C CMOS sensor capable of acquiring 24 megapixels (6000 x 4000 pixels). The RGNIR camera was modified to capture information in both the NIR and visible light (green and red) by adding a 49-mm filter ring to the front nose of the lens, manufactured by Mosaicmill (Mosaicmill Oy, Vantaa, Finlandia), where a focus calibration process was carried out.



Figure 1. a) Quadcopter microdrone MD4-1000 with the Red-Green-Near Infrared (RGNIR) camera attached, flying over one of the vineyards and b) detail of an RGB-image taken by the UAV from field A-2017. The circles in blue color represent bermudagrass patches growing in the inter-rows.

The flight missions were conducted in mid-June 2016 (field A) and 2017 (fields A and B), when bermudagrass was at the vegetative growth stage, showing the typical green color of this phenological stage (Fig 1b), and, therefore, had a spectral response very similar to that of the grapevines. During each flight, the UAV route was configured to fly at 30 meters altitude with a forward lap of at least 90%. In addition, a side lap of 60% was programmed. The flights were carried out at noon, to take advantage of the sun's position and thus minimize shadows on acquired images. All flight operations fulfilled the list of requirements established by the Spanish National Agency of Aerial Security including pilot license, safety regulations, and limited flight distance (AESA, 2017).

4.2. Geomatic products generation

The images acquired from each camera were processed using PhotoScan Professional software, version 1.2.4 build 2399 (Agisoft LLC, St. Petersburg, Russia) to generate three geomatic products: (1) a three-dimensional (3D) point cloud, by applying the Structure-from-Motion (SfM) technique; (2) a digital surface model (DSM) created from the 3D point cloud that provides height information; and (3) an orthomosaic (Fig 2), where every pixel contained RGB or RGNIR information depending on the camera used as well as the spatial information.

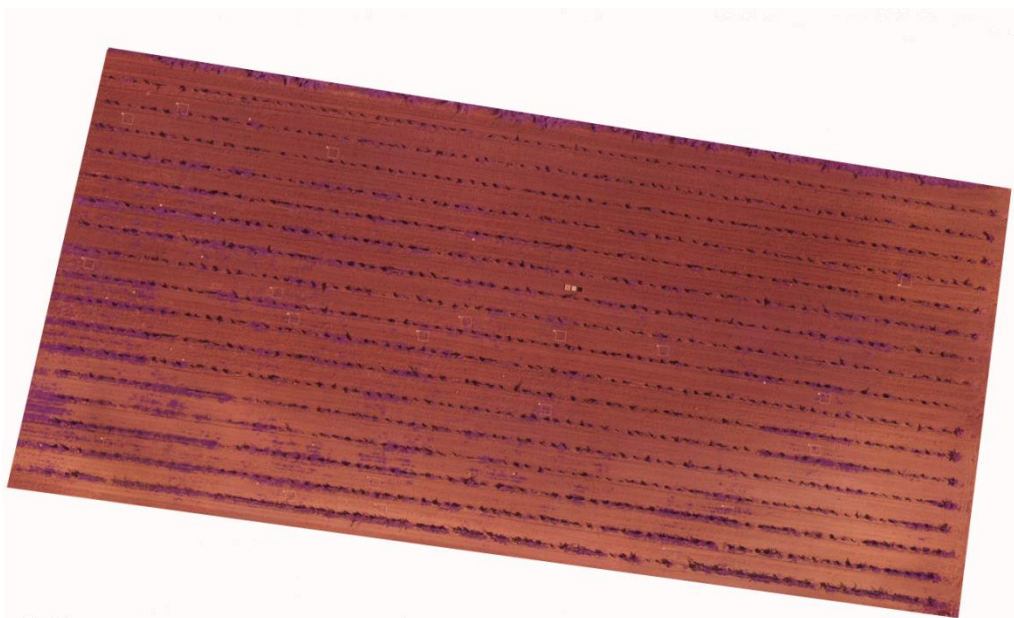


Figure 2. RGNIR orthomosaic corresponding to field A-2016.

The mosaicking process was fully automatic, except for the manual localization of six ground control points (GCPs), with four placed in the corners and two in the center of each field to georeference the geomatic products. These GCPs coordinates were measured using two GNSS receivers: one was a reference station from the GNSS RAP network from the Institute for Statistics and Cartography of Andalusia (Spain), and the other was a GPS with a centimeter accuracy (model Trimble R4, Trimble company, Sunnyvale, California, United States) as a rover receiver. First, the software matched the camera position and common points for each image, which facilitated the refinement of the camera calibration parameters. Once the images were aligned, the 3D point cloud was generated by applying SfM technique to the images, which was used as the basis to generate the DSM. The DSM represents the irregular geometry of the ground and the objects on it by means of a 3D polygon mesh. Next, the individual images were projected over the DSM, and the orthomosaicked image was generated. Finally, the DSM was joined to the orthomosaic as a TIFF file consisting of a 4-band multi-layer file (Red, Green, Blue and DSM, for the visible-light camera; and Red, Green, NIR, and DSM, for the modified one). A further description about the PhotoScan function is given in Dandois and Ellis (2013).

The geomatic products had different spatial resolutions according to the technical characteristics of each sensor. For example, in 2016: (1) 0.86 and 1.72 cm/pixel for the orthomosaic and DSM generated from the RGB camera; and (2) 0.54 and 1.07 cm/pixel for the RGNIR camera, which was almost half of the values obtained with the RGB camera. The methodology to build these accurate geomatic products has been validated in previous studies (Torres-Sánchez et al., 2015b).

4.3. Ground truth data

A set of 18 1 x 1 m georeferenced sampling frames was placed in every field to represent the current weed infestation in the vineyard, ensuring that the entire field had an equal chance of being sampled without operator bias (McCoy, 2005). The frames were set covering bare soil and bermudagrass patches, and georeferenced as described for the GCPs (Fig 3).

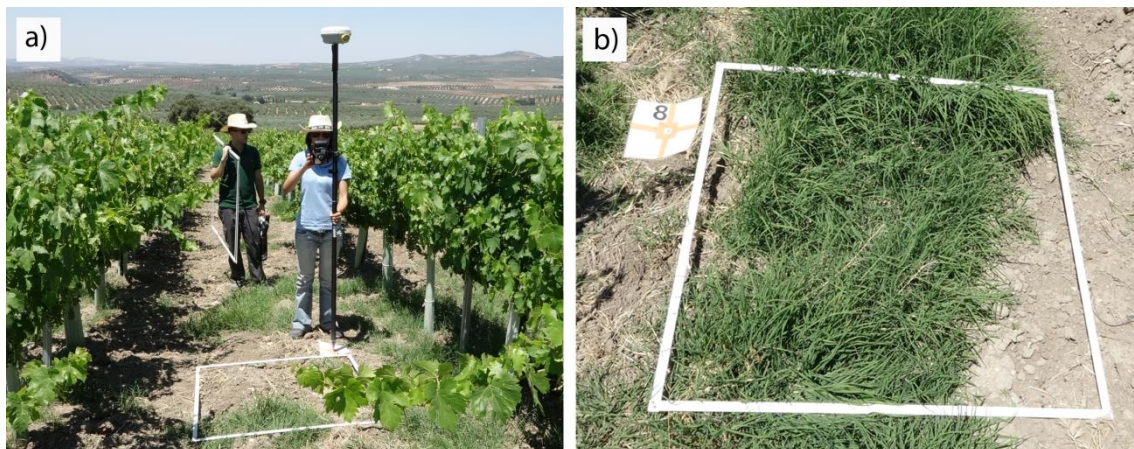


Figure 3. a) Placing and georeferencing the frames in field A-2017 and b) detail of a frame covering bermudagrass and bare soil classes. The individuals in this manuscript have given written informed consent (as outlined in PLOS consent form) to publish these case details.

The high resolution of the orthomosaic (Fig 4a) made it possible to visually identify the bermudagrass patches in every sampling frame and conduct a manual classification of weed infestation and bare-soil (Fig 4b) using ENVI software (Exelis Visual Information, Solutions, Boulder, Colorado, United States), which resulted in the ground truth (GT) data for the procedure. 25 % of the GT full dataset corresponding to field A-2016 as well as 25 % the GT full dataset of field A-2017 were used for the spectral analysis, whereas the remaining 75% of every field-year were employed for the validation of the image analysis (OBIA algorithm) of each orthomosaic. Additionally, field B-2017 was selected to generalize the procedure, using the GT full dataset only for validation purposes of the classification of bermudagrass infestation map.

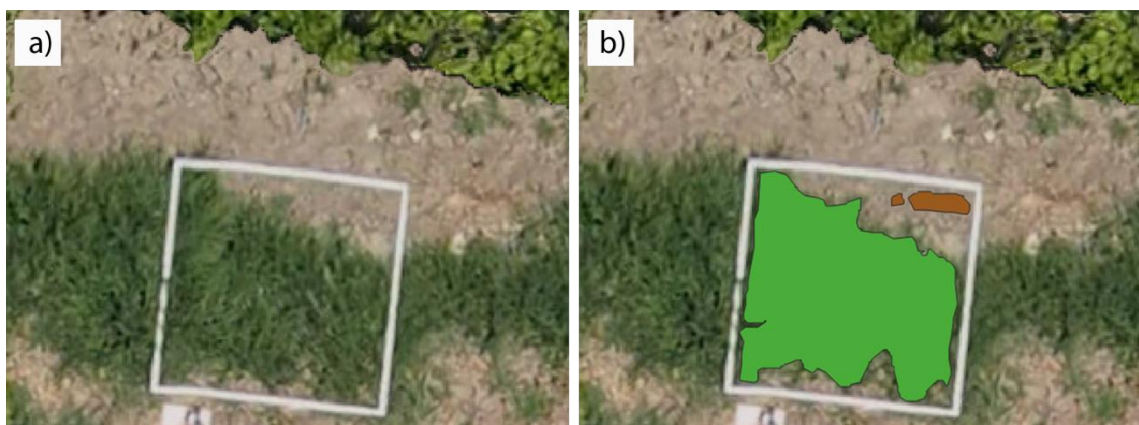


Figure 4. Detail of RGB-orthomosaic of field A-2017 showing: a) sampling frames covering bermudagrass and bare soil and b) manual classification of bermudagrass (green color) and bare soil (brown color) classes that made up the ground truth data.

4.4. Spectral analysis: optimum vegetation index

In order to spectrally separate bare soil and bermudagrass, the following analysis was performed. As explained above, 25 % of the GT full dataset from both the A-2016 and A-2017 fields was used in the spectral analysis to select the optimal vegetation index (VI) that best discriminated bermudagrass and bare soil for each camera (visible and modified). The mean spectral reflectance calculated for the three spectral bands of each camera (RGB and RGNIR) for each class (weed and bare soil) were used to calculate 14 and 18 vegetation indices and band ratios, respectively (Table 1). The VIs in this study are related to vegetation conditions and plant structure and are widely used in agricultural studies (de Castro et al., 2015; Peña-Barragán et al., 2011).

The VIs were analyzed by performing a one-way analysis of variance (ANOVA) followed by Tukey's Honest Significant Difference test ($P < 0.05$) and finally, applying the M-statistic (Equation 1) (Kaufman and Reamer, 1994) to quantify the histogram separation of vegetation indices. The M-statistic value expresses the difference in the means of the class 1 and class 2 histograms normalized by the sum of their standard deviations (σ). According to Kaufman and Reamer (1994), the same difference in means can give different measures of separability depending on the spread of the histograms, i.e., narrow histograms (smaller σ) will cause less overlap and more separability than wider histograms for the same difference in means.

$$M = \frac{Mean_{class1} - Mean_{class2}}{\sigma_{class1} + \sigma_{class2}} \quad (1)$$

Statistical analysis was conducted using the software JMP (JMP 10, SAS Institute Inc., Campus Drive, Cary, NC, USA 27513). The selected VI for each camera was subsequently implemented in the OBIA algorithm for bermudagrass, bare soil, and grapevine classification.

Table 1. Spectral vegetation indices and their equations used for both cameras.

Vegetation index	Equation	Camera ^a
R/B index (Everitt and Villarreal, 1987)	$\frac{R}{B}$	1
R/G index (<i>This study</i>)	$\frac{R}{G}$	1, 2
Normalized Red Green difference index (Gitelson et al., 2002a)	$NRGDI = \frac{G - R}{G + R}$	1, 2
Normalized pigment chlorophyll index (Peñuelas et al., 1994)	$NPCI = \frac{R - B}{R + B}$	1
Visible atmospherically resistant index (Gitelson et al., 2002b)	$VARI = \frac{G - R}{G + R - B}$	1
Woebbecke index (Woebbecke et al., 1995a)	$WI = \frac{G - B}{R - G}$	1
Excess Blue (Guijarro et al., 2011)	$ExB = 1.4 B - G$	1
Excess Green (Woebbecke et al., 1995b)	$ExG = 2 G - R - B$	1
Excess Red (Meyer et al., 1998)	$ExR = 1.4 R - G$	1, 2
Excess Green-Red (Camargo Neto, 2004)	$ExGR = ExG - ExR$	1
Color index of vegetation (Kataoka et al., 2003)	$CIVE = 0.441 R - 0.811 G + 0.385 B + 18.78745$	1
Vegetative index (Hague et al., 2006)	$VEG = \frac{G}{(R^{0.667}) \times (B^{1-0.667})}$	1
Indices combination1 (Guijarro et al., 2011)	$COMB1 = 0.25 ExG + 0.3 ExGR + 0.33 CIVE + 0.12 VEG$	1
Indices combination2 (Guerrero et al., 2012)	$COMB2 = 0.36 ExG + 0.47 CIVE + 0.17 VEG$	1
Chlorophyll index green (Gitelson et al., 2003)	$CI = \frac{NIR}{G} - 1$	2
Difference vegetation index (Jordan, 1969)	$DVI = NIR - R$	2
Vegetation index faster (Crippen, 1990)	$VIF = \frac{NIR}{NIR + R}$	2
Green normalized difference vegetation index (Gitelson et al., 1996)	$GNDVI = \frac{NIR - G}{NIR + G}$	2
Ratio vegetation index (Richardson and Wiegand, 1977)	$RFI = \frac{R}{NIR}$	2
Modified normalized difference vegetation index (Baret and Guyot, 1991)	$MRVI = \frac{RFI - 1}{RFI + 1}$	2
Modified simple ratio (Chen, 1996)	$MSR = \frac{\frac{NIR}{R} - 1}{\sqrt{\frac{NIR}{R} + 1}}$	2
Modified soil-adjusted vegetation Index (Qi et al., 1994)	$MSAVI = \frac{2NIR + 1 - \sqrt{(2NIR + 1)^2 - 8 \times (NIR - R)}}{2}$	2
NIR-G index (Sripada et al., 2006)	$NIR - G$	2
NIR/G index (Sripada et al., 2006)	$\frac{NIR}{G}$	2
Non-linear vegetation index (Goel and Qin, 1994)	$NLI = \frac{NIR^2 - R}{NIR^2 + R}$	2
Normalized difference vegetation Index (Rouse et al., 1974)	$NDVI = \frac{NIR - R}{NIR + R}$	2
Optimization soil-adjusted vegetation index (Rondeaux et al., 1996)	$OSAVI = \frac{NIR - R}{NIR + R + 0.16}$	2
Transformed vegetation index 1 (Perry and Lautenschlager, 1984)	$TVI1 = \frac{NDVI + 0.5}{ABS(NDVI + 0.5)} \times \sqrt{ABS(NDVI + 0.5)}$	2
Transformed vegetation index 2 (Broge and Leblanc, 2001)	$TVI2 = 0.5 \times (120 \times (NIR - G) - 200 \times (R - G))$	2

^a 1: RGB; 2: RGNIR

4.5. Image analysis: bermudagrass mapping

4.5.1. OBIA algorithm

Once the VIs that best separated bare soil and bermudagrass were selected, a novel OBIA algorithm was developed to classify the grapevines, bare soil, and bermudagrass using Cognition Network programming language with the eCognition Developer 9.2 software (Trimble GeoSpatial, Munich, Germany). The algorithm is fully automatic and requires no user intervention. Besides this, the same algorithm was used to analyze the orthomosaics generated by each camera, with the only difference being the VI implemented by selecting the optimal one for each. The sequence of phases that compose this algorithm is detailed below:

- i) Vine classification: Height information contained in the DSM model was used to detect and classify grapevine objects (Fig 5b), as fully described in a previous work (de Castro et al., 2018a), which first consisted of orthomosaic-image segmentation based on spatial information for object generation (chessboard segmentation). Then, the DSM standard deviation was used to create "vine candidates" that were analyzed at the pixel level to achieve a more refined grapevine classification. Finally, the algorithm classified every pixel as vineyard or not-vineyard by comparing their height value from the DSM with that of the adjacent bare soil. Therefore, spatial information proved to be very suitable for grapevine classification, avoiding errors related to field slope by considering average soil altitude as well as avoiding confusion due to spectral similarities. Finally, the objects in the images were classified as vineyard or not-vineyard objects (Fig 5c).
- ii) Bermudagrass and bare soil classification: Once the grapevines were correctly classified, the orthomosaic was segmented using a multiresolution segmentation where the layers Red, Green, and Blue for the RGB camera, and Red, Green, and NIR for the RGNIR camera were weighted to 1, whereas the DSM layer was weighted to 0 in both cases. Multiresolution segmentation is a bottom-up segmentation algorithm based on a pairwise region merging technique in which, based on several parameters defined by the operator (scale, color/shape, smoothness/compactness), the image is subdivided into homogeneous objects. The scale parameter established was 5, whereas 0.3 and 0.5 were chosen for shape and compactness, respectively. These values were chosen after performing several tests for showing a better visual adjustment by delineating bermudagrass patches and bare soil. Therefore, these values could also be used in other vineyards with similar characteristics where bermudagrass classification is required.

Subsequently, the no-vineyard objects, consisting of bare soil and bermudagrass were classified using the VI selected for each camera in the previous section. The optimum ratio value was conducted using an automatic and iterative threshold approach

following the Otsu method (Otsu, 1979) implemented in eCognition, in accordance with Torres-Sánchez et al. (2015a). Finally, a classified map was generated where bermudagrass patches, bare soil, and grapevine objects were defined (Fig 5d).

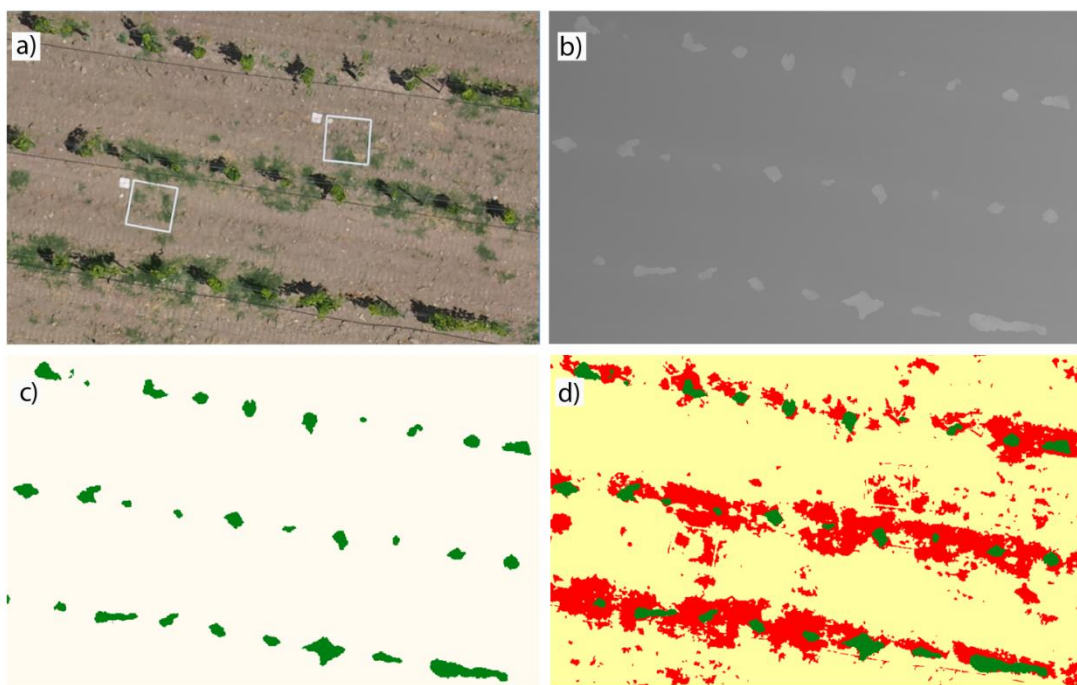


Figure 5. Several stages of the OBIA algorithm for an enlarged view belonging to field A-2016 and RGB camera. a) the RGB bands, b) the DSM of the orthomosaic, c) vine line classification (grapevines in green color and no-vineyard objects in white color), and d) classified map (grapevines in green color, bermudagrass patches in red color, and bare soil in yellow color).

iii) Site-specific bermudagrass management maps: After vineyard–weed–bare soil classification, information relative to bermudagrass patches was available such as number, location (X and Y UTM coordinates), and area covered by weed patches and vines from the classified map. As an additional phase of the process, the algorithm has the option to design site-specific bermudagrass management maps that are user-configurable depending on the management strategy. For this purpose, the algorithm created a new level by copying the classified object level to an upper level and a chessboard segmentation was applied to build a user-adjustable grid framework following the grapevine row orientation. In this experiment, a customizable 1 x 0.5 m grid size was selected according to the specifications of the intra- and inter-row weeder usually used in organic vineyards (Mudarra Prieto and García Trujillo, 2005). A hierarchical structure was generated in the inter-row area between the grid super-objects (upper level) and the bermudagrass and bare-soil sub-objects (lower level). Next, the weed coverage (% of bermudagrass) was automatically calculated from the ratio of

bermudagrass coverage to total area per grid, as it is considered as one of the main variables in the weed control decision-making process (Peña et al., 2013). Thus, based on the information related to weed-free zones and weed-infested zones, site-specific treatment maps were created.

4.5.2. Bermudagrass map validation

The accuracy of the algorithm was assessed by comparing the GT data corresponding to bermudagrass infestation and bare soil (manual weed coverage and bare soil area) with the output of every image classification process (estimated bare soil and weed coverage) through a confusion matrix. As commented before, 75% of the GT full datasets corresponding to field A for both 2016 and 2017 were used to assess the classification accuracy. In the case of field B-2017, the GT full dataset was used, so this set of examples was used only to assess the performance (i.e., generalization) of the developed algorithm. The confusion matrix provided overall accuracy (OA) (Equation 2) of each orthomosaic classification, which represented the percentage of correctly classified area (bare soil and bermudagrass); and the producer's accuracy (PA) that indicated the probability that a classified object actually represents that category, i.e., the category of the ground truth data (Congalton, 1991). The omission error, i.e., the complementary value to PA, was also calculated from the confusion matrix and quantified the proportion of bermudagrass coverage misclassified as bare soil.

$$\text{Overall classification accuracy (\%)} = 100 \times \frac{\text{Area correctly classified}}{\text{Total area classified}} \quad (2)$$

The methodology to identify vine rows based on DSM information has been validated in a previous study (de Castro et al., 2018a), where a high level of precision was reached.

5. Results and Discussion

5.1. Spectral analysis: vegetation index selected

Spectral information from every orthomosaic was evaluated to select the VI that best discriminated between the bermudagrass and bare soil, as affected by the spectral range of each camera, i.e., RGB and RGNIR. Significant differences between both classes were observed in all the VI calculated. These results confirmed the potential of discriminating bermudagrass from bare soil by using UAV-images taken at the vegetative stage with any of the cameras (RGB and RGNIR) onboard the UAV, when bermudagrass plants showed a very different green color from the brown of the bare soil. The best results obtained with the

M-statistic for images taken with each type of camera were ranked and are shown in Table 2.

Table 2. Vegetation indices analyzed with the highest values of M-statistical obtained for each camera.

Camera	Vegetation Index	M-statistical value
RGB	Excess Green-Red (ExGR)	3.50
	Indices combination1 (COMB1)	3.48
	Excess Red (ExR)	3.16
	Color index of vegetation (CIVE)	3.06
RGNIR	Excess Green (ExG)	2.87
	Green normalized difference vegetation index (GNDVI)	2.27
	Difference vegetation index (DVI)	2.15
	Chlorophyll index Green (CI)	2.14
NIR/G	NIR/G	2.14
	NIR-G	2.10

Letters in bold correspond the spectral vegetation indices that showed the highest M values and were then used in the further OBIA algorithm.

According to Smith et al. (2007), two classes exhibit moderate separability when M exceeds 1 and good discrimination when it exceeds 2. In this experiment, most of the VIs extracted for each camera achieved M values larger than 2, therefore showing high discriminatory power to separate bermudagrass from bare soil. ExGR showed the best spectral separability in the analysis of the RGB-range, reaching an M value of 3.50, whereas GNDVI was the selected index for the RGNIR-range spectral analysis, as obtained by the highest M value (2.27). As a result of the spectral analysis, ExGR and GNDVI were the optimum VIs selected to carry out the discrimination between both classes for the RGB- and RGNIR-orthomosaic, respectively, thus, the corresponding index was implemented in the classification algorithm developed.

ExGR is a combination of redness (ExR) and greenness (ExG) indices widely used for vegetation identification with visible spectral-index based methods under the assumption that plants display a high degree of greenness due to chlorophyll in the leaves. In this context, Guijarro et al. (2011) and Meyer and Camargo Neto (2008) used ExGR to separate the plants from the soil and residue background in the RGB images. On the other hand, GNDVI has been used to measure several plant parameters including N status (Bell et al., 2004, 2002), plant biomass (Hunt et al., 2011), and early disease detection (de Castro et al., 2015) due to the high sensitivity to the chlorophyll concentration variation of this vegetation index. Thus, based on that premise and the results obtained in the spectral analysis in this investigation, GNDVI showed high robustness in the ability of separating bare soil (no chlorophyll) from bermudagrass at the vegetative stage (in green color due to the high concentration of chlorophyll pigment) as a part of the developed algorithm for the

image analysis. These results showed the importance of the timing for this analysis, as it is feasible when BG plants are at vegetation phenological stage and green. On the other hand, these VIs would not be suitable for bermudagrass discrimination in another season, e.g. in winter when bermudagrass is dormant (light brown) and shows a similar spectral response to bare soil. At that time, it would therefore be necessary to apply a different analysis such as this one based on texture characteristics (Wood et al., 2012).

5.2. Image analysis

5.2.1. Classified maps

After the spectral analysis was carried out, the study focused on image analysis. An OBIA algorithm was developed to parse the orthomosaics as affected by kind of sensor for the suitable discrimination of bermudagrass patches. Next, the algorithm automatically mapped grapevines, bermudagrass, and bare soil by classifying every image object according to these three classes. Thus, a classified map for each field, year, and camera was created (Figs 6 and 7), where clear differences in grapevine size were observed when analyzing the two years studied. Moreover, the developed methodology was able to map bermudagrass within the grapevine rows in the first study year (2016) since at that time the vines were at an initial stage of growth so that the canopy was not closed and it was possible to get information down to ground level. Nevertheless, the growth of the grapevines in the second year (2017) made it unfeasible to obtain that information up to ground level within the row as the vines showed overlapping crowns. Consequently, using the developed UAV-based OBIA algorithm at the proper timing of grapevine growth would enable accurate mapping of weeds within vine rows. The total area occupied by grapevines and bare soil as well as the area infested by bermudagrass was quantified and extracted from these classified maps (Table 3).

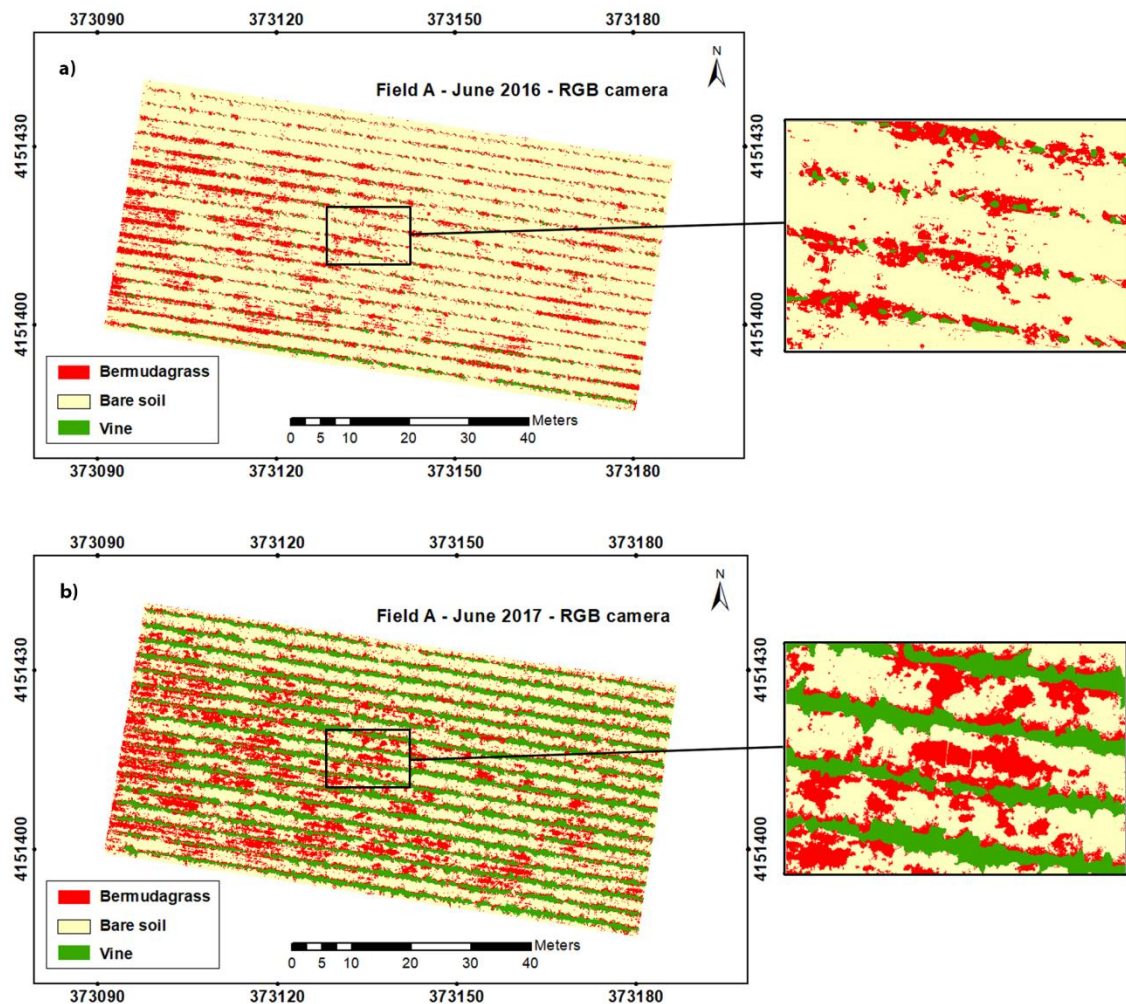


Figure 6. Classified maps developed by the OBIA-algorithm using RGB-imagery for field A in: a) 2016 and b) 2017.

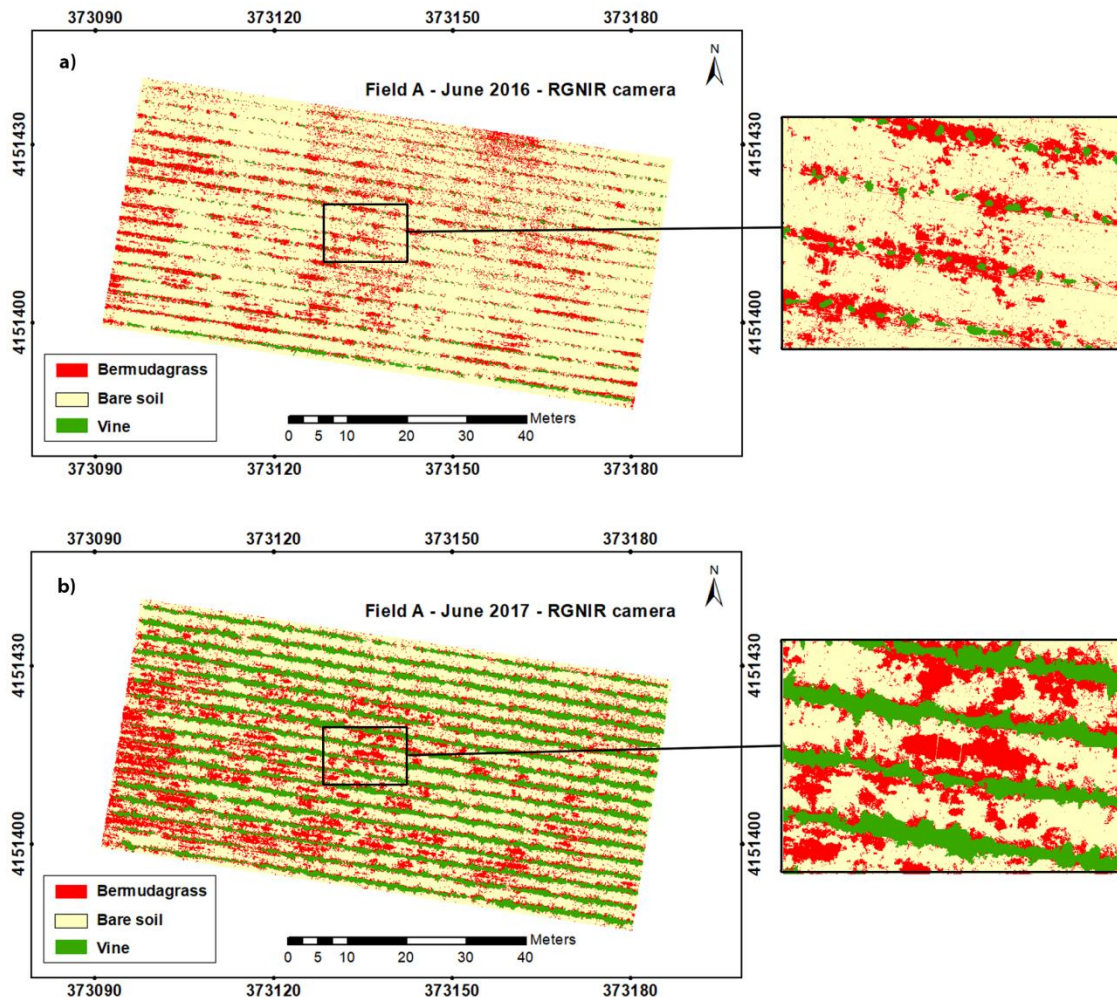


Figure 7. Classified maps developed by the OBIA-algorithm using RGNIR-imagery for field A in: a) 2016 and b) 2017.

Table 3. Classified area of grapevine, bermudagrass and bare soil obtained from the RGB and RGNIR images analyses at every location and year studied.

Camera	Field	Year	Classified Area (%) ^a		
			Vine	Bermudagrass	Bare soil
RGB	A	2016	3.4	13.8	82.8
		2017	24.4	21.3	54.3
RGNIR	B	2017	20.8	21.9	57.3
		2016	3.7	14.6	81.7
	B	2017	24.5	19.7	55.8
		2017	21.3	20.5	58.2

^a Percentage of surface occupied for each class respect to total field area.

Similar results of the classified area were obtained by using any of the sensors, e.g., 24.4% and 24.5% for the vine class in field A-2017 when employing the RGB-sensor and RGNIR-sensor orthomosaic, respectively; and similarly, for bare soil in field A-2016, reporting 82.8% and 81.7% of the classified area, which demonstrated the algorithm robustness.

An increase of approximately 21% in the vineyard was observed in the comparison of 2016 and 2017 orthomosaics for both sensors. These differences in grapevine size were the result of usual growth as a relevant rate of development was experienced by vines in those years (Lopes et al., 2008).

The surface infested by bermudagrass also augmented in the context of that temporal comparison, obtaining an increased value of 7.5% when the RGB imagery was analyzed, despite uniform weed management in the inter-row spaces was carried out. This management consisted of biannual tillage and manual mowing using a brush cutter; no synthetic chemicals were used as both fields were organic. Thus, the increase of bermudagrass coverage could be due to inefficient weed management since perennial weeds established by rhizomes or stolons are considered the most difficult to manage in organic orchards, and in fact, they can become a permanent control target as the removal of aerial parts does not eliminate weeds and portions of stolons or rhizomes may re-grow and colonize new areas (Hammermeister, 2016). According to Cudney et al. (2007), among the recommendations for bermudagrass management, mowing should be minimized as stolons can cause weed dispersion. They advised a single deep cultivation (up to six inches), avoiding very moist soils, which brings most shoots to the surface to dry them out, and pointed out that this weed management (tilling and drying) did not eradicate seeds in the soil. In addition, deep cultivation risks damaging the roots, trunks, and arms of the grapevines (Guerra and Steenwerth, 2012). Other alternatives for weed control include the use of cover crops such as perennial or annual grasses (*Festuca arundinacea* or *Hordeum vulgare*, respectively) or legumes (*Medicago rugosa*), which compete with the bermudagrass and reduce its infestation (Valencia et al., 2017).

Furthermore, a reduction in the area occupied by bare soil was found using any of the sensors, which was quantified as 28.5% for the RGB-orthomosaic image and 25.9% for the RGNIR-orthomosaic.

5.2.2. Bermudagrass mapping accuracy

As mentioned in the OBIA algorithm description, the vine class was first separated from the rest of classes using DSM height information as described in [3], where overall accuracy values higher than 93.6 % were achieved in the vine classification. The classification statistics of the bare soil and bermudagrass classes obtained in the confusion

matrix (OA and PA) for the orthomosaic corresponding to each sensor, field, and year are shown in Table 4. The matrix indicated an overall accuracy higher than 97.7% in all of the cases studied, well above the minimum accepted value standardized at 85% by Thomlinson et al. (1999). These consistent results proved the suitability of the VIs selected in the previous spectral analysis and demonstrated that the VI-based OBIA algorithm correctly identified and mapped the bermudagrass patches in the inter-rows of the vineyards in both years of the study. Moreover, high degrees of producer's accuracy with values close to or even 100% were achieved in all the studied cases, which corresponded to null or very low values of omission error.

Table 4. Classification statistics obtained in confusion matrix for each year, field and camera.

Year	Field	Camera	Producer's Accuracy (%)		Overall Accuracy (%)
			Bg ^a	Bs	
2016	A	RGB	98.3	99.9	98.7
		RGNIR	95.7	99.9	97.7
	A	RGB	99.6	100	99.7
		RGNIR	99.9	99.9	99.9
2017	B	RGB	99.9	100	99.9
		RGNIR	99.9	100	99.9

^a Bg: Bermudagrass; Bs: Bare soil. The algorithm was executed with the selected VI for each camera in the previous section, i.e. ExGR for RGB-orthomosaic and GNDVI for RGNIR-orthomosaic.

Similar classification accuracy was achieved using images from both cameras, proving that it is possible to map bermudagrass at the vegetative stage based on RGB-imagery and RGNIR-imagery taken by UAV. For example, 99.6% and 99.9% of PA were obtained for the bermudagrass class using the RGB and RGNIR cameras in field A-2017, respectively; and moreover, OA values of 98.7% and 97.7% were reached for those respective cameras and field in 2016. Therefore, due to the similar results as well as the handling and cheaper costs of the conventional camera, as a preliminary conclusion of this experiment, we recommend the use of an RGB sensor for bermudagrass mapping at the vegetative stage during early summer in vineyards. Thereby, only results for this camera are shown throughout the rest of the manuscript.

The highly accurate results achieved in the image analysis proved that the combination of UAV imagery and OBIA is a suitable tool to map the usual classes including weeds in vineyards. In this context, Peña et al. (2013) used a similar image-based UAV

technology to discriminate weeds in maize (*Zea mays* L.) fields in the early season obtaining 86% of OA in the confusion matrix; however, the precision of the OBIA algorithm was evaluated by comparing weed coverage over grid units, not over objects. Consequently, the OA was related to the percentage of frames correctly classified (the number of correct frames as a percentage of the total number of sampling frames) and unsuitable spatial accuracy measures for OBIA were performed. In our research, the shape and location of weeds were evaluated, as first proposed by de Castro et al. (2018b), who obtained a high level of agreement in the comparison between the manual weed classification in herbaceous crops and that automatically performed by the OBIA algorithm; however, no matrix confusion was calculated in that experiment. Furthermore, although a confusion matrix was performed in the previous paper for the 3D characterization of vineyards (de Castro et al., 2018a), the matrix evaluated the precision in the grapevine vs the non-grapevine classification (composed by inter-row cover crops and bare soil), so this methodology remained non-validated for weed detection in the inter-row of the vineyards.

The omission errors (OE), as complementary to PAs, are shown in Table 5, where values lower than 0.4 were obtained in 2017 for both fields and 1.7 in 2016 for field A. Thus, only 1.7% of the bermudagrass objects were misclassified as bare soil, whereas less than 0.4% of weed patches were misclassified in the rest of the cases, being far below those obtained by Peña et al. (2013), who reported values of 17% for frames at moderate weed coverage, and by Laliberte and Rango (2011), who obtained a 12% omission error in the classification of grass (*Bouteloua eriopoda* Torrey) using UAV and OBIA techniques. Moreover, no errors were quantified in the bare soil classification. From an agronomic perspective, a key issue for successful management is to report low OE values as it increases the chance of controlling all of the weed patches and also reduces the risk of allowing weeds to go untreated (Gibson et al., 2004). Therefore, bermudagrass maps obtained from the automatic VI-based OBIA algorithm can be an accurate and suitable tool for farmers to control this species in vineyards.

Table 5. Omission error statistics obtained for each year and field using RGB camera.

Year	Field	Omission error (%)	
		Bg ^a	Bs
2016	A	1.7	0.0
	A	0.4	0.0
2017	B	0.1	0.0

^a Bg: Bermudagrass; Bs: Bare soil.

5.2.3. Site-specific weed management

The bermudagrass maps could help farmers improve weed control through a rational-programmed strategy based on site-specific weed management (SSWM), targeting suitable control measures only where they are needed, either intra- or inter-rows. In addition, these maps could also be used to both design a control management strategy for organic vineyards through spraying organic herbicides such as clove oil, acetic and citric acid products (Lanini et al., 2011; Roig et al., 2017), and using herbicides in the case of non-organic vineyards, according to the weed coverage. In this context, site-specific bermudagrass treatment maps were designed by the OBIA algorithm (Fig 8) based on the weed maps as explained in the Materials and Methods section, through delineating site-specific treatment zones according to the several weed cover thresholds. Three user-adaptable treatment thresholds were selected in this experiment: 0, 2.5, and 5%, where 0% implies that herbicides must be applied in the treatment zone just when there is the presence of bermudagrass, and 5% that the herbicide must be applied when weed coverage is equal or higher than 5%.

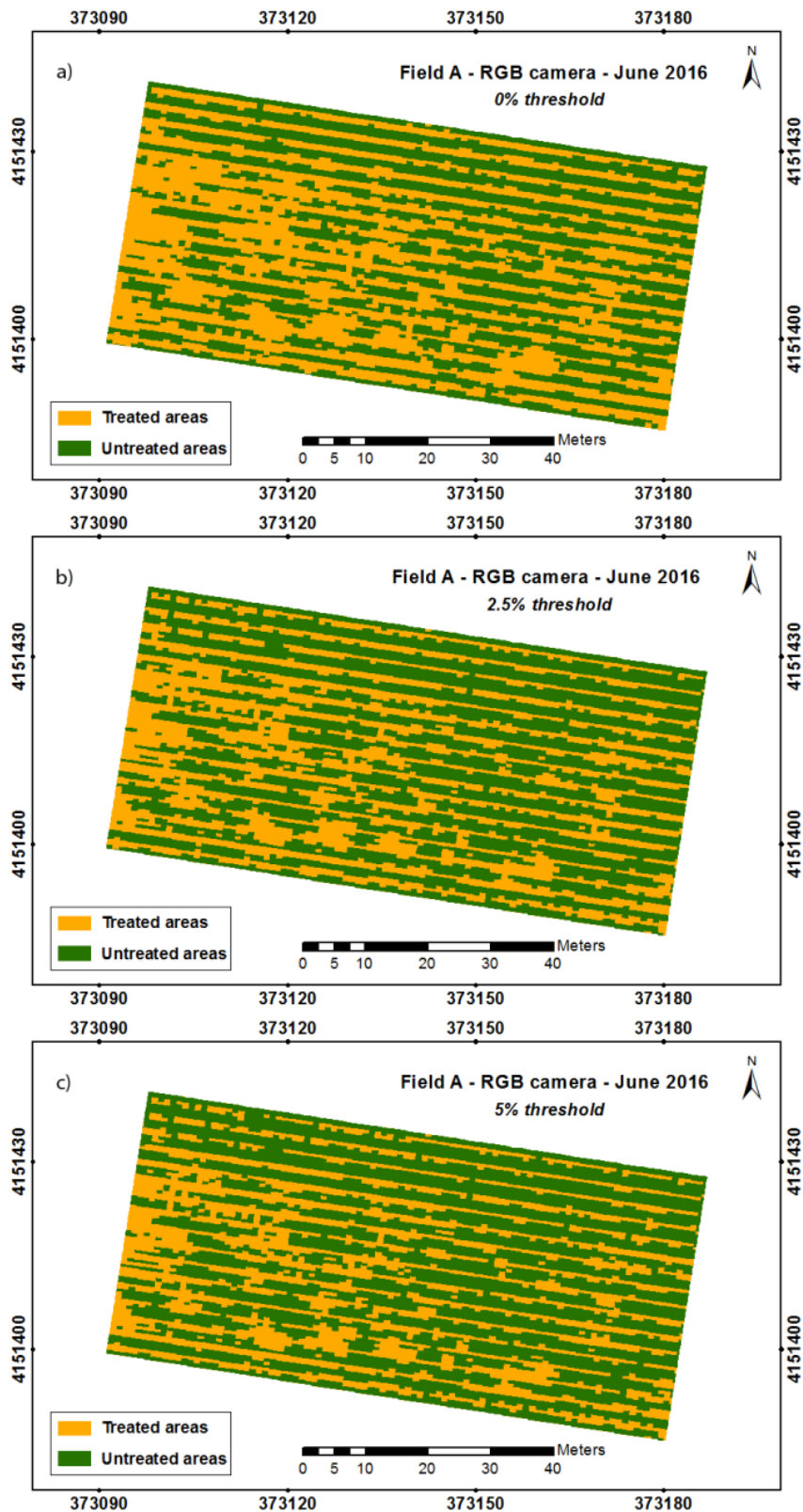


Figure 8. Site-specific treatment maps for bermudagrass patches in field A-2016 according to treatment thresholds: a) 0%, b) 2.5%, and c) 5%. Only results for RGB camera are shown.

The potential herbicide savings, calculated in terms of untreated areas, extracted from the SSWM maps are shown in Table 6. Since savings percentages were calculated based on bermudagrass coverage, savings values varied for each scenario, e.g., the potential savings for field A-2016 consisted of 48.3% from the more conservative prescription maps, since any grid with the presence of bermudagrass was considered a treatment area, while potential savings of 23.4% would be obtained for field B-2017 under the same conservative circumstance. Furthermore, as expected, higher potential savings were observed for higher treatment thresholds (Peña et al., 2013). In that sense, about a 14% raise in potential savings was achieved using a 5% weed threshold when compared to the more conservative one for the three cases analyzed. Consequently, the reduction in the bare soil area resulted from the growth of grapevines and the increase in the area infested by bermudagrass.

Table 6. Herbicide saving obtained from herbicide application maps as affected by treatment thresholds for RGB imagery by year and field analyzed.

Year	Field	Herbicide saving by treatment thresholds (%)		
		0	2.5	5
2016	A	48.3	58.5	62.2
	B	24.4	33.5	38.7
2017	A	23.4	31.9	36.5
	B			

These values correspond to a 1 x 0.5 m grid cell size.

In summary, the combination of UAV imagery and the VI-OBIA algorithm developed provides automatic and accurate bermudagrass mapping. These weed maps could be used to design site-specific bermudagrass management in organic vineyards as well as to create site-specific prescription maps according to weed coverage for non-organic vineyards. These prescription maps could aid in controlling bermudagrass in several agricultural seasons so that the species could be eradicated. This PV-based approach could lead to herbicide reductions, and also optimize fuel, field operating time and cost (de Castro et al., 2018b).

6. Conclusions

Based on the high competition caused by bermudagrass infestation in the inter-row of vineyards, the possibility of mapping this weed using UAV-imagery was evaluated to facilitate site-specific weed management in the context of PV. Aerial images of several fields were captured using two sensors (RGB and RGNIR) attached to the UAV that allowed us to obtain ultra-high spatial resolution imagery and operate on demand according to the necessities of the grapevines. First, the spectral data analyses showed significant differences

between the bare soil and bermudagrass, then ExGR and GNDVI were the optimum VIs selected to carry out the discrimination between both classes for the RGB- and RGNIR-orthomosaic, respectively. Second, an accurate and fully automatic VI-based OBIA algorithm was developed to map bermudagrass infesting the inter-row of vineyards, where the optimum VI for each camera was implemented. Grapevines were mapped using photogrammetric-based DSMs, thus avoiding misclassification due to the spectral similarity between the vines and bermudagrass. High values of map classification accuracy (>97.7%) were achieved with each of the cameras, proving that it is possible to map bare soil, grapevines, and bermudagrass at the vegetative stage based on RGB- and RGNIR-imagery. Thus, due to the similar results and handling and cheaper cost of the conventional camera, the use of an RGB sensor was recommended for that objective.

The analysis of the classified area from maps allowed us to quantify grapevine growth in those years and revealed the area infested by bermudagrass. Thus, these bermudagrass maps generated by the VIs-based OBIA algorithm could help farmers improve weed control in organic vineyards through a well-programmed strategy based on site-specific weed management (SSWM). Moreover, site-specific bermudagrass treatment maps, according to the weed coverage of the field, were designed by the algorithm to spray herbicides to be used for non-organic vineyards in the context of precision viticulture. Using these prescription maps could aid in controlling bermudagrass across several agricultural seasons and eradicating this species. This PV-based approach could reduce herbicide use, and optimize fuel, field operating time, and costs.

7. References

- AESA, 2017. URL
http://www.seguridadaerea.gob.es/LANG_EN/cias_empresas/trabajos/rpas/marco/default.aspx (accessed 6.2.17).
- Arnó Satorra, J., Casasnovas, M., Antonio, J., Ribes Dasi, M., Polo, R., Ramón, J., 2009. Review. Precision viticulture. Research topics, challenges and opportunities in site-specific vineyard management. *Span. J. Agric. Res.* 7(4): 779-790.
<https://doi.org/10.5424/sjar/2009074-1092>
- Baret, F., Guyot, G., 1991. Potentials and limits of vegetation indices for LAI and APAR assessment. *Remote Sens. Environ.* 35, 161–173. [https://doi.org/10.1016/0034-4257\(91\)90009-U](https://doi.org/10.1016/0034-4257(91)90009-U)

- Bell, G.E., Howell, B.M., Johnson, G.V., Raun, W.R., Solie, J.B., Stone, M.L., 2004. Optical sensing of turfgrass chlorophyll content and tissue nitrogen. *HortScience* 39, 1130–1132.
- Bell, G.E., Martin, D.L., Stone, M.L., Solie, J.B., Johnson, G.V., 2002. Turf area mapping using vehicle-mounted optical sensors. *Crop Sci.* 42, 648–651.
<https://doi.org/10.2135/cropsci2002.6480>
- Blaschke, T., Hay, G.J., Kelly, M., Lang, S., Hofmann, P., Addink, E., Queiroz Feitosa, R., van der Meer, F., van der Werff, H., van Coillie, F., Tiede, D., 2014. Geographic object-based image analysis – towards a new paradigm. *Isprs J. Photogramm. Remote Sens.* 87, 180–191. <https://doi.org/10.1016/j.isprsjprs.2013.09.014>
- Bramley, R., Pearse, B., Chamberlain, P., 2003. Being profitable precisely -a case study of precision viticulture from Margaret river. *Aust. N. Z. Grapegrow. Winemak. Annu. Tech.* 473a, 84–87.
- Bramley, R.G.V., Hamilton, R.P., 2004. Understanding variability in winegrape production systems. *Aust. J. Grape Wine Res.* 10, 32–45. <https://doi.org/10.1111/j.1755-0238.2004.tb00006.x>
- Broge, N.H., Leblanc, E., 2001. Comparing prediction power and stability of broadband and hyperspectral vegetation indices for estimation of green leaf area index and canopy chlorophyll density. *Remote Sens. Environ.* 76, 156–172.
[https://doi.org/10.1016/S0034-4257\(00\)00197-8](https://doi.org/10.1016/S0034-4257(00)00197-8)
- Camargo Neto, J., 2004. A combined statistical-soft computing approach for classification and mapping weed species in minimum-tillage systems. Univ. Neb. Linc.
- Chen, J.M., 1996. Evaluation of vegetation indices and a modified simple ratio for boreal applications. *Can. J. Remote Sens.* 22, 229–242.
<https://doi.org/10.1080/07038992.1996.10855178>
- Congalton, R.G., 1991. A review of assessing the accuracy of classifications of remotely sensed data. *Remote Sens. Environ.* 37, 35–46. [https://doi.org/10.1016/0034-4257\(91\)90048-B](https://doi.org/10.1016/0034-4257(91)90048-B)
- Crippen, R.E., 1990. Calculating the vegetation index faster. *Remote Sens. Environ.* 34, 71–73.
- Cudney, D.W., Elmore, C.L., Bell, C.E., 2007. Bermudagrass - integrated pest management for home gardeners and landscape professionals. Pest Notes - Publ. 7453 4.
- Cunha, M., Marçal, A.R.S., Silva, L., 2010. Very early prediction of wine yield based on satellite data from vegetation. *Int. J. Remote Sens.* 31, 3125–3142.
<https://doi.org/10.1080/01431160903154382>

- Dandois, J.P., Ellis, E.C., 2013. High spatial resolution three-dimensional mapping of vegetation spectral dynamics using computer vision. *Remote Sens. Environ.* 136, 259–276. <https://doi.org/10.1016/j.rse.2013.04.005>
- de Castro, A.I., Ehsani, R., Ploetz, R., Crane, J.H., Abdulridha, J., 2015. Optimum spectral and geometric parameters for early detection of laurel wilt disease in avocado. *Remote Sens. Environ.* 171, 33–44. <https://doi.org/10.1016/j.rse.2015.09.011>
- de Castro, A.I., Jiménez-Brenes, F.M., Torres-Sánchez, J., Peña, J.M., Borra-Serrano, I., López-Granados, F., 2018a. 3-D characterization of vineyards using a novel UAV imagery-based OBIA procedure for precision viticulture applications. *Remote Sens.* 10, 584. <https://doi.org/10.3390/rs10040584>
- de Castro, A.I., Torres-Sánchez, J., Peña, J.M., Jiménez-Brenes, F.M., Csillik, O., López-Granados, F., 2018b. An automatic random forest-OBIA algorithm for early weed mapping between and within crop rows using UAV imagery. *Remote Sens.* 10, 285. <https://doi.org/10.3390/rs10020285>
- Everitt, J.H., Villarreal, R., 1987. Detecting huisache (*Acacia farnesiana*) and mexican palo-verde (*Parkinsonia aculeata*) by aerial photography. *Weed Sci.* 35, 427–432. <https://doi.org/10.1017/S0043174500053947>
- FAO, 2016. *Cynodon dactylon* [WWW Document]. URL <http://www.fao.org/ag/agp/AGPC/doc/gbase/data/Pf000208.HTM> (accessed 9.7.17).
- Gibson, K.D., Dirks, R., Medlin, C.R., Johnston, L., 2004. Detection of weed species in soybean using multispectral digital images. *Weed Technol.* 18, 742–749. <https://doi.org/10.1614/WT-03-170R1>
- Gitelson, A.A., Gritz, Y., Merzlyak, M.N., 2003. Relationships between leaf chlorophyll content and spectral reflectance and algorithms for non-destructive chlorophyll assessment in higher plant leaves. *J. Plant Physiol.* 160, 271–282.
- Gitelson, A.A., Kaufman, Y.J., Merzlyak, M.N., 1996. Use of a green channel in remote sensing of global vegetation from EOS-MODIS. *Remote Sens. Environ.* 58, 289–298.
- Gitelson, A.A., Kaufman, Y.J., Stark, R., Rundquist, D., 2002a. Novel algorithms for remote estimation of vegetation fraction. *Remote Sens. Environ.* 80, 76–87. [https://doi.org/10.1016/S0034-4257\(01\)00289-9](https://doi.org/10.1016/S0034-4257(01)00289-9)
- Gitelson, A.A., Stark, R., Grits, U., Rundquist, D., Kaufman, Y., Derry, D., 2002b. Vegetation and soil lines in visible spectral space: A concept and technique for remote estimation of vegetation fraction. *Int. J. Remote Sens.* 23, 2537–2562. <https://doi.org/10.1080/01431160110107806>

- Goel, N.S., Qin, W., 1994. Influences of canopy architecture on relationships between various vegetation indices and LAI and Fpar: A computer simulation. *Remote Sens. Rev.* 10, 309–347. <https://doi.org/10.1080/02757259409532252>
- Guerra, B., Steenwerth, K., 2012. Influence of floor management technique on grapevine growth, disease pressure, and juice and wine composition: A Review. *Am. J. Enol. Vitic.* 63, 149–164. <https://doi.org/10.5344/ajev.2011.10001>
- Guerrero, J.M., Pajares, G., Montalvo, M., Romeo, J., Guijarro, M., 2012. Support vector machines for crop/weeds identification in maize fields. *Expert Syst. Appl.* 39, 11149–11155. <https://doi.org/10.1016/j.eswa.2012.03.040>
- Guijarro, M., Pajares, G., Riomoros, I., Herrera, P.J., Burgos-Artizzu, X.P., Ribeiro, A., 2011. Automatic segmentation of relevant textures in agricultural images. *Comput. Electron. Agric.* 75, 75–83. <https://doi.org/10.1016/j.compag.2010.09.013>
- Hague, T., Tillett, N.D., Wheeler, H., 2006. Automated crop and weed monitoring in widely spaced cereals. *Precis. Agric.* 7, 21–32. <https://doi.org/10.1007/s11119-005-6787-1>
- Håkansson, S., 1982. Multiplication, growth and persistence of perennial weeds, in: Biology and Ecology of Weeds, Geobotany. Springer, Dordrecht, pp. 123–135. https://doi.org/10.1007/978-94-017-0916-3_11
- Hall, A., Lamb, D.W., Holzapfel, B., Louis, J., 2002. Optical remote sensing applications in viticulture - a review. *Aust. J. Grape Wine Res.* 8, 36–47. <https://doi.org/10.1111/j.1755-0238.2002.tb00209.x>
- Hammermeister, A.M., 2016. Organic weed management in perennial fruits. *Sci. Hortic.*, Recent advances in organic horticulture technology and management - Part 1 208, 28–42. <https://doi.org/10.1016/j.scienta.2016.02.004>
- Hernández, A.J., Lacasta, C., Pastor, J., 2000. Cubiertas vegetales para un viñedo ecológico en zonas semiáridas, in: Actas IV Congreso SEAE. Armonía entre Ecología y Economía. Córdoba, p. 11.
- Hunt, E.R., Hively, W.D., McCarty, G.W., Daughtry, C.S.T., Forrestal, P.J., Kratochvil, R.J., Carr, J.L., Allen, N.F., Fox-Rabinovitz, J.R., Miller, C.D., 2011. NIR-Green-Blue high-resolution digital images for assessment of winter cover crop biomass. *GIScience Remote Sens.* 48, 86–98. <https://doi.org/10.2747/1548-1603.48.1.86>
- Johnson, L.F., Roczen, D.E., Youkhana, S.K., Nemani, R.R., Bosch, D.F., 2003. Mapping vineyard leaf area with multispectral satellite imagery. *Comput. Electron. Agric.* 38, 33–44. [https://doi.org/10.1016/S0168-1699\(02\)00106-0](https://doi.org/10.1016/S0168-1699(02)00106-0)
- Jordan, C.F., 1969. Derivation of leaf-area index from quality of light on the forest floor. *Ecology* 50, 663–666. <https://doi.org/10.2307/1936256>

- Kataoka, T., Kaneko, T., Okamoto, H., Hata, S., 2003. Crop growth estimation system using machine vision, in: Proceedings 2003 IEEE/ASME International Conference on Advanced Intelligent Mechatronics (AIM 2003). Presented at the Proceedings 2003 IEEE/ASME International Conference on Advanced Intelligent Mechatronics (AIM 2003), pp. b1079-b1083 vol.2. <https://doi.org/10.1109/AIM.2003.1225492>
- Kaufman, Y.J., Remer, L.A., 1994. Detection of forests using mid-IR reflectance: an application for aerosol studies. *IEEE Trans. Geosci. Remote Sens.* 32, 672–683. <https://doi.org/10.1109/36.297984>
- Laliberte, A.S., Rango, A., 2011. Image processing and classification procedures for analysis of sub-decimeter imagery acquired with an unmanned aircraft over arid rangelands. *GIScience Remote Sens.* 48, 4–23. <https://doi.org/10.2747/1548-1603.48.1.4>
- Lanini, W.T., McGourty, G.T., Thrupp, L.A., 2011. Weed management for organic vineyards. *Org. Winegrowing Man.* 69–82.
- Lopes, C.M., Monteiro, A., Machado, J.P., Fernandes, N., Araújo, A., 2008. Cover cropping in a sloping non-irrigated vineyard: II - effects on vegetative growth, yield, berry and wine quality of “cabernet sauvignon” grapevines. *Ciênc. E Téc. Vitivinícola* 23, 37–43.
- Mahlein, A.-K., Oerke, E.-C., Steiner, U., Dehne, H.-W., 2012. Recent advances in sensing plant diseases for precision crop protection. *Eur. J. Plant Pathol.* 133, 197–209. <https://doi.org/10.1007/s10658-011-9878-z>
- Matese, A., Gennaro, S.F.D., Berton, A., 2017. Assessment of a canopy height model (CHM) in a vineyard using UAV-based multispectral imaging. *Int. J. Remote Sens.* 38, 2150–2160. <https://doi.org/10.1080/01431161.2016.1226002>
- Matese, A., Toscano, P., Di Gennaro, S.F., Genesio, L., Vaccari, F.P., Primicerio, J., Belli, C., Zaldei, A., Bianconi, R., Gioli, B., 2015. Intercomparison of UAV, aircraft and satellite remote sensing platforms for precision viticulture. *Remote Sens.* 7, 2971–2990. <https://doi.org/10.3390/rs70302971>
- McCoy, R.M., 2005. Field methods in remote sensing. Guilford Press, New York, NY.
- Meyer, G.E., Camargo Neto, J., 2008. Verification of color vegetation indices for automated crop imaging applications. *Comput. Electron. Agric.* 63, 282–293. <https://doi.org/10.1016/j.compag.2008.03.009>
- Meyer, G.E., Hindman, T.W., Laksmi, K., 1998. Machine vision detection parameters for plant species identification. pp. 327–335. <https://doi.org/10.1117/12.336896>
- Monteiro, A., Caetano, F., Vasconcelos, T., Lopes, C.M., 2013. Vineyard weed community dynamics in the dão winegrowing region. *Ciênc. E Tec. Vitivinic.* 27, 73–82.

- Mudarra Prieto, I., García Trujillo, R., 2005. El viñedo ecológico. Consejería de Medio Ambiente. Junta de Andalucía.
- Otsu, N., 1979. A threshold selection method from gray-level histograms. *IEEE Trans. Syst. Man Cybern.* 9, 62–66. <https://doi.org/10.1109/TSMC.1979.4310076>
- Peña, J.M., Torres-Sánchez, J., Castro, A.I. de, Kelly, M., López-Granados, F., 2013. Weed mapping in early-season maize fields using object-based analysis of unmanned aerial vehicle (UAV) images. *PLoS ONE* 8, e77151. <https://doi.org/10.1371/journal.pone.0077151>
- Peña-Barragán, J.M., Ngugi, M.K., Plant, R.E., Six, J., 2011. Object-based crop identification using multiple vegetation indices, textural features and crop phenology. *Remote Sens. Environ.* 115, 1301–1316. <https://doi.org/10.1016/j.rse.2011.01.009>
- Peñuelas, J., Gamon, J.A., Fredeen, A.L., Merino, J., Field, C.B., 1994. Reflectance indices associated with physiological changes in nitrogen- and water-limited sunflower leaves. *Remote Sens. Environ.* 48, 135–146. [https://doi.org/10.1016/0034-4257\(94\)90136-8](https://doi.org/10.1016/0034-4257(94)90136-8)
- Perry, C.R., Lautenschlager, L.F., 1984. Functional equivalence of spectral vegetation indices. *Remote Sens. Environ.* 14, 169–182.
- Poblete-Echeverría, C., Olmedo, G.F., Ingram, B., Bardeen, M., 2017. Detection and segmentation of vine canopy in ultra-high spatial resolution RGB imagery obtained from unmanned aerial vehicle (UAV): a case study in a commercial vineyard. *Remote Sens.* 9, 268. <https://doi.org/10.3390/rs9030268>
- Puletti, N., Perria, R., Storchi, P., 2014. Unsupervised classification of very high remotely sensed images for grapevine rows detection. *Eur. J. Remote Sens.* 47, 45–54. <https://doi.org/10.5721/EuJRS20144704>
- Qi, J., Chehbouni, A., Huete, A.R., Kerr, Y.H., Sorooshian, S., 1994. A modified soil adjusted vegetation index. *Remote Sens. Environ.* 48, 119–126. [https://doi.org/10.1016/0034-4257\(94\)90134-1](https://doi.org/10.1016/0034-4257(94)90134-1)
- Rey, C., Martín, M.P., Lobo, A., Luna, I., Diago, M.P., Millan, B., Tardáguila, J., 2013. Multispectral imagery acquired from a UAV to assess the spatial variability of a Tempranillo vineyard, in: Precision Agriculture '13. Wageningen Academic Publishers, Wageningen, pp. 617–624. https://doi.org/10.3920/978-90-8686-778-3_76
- Richardson, A.J., Wiegand, C.L., 1977. Distinguishing vegetation from soil background information. *Photogramm. Eng. Remote Sens.* 43, 1541–1552.

- Roig, G., Montull Daniel, J.M., Llenes, J.M., Palou, A.T., 2017. Herbicidas alternativos en viña ecológica, in: Actas XVI Congreso de la Sociedad Española de Malherbología. Universidad Pública de Navarra. pp. 381-384. pp. 381–384.
- Romboli, Y., Gennaro, S.F.D., Mangani, S., Buscioni, G., Matese, A., Genesio, L., Vincenzini, M., 2017. Vine vigour modulates bunch microclimate and affects the composition of grape and wine flavonoids: an unmanned aerial vehicle approach in a sangiovese vineyard in Tuscany. *Aust. J. Grape Wine Res.* 23, 368–377.
<https://doi.org/10.1111/ajgw.12293>
- Rondeaux, G., Steven, M., Baret, F., 1996. Optimization of soil-adjusted vegetation indices. *Remote Sens. Environ.* 55, 95–107.
- Rouse, J., Haas, R.H., Schell, J.A., Deering, D.W., 1974. Monitoring vegetation systems in the Great Plains with ERTS. Proc. Third ERTS Symp. Wash. DC 309–317.
- Santesteban, L.G., Di Gennaro, S.F., Herrero-Langreo, A., Miranda, C., Royo, J.B., Matese, A., 2017. High-resolution UAV-based thermal imaging to estimate the instantaneous and seasonal variability of plant water status within a vineyard. *Agric. Water Manag.*, Special Issue: Advances on ICTs for Water Management in Agriculture 183, 49–59. <https://doi.org/10.1016/j.agwat.2016.08.026>
- Schieffer, J., Dillon, C., 2015. The economic and environmental impacts of precision agriculture and interactions with agro-environmental policy. *Precis. Agric.* 16, 46–61.
<https://doi.org/10.1007/s11119-014-9382-5>
- Smith, A.M.S., Drake, N.A., Wooster, M.J., Hudak, A.T., Holden, Z.A., Gibbons, C.J., 2007. Production of Landsat ETM+ reference imagery of burned areas within Southern African savannahs: comparison of methods and application to MODIS. *Int. J. Remote Sens.* 28, 2753–2775. <https://doi.org/10.1080/01431160600954704>
- Sripada, R.P., Heiniger, R.W., White, J.G., Meijer, A.D., 2006. Aerial color infrared photography for determining early in-season nitrogen requirements in corn. *Agron. J.* 98, 968–977.
- Thomlinson, J.R., Bolstad, P.V., Cohen, W.B., 1999. Coordinating methodologies for scaling landcover classifications from site-specific to global: Steps toward validating global map products. *Remote Sens. Environ.* 70, 16–28.
- Torres-Sánchez, J., López-Granados, F., Peña, J.M., 2015a. An automatic object-based method for optimal thresholding in UAV images: application for vegetation detection in herbaceous crops. *Comput. Electron. Agric.* 114, 43–52.
<https://doi.org/10.1016/j.compag.2015.03.019>
- Torres-Sánchez, J., López-Granados, F., Serrano, N., Arquero, O., Peña, J.M., 2015b. High-throughput 3-d monitoring of agricultural-tree plantations with unmanned aerial

- vehicle (UAV) technology. *PLoS ONE* 10.
<https://doi.org/10.1371/journal.pone.0130479>
- Valencia, F., Mas, N., Recasens, J., 2017. El uso de cubiertas vegetales y sus labores de implantación en el manejo de *Cynodon dactylon* en viñedo. Actas XVI Congreso de la Sociedad Española de Malherbología. Universidad Pública de Navarra. pp 147-152.
- Weiss, M., Baret, F., Weiss, M., Baret, F., 2017. Using 3D point clouds derived from uav rgb imagery to describe vineyard 3d macro-structure. *Remote Sens.* 9, 111.
<https://doi.org/10.3390/rs9020111>
- Woebbecke, D.M., Meyer, G.E., Bargen, K.V., Mortensen, D.A., 1995a. Color indices for weed identification under various soil, residue, and lighting conditions. *Trans. ASAE* 38, 259–269. <https://doi.org/10.13031/2013.27838>
- Woebbecke, D.M., Meyer, G.E., Von Bargen, K., Mortensen, D.A., 1995b. Shape features for identifying young weeds using image analysis. *Trans. ASAE USA*.
- Wood, E.M., Pidgeon, A.M., Radeloff, V.C., Keuler, N.S., 2012. Image texture as a remotely sensed measure of vegetation structure. *Remote Sens. Environ.* 121, 516–526.
<https://doi.org/10.1016/j.rse.2012.01.003>

Capítulo 5

Conclusiones



Esta Tesis Doctoral ha contribuido a generar conocimiento para alcanzar el objetivo global centrado en la optimización del manejo de dos cultivos leñosos de gran relevancia socioeconómica (olivar y viñedo) en el contexto de la agricultura de precisión. Ello se ha conseguido mediante el uso de tecnología UAV y análisis OBIA, avanzando en dos aspectos fundamentales: 1) evaluación multitemporal del impacto de varios tipos de poda sobre la arquitectura 3D en cada olivo, y 2) racionalización de las aplicaciones de fitosanitarios en viñedo, tanto foliares según tamaño y estructura de cada cepa, como de herbicidas para el control localizado de malas hierbas según su posición y nivel de infestación.

Para la consecución de lo anterior, se plantearon los siguientes objetivos específicos:

- d) Monitorización multitemporal 3D de cada árbol de una parcela de olivar bajo marco de plantación intensivo para cuantificar la influencia de tres tipos diferentes de poda (adaptada, tradicional y mecánica) sobre los parámetros morfológicos de la copa (altura, área proyectada y volumen), así como evaluar su respuesta vegetativa después de un año de realizarse cada tratamiento de poda (**Capítulo 2**).
- e) Caracterización espacio-temporal 3D de alto rendimiento (*high-throughput*) de la arquitectura de cada cepa en tres viñedos en espaldera en dos momentos fenológicos distintos para computar los parámetros morfológicos de cada cepa, detectar huecos por marras en la parcela y sentar las bases metodológicas para crear mapas de tratamientos foliares de fitosanitarios según tamaño del dosel (**Capítulo 3**).
- f) Detección y cartografía multitemporal automática de las infestaciones de la mala hierba gramínea y perenne *Cynodon dactylon* L. (grama) en dos viñedos en espaldera durante dos años consecutivos para establecer estrategias de control localizado incorporando un rango de umbrales de tratamiento según niveles de infestación permitiendo una racionalización de su manejo (**Capítulo 4**).

De las investigaciones realizadas para lograr los objetivos específicos recogidos en los **Capítulos 2, 3 y 4** de esta Tesis Doctoral se han obtenido las siguientes conclusiones:

Capítulo 2.- JIMÉNEZ-BRENES, F.M.; LÓPEZ-GRANADOS, F.; DE CASTRO, A.I.; TORRES-SÁNCHEZ, J.; CASTILLO, N.; PEÑA, J.M. (2017). Quantifying pruning impacts on olive tree architecture and annual canopy growth by using UAV-based 3D modelling. *Plant Methods*, 13:55. doi:10.1186/s13007-017-0205-3 (Open Access).

1. La combinación de tecnología UAV y modelización 3D a partir del Modelo Digital de Superficie (*DSM*, *en inglés*) junto con el desarrollo de un algoritmo OBIA automatizado de análisis de las imágenes-UAV permitió una monitorización multitemporal de cada individuo de una parcela de 648 olivos sometidos a tres tipos de poda (*adaptada, tradicional y mecánica*).

2. El algoritmo OBIA identificó y clasificó automáticamente cada olivo a partir de las imágenes obtenidas con una cámara RGB de bajo coste acoplada al UAV, exportando los valores de altura, área proyectada y volumen para cada olivo en cada vuelo realizado considerando tres fechas: antes de la poda, un mes después y transcurrido un año de ésta.
3. La cuantificación de los parámetros geométricos de cada árbol permitió realizar un seguimiento temporal de los efectos de cada poda sobre la arquitectura de copa de cada árbol. Como tendencia general, los olivos sometidos a la poda *adaptada* registraron las mayores pérdidas de follaje un mes después de la poda, seguidos por los olivos bajo poda *tradicional*. Sin embargo, estos últimos presentaron el mayor crecimiento de la copa un año después de la poda, es decir, mayor respuesta vegetativa. Debido a la tipología de la poda *mecanizada* que mantiene el corte a una altura fija, los olivos bajo dicho tratamiento no mostraron una respuesta tan acusada como los otros tipos de poda respecto a su crecimiento, ya que no disminuyeron en gran medida su tamaño al mes de la poda ni lo aumentaron al año de la misma. La tecnología y metodología presentadas en este artículo son adaptables y transferibles a otros cultivos como viñedos o árboles frutales, si bien es necesario realizar previamente ajustes sobre el algoritmo OBIA dependiendo del cultivo.
4. Esta investigación ofrece información cartográfica y tabulada útil para el diseño de estrategias de manejo localizado del olivar en el contexto de la agricultura de precisión, no solo para aplicaciones optimizadas de poda, sino también para fertilización, fitosanitarios y/o riegos en función de la arquitectura de cada olivo, lo cual reporta beneficio medioambiental y ahorro económico para el agricultor.

Capítulo 3.- DE CASTRO, A.I.; JIMÉNEZ-BRENES, F.M.; TORRES-SÁNCHEZ, J.; PEÑA, J.M.; BORRA-SERRANO, I.; LÓPEZ-GRANADOS, F. (2018). 3-D characterization of vineyards using a novel UAV imagery-based OBIA procedure for precision viticulture applications. *Remote Sensing*, 10(4): 584. doi:10.3390/rs10040584 (Open Access).

1. Un novedoso algoritmo automático OBIA fue desarrollado para caracterizar tridimensionalmente tres viñedos con cubiertas vegetales entre las calles en dos momentos fenológicos distintos a partir de imágenes tomadas por una cámara RGB de bajo coste a bordo de un UAV.
2. La utilización de técnicas fotogramétricas y el *DSM* permitieron al algoritmo separar cada cepa de la cubierta vegetal del viñedo en base a la diferencia de altura entre ambas clases, superando así el problema de similitud espectral entre cepas y cubierta vegetal en los momentos de adquisición de las imágenes.

3. El algoritmo OBIA diseñado clasificó con un alto grado de precisión (90-95 %) cada cepa de vid, computando su altura, área proyectada y volumen, además de la existencia de huecos en cada hilera (marras). Las alturas obtenidas por el algoritmo fueron validadas con datos verdad-terreno tomados en campo, obteniéndose un error medio cuadrático de 0,19 metros para los tres viñedos analizados.
4. El algoritmo OBIA exportó mapas georreferenciados con la localización y dimensiones de cada cepa, mostrando así la variabilidad espacio-temporal existente en el viñedo, información clave para el diseño de estrategias de manejo localizado del dosel.
5. En resumen, la combinación tecnológica UAV-OBIA mostró un gran potencial en para la monitorización multitemporal del crecimiento de un viñedo, lo cual tiene múltiples aplicaciones en el contexto de la viticultura de precisión: tratamiento variable de fitosanitarios foliares, determinación del momento óptimo de cosecha o evaluación del efecto de diferentes tratamientos de poda según la estructura 3-D de cada cepa.

Capítulo 4.- JIMÉNEZ-BRENES, F.M.; LÓPEZ-GRANADOS, F.; TORRES-SÁNCHEZ, J.; PEÑA, J.M.; RAMÍREZ, P.; CASTILLEJO-GONZÁLEZ, I.L.; DE CASTRO, A.I. (2019). Automatic UAV-based detection of *Cynodon dactylon* for site-specific vineyard management. *PLoS ONE*, 14(6): e0218132. doi.org/10.1371/journal.pone.0218132 (Open Access).

1. Se desarrolló un algoritmo OBIA capaz de detectar y cartografiar de forma precisa los rodales de grama (*Cynodon dactylon* L.) que infestan viñedos. Este algoritmo analizó automáticamente las imágenes tomadas por dos sensores con distinto rango espectral (RGB y RGNIR) a bordo de un UAV en dos viñedos durante dos años consecutivos.
2. El DSM hizo posible la clasificación de la viña en base a información de altura, superando así el problema de similitud espectral entre ésta y los rodales de grama en el momento en el que se llevó a cabo la investigación. Además, se realizó un análisis espectral que permitió separar la grama y el suelo desnudo, siendo los índices de vegetación ExGR y GNDVI los más precisos y, por tanto, los implementados en el correspondiente algoritmo OBIA de análisis de las imágenes generadas para las cámaras RGB y RGNIR, respectivamente.
3. Se alcanzaron altos valores de precisión de la clasificación (> 97,7 %) con cada una de las cámaras empleadas, mostrando que es posible la cartografía automática de todas las clases presentes en el viñedo: cepas, grama y suelo desnudo con cualquiera de los sensores evaluados (RGB y RGNIR). Considerando estos resultados similares, se recomienda el uso del sensor RGB por ser más manejable y económico.

4. Los mapas y la información tabulada generados por el algoritmo OBIA constituyen una herramienta útil y precisa para los viticultores ya que podrían ser utilizados en la optimización del manejo de grama en viñedos, tanto ecológicos como no ecológicos. Ello sería posible a través de un programa basado en estrategias de control localizado según la posición de los rodales de grama y el umbral de infestación.

LÍNEAS DE INVESTIGACIÓN COLATERALES Y FUTURAS (EN INICIO O PLENO DESARROLLO)

Esta Tesis Doctoral ha sentado las bases tecnológicas y metodológicas para abordar un conjunto de líneas de investigación no incluidas en este manuscrito y en las que ha estado involucrado el doctorando. Estos trabajos, que han sido publicados o están actualmente en revisión, se exponen a continuación indicando su grado de desarrollo:

1. Objetivo: Arquitectura y fenotipado de cultivares de cultivos leñosos en programas de mejora genética y en condiciones de campo.

- i) Cultivo de Almendro, en colaboración con investigadores del IFAPA Alameda del Obispo-Córdoba:
 - Trabajo publicado: TORRES-SÁNCHEZ, J.; DE CASTRO, A.I.; PEÑA, J.M.; **JIMÉNEZ-BRENES, F.M.**; ARQUERO, O.; LOVERA, M.; LÓPEZ-GRANADOS, F. (2019). Mapping the 3D structure of almond trees using UAV acquired photogrammetric point clouds and object-based image analysis. *Biosystems Engineering*, 176: 172-184. <https://doi.org/10.1016/j.biosystemseng.2018.10.018>.
 - Trabajo en revisión: LÓPEZ-GRANADOS, F.; TORRES-SÁNCHEZ, J.; **JIMÉNEZ-BRENES, F.M.**; ARQUERO, O.; LOVERA, M.; DE CASTRO, A.I. (2019). An efficient RGB-UAV-based platform for field almond tree phenotyping: 3-D architecture and flowering traits. *Plant Methods* (Open Access).
- ii) Olivar, en colaboración con investigadores de la Universidad de Sevilla:
 - Trabajo en revisión: DE CASTRO, A.I.; RALLO, P.; SUÁREZ, M.P.; TORRES-SÁNCHEZ, J.; CASANOVA, L.; **JIMÉNEZ-BRENES, F.M.**; MORALES-SILLERO, A.; JIMÉNEZ, R.; LÓPEZ-GRANADOS, F. (2019). High-throughput system for the early quantification of major architectural traits in olive breeding trials using UAV images and OBIA techniques. *Frontiers in Plant Science* (Open Access).
- iii) Frutales de hueso, en colaboración con investigadores de la Universitat de Lleida y del Centro de Automática y Robótica (CAR-CSIC) de Arganda (Madrid):

- En pleno desarrollo

2. Objetivo: Monitorización y cuantificación de las intervenciones en verde (deshojado, despuntado y esbergurado) sobre la estructura tridimensional en viñedo. En colaboración con investigadores de la Universidad Pública de Navarra.

- Trabajo publicado: TORRES-SÁNCHEZ, J.; MARÍN, D.; DE CASTRO, A.I.; ORIA, I.; **JIMÉNEZ-BRENES, F.M.**; MIRANDA, C.; SANTESTEBAN, L.G.; LÓPEZ-GRANADOS, F. (2019). Assessment of vineyard trimming and leaf removal using UAV photogrammetry. *12th European Conference on Precision Agriculture*, 8th-11th July 2019. Montpellier, Francia, pp: 187-192.
- Artículo en preparación con resultados de cuatro parcelas de viñedo.

3. Objetivo: Análisis cuantitativo y dinámica de poblaciones de las emergencias de grama en viñedo.

- En pleno desarrollo. Este trabajo es continuación de los estudios presentados en el **Capítulo 4** de esta Tesis.

4. Objetivo: Detección temprana de enfermedades fúngicas en diferentes variedades de almendro: tolerancia varietal según grado de afectación de la copa. En colaboración con investigadores del IFAPA Alameda del Obispo de Córdoba y Universidad de Córdoba.

- En pleno desarrollo

5. Objetivo: Detección temprana de malas hierbas monocotiledóneas y dicotiledóneas en cultivos herbáceos.

- En pleno desarrollo

